

EVALUATING PHOTOLYSIS AND SORPTION OF ANTIBIOTICS IN BOTH
LABORATORY AND ENVIRONMENTAL SETTINGS

Katherine M. Stauffenberg

A thesis submitted to the faculty of the University of North Carolina at Chapel Hill in partial fulfillment of the requirements for the degree of Master of Science in the Department of Environmental Sciences and Engineering, School of Public Health

Chapel Hill
2007

Approved by:

Dr. Howard S. Weinberg, Advisor

Dr. Michael D. Aitken, Reader

Dr. Stephen C. Whalen, Reader

© 2007
Katherine M. Stauffenberg
ALL RIGHTS RESERVED

ABSTRACT

Katherine M. Stauffenberg

Evaluating Photolysis and Sorption of Antibiotics in both Laboratory
and Environmental Settings

(Under the direction of Howard S. Weinberg)

There is growing public health concern about the development of antimicrobial strains of bacteria and the possibility that the continuous exposure of natural microbes to antibiotic residues in the environment could be one pathway. For a complete perspective on fate and transport of antibiotics in the aquatic environment and their potential role in this process, both aqueous phase and sediment concentrations are important to determine environmental exposure. Sulfamethoxazole (SMX), trimethoprim (TMP), ciprofloxacin (CPX), and tetracycline (TCC) were quantified in surface water and sediment extracts using standard addition and isotopically labeled surrogates. While SMX was found at the highest concentrations in surface waters (198-328 ng/L), CPX was the most concentrated in the sediments (20-25 ng/g). An alternative fate for aqueous phase antibiotics is that of photolysis. To evaluate this process under laboratory conditions, a reactor was constructed to simulate a controlled stream environment. SMX was shown to degrade in the presence of UV-light into sulfanilic acid and a photoisomer. Highly organic sediments were the most efficient at removing SMX from the aqueous phase.

ACKNOWLEDGEMENTS

Eternal gratitude is owed to Maryanne Boundy, Joe Pedit, and Jack Whaley. Without these reanimators, this Frankenstein would never have been resurrected from its grave.

TABLE OF CONTENTS

	Page
LIST OF TABLES.....	ix
LIST OF FIGURES	xi
LIST OF ABBREVIATIONS AND SYMBOLS	xvi
CHAPTER 1: BACKGROUND AND LITERATURE REVIEW	1
1.1 Introduction	1
1.2 Target Antibiotics	2
1.3 Environmental Occurrence Data of Antibiotics.....	6
1.3.1 Wastewater Treatment Plants	6
1.3.2 Streams.....	6
1.4 Photochemistry	7
1.4.1 Actinometry	10
1.4.2 Light Sources	11
1.4.3 Photolysis of Antibiotics.....	11
1.5 Sorption of Antibiotics.....	15
1.6 Water Sediment Systems	17
1.7 Current Analytical Methods.....	18
1.8 Public Health Related Issues.....	19
1.9 Research Overview	20

CHAPTER 2: MATERIALS AND METHODS	21
2.1 Materials	21
2.2 Glassware Cleaning Procedure	22
2.3 Autosampler Vial Deactivation.....	22
2.4 Standards.....	22
2.5 Sampling Site	22
2.6 Surface Water Extraction.....	24
2.6.1 Sample Collection and Storage.....	25
2.6.2 Sample Preparation.....	25
2.7 Sediment Extraction.....	26
2.7.1 Sample Collection and Storage.....	26
2.7.2 Sample Preparation.....	26
2.8 Photolysis.....	28
2.8.1 Artificial Light Sources.....	28
2.8.2 Reactor Design Evolution.....	30
2.8.3 Actinometry	33
2.8.4 Final Reactor Procedure.....	34
2.9 HPLC Analysis	35
2.9.1 LC/MS Analysis.....	36
2.9.2 HPLC-PDA Analysis.....	37
2.10 Soil Characterization.....	37
2.11 pH.....	38
2.12 Total Organic Carbon (TOC) Analysis.....	38

2.13 UV-VIS Spectrometry	38
CHAPTER 3: RESULTS AND DISCUSSION.....	39
3.1 Stability of the Antibiotics During Analysis.....	39
3.2 Soil and Sediment Characterization.....	43
3.3 Photolysis of SMX.....	43
3.3.1 Batch Reactor Results	43
3.3.2 Second Reactor Design.....	45
3.3.3 Final Reactor Design.....	48
3.3.4 Photolysis Byproducts	57
3.4 Optimizing Soil and Sediment Extraction	65
3.4.1 Extraction Method	65
3.4.2 Soil Extraction Solvent	66
3.4.3 Final Sample Solvent.....	68
3.4.4 Instrument Analysis	71
3.4.5 Standard Addition	76
3.4.6 Isotopic Dilution	78
3.5 Environmental Surface Water and Sediment Extractions.....	82
CHAPTER 4: CONCLUSIONS	85
APPENDICES	87
Appendix A. Soil Characterization Procedures	87
Determination of Soil pH.....	87
Gravimetric Soil Moisture Determination (%M).....	87
Organic Matter Content of Soils.....	87

Determination of Soil Texture	88
Determination of Soil Particle Density (D_p)	89
Determination of Water Holding Capacity (WHC)	90
Appendix B: Procedure for Total Organic Carbon (TOC) Analysis	92
Sample storage and preparation	92
Preparation of calibration standards.....	92
Preparation of the TOC analyzer	93
Data Analysis	97
Quality Control and Assurance	98
REFERENCES	100

LIST OF TABLES

	Page
Table 1.1 Chemical information regarding commonly used classes of antibiotics (Thiele-Bruhn, 2003).....	4
Table 1.2a: Structure and some physical properties of target antibiotics.....	4
Table 1.2b: Structures and some physical properties of target antibiotics	5
Table 1.3: Daily prescribed human dose and metabolism of the target antibiotics (Lorian, 1996).....	5
Table 1.4: Environmentally relevant photooxidants (* denoting free radical) and standard one electron reaction potentials (E_H) (Schwarzenbach, Geschwend <i>et al.</i> , 1993).....	10
Table 1.5: Direct rate constants for sulfamethoxazole in various buffered solutions measured under natural sunlight (Boreen, Arnold <i>et al.</i> , 2004).....	12
Table 1.6: Sorption coefficients of antibiotics determined from batch sorption and isotherm experiments.....	16
Table 2.1: Effects of the Pyrex filter on the Phillips T20W lamp intensity	30
Table 2.2: Gradient Run 1 for HPLC analysis of sulfamethoxazole and related photodegradation byproducts	35
Table 2.3: Gradient Run 2 for HPLC analysis of antibiotic mixtures	36
Table 2.4: Target analytes and the MS/MS breakdown information	37
Table 3.1: Comparing the responses of consecutive injections of the same aqueous solutions of SMX, CPX, and TCC in LGW analyzed by HPLC-PDA at 271nm	42
Table 3.2: Comparing the LC-MS/MS response of aqueous solutions of CPX (0.43 mg/L), TCC (1.1 mg/L) and SMX (0.22 mg/L) in untreated and deactivated glass vials	42
Table 3.3: Soil and sediment characterization from six different North Carolina locations.....	43

Table 3.4: Summary of kinetics for 10 mg/L SMX in BR assuming pseudo first order degradation (n = 3).....	45
Table 3.5: Summary of kinetics information for 1 mg/L SMX in BR assuming pseudo first order degradation (n = 2).....	45
Table 3.6: Summary of kinetics information for 1 mg/L SMX in BR assuming pseudo first order degradation (n = 5).....	47
Table 3.7: Results of sonicated extracts compared to the shaken extracts of the Eastern NC agricultural soil spiked with sulfamethoxazole (200 µg SMX/g soil) (n = 3)	66
Table 3.8: Results of three consecutive exactions of the same soil sample with three commonly used solvents (200 µg/g) (n = 3)	67
Table 3.9a: Isotopic dilution relative response of sulfamethoxazole in solvent matrix (LGW) analyzed by LC/MS/MS.....	79
Table 3.9b: Isotopic dilution relative response of ciprofloxacin in solvent matrix (LGW) analyzed by LC/MS/MS	80
Table 3.9c: Isotopic dilution relative response of levofloxacin in solvent matrix (LGW) analyzed by LC/MS/MS	80
Table 3.10: Comparing standard addition calculated concentrations to isotopic dilution concentrations from Morgan Creek effluent sediment (2/14/06).....	82
Table 3.11: Aqueous antibiotic concentrations in surface water (Morgan Creek) around the OWASA WWTP (2/6/2006) (nd=not detected).....	83
Table 3.12: Sediment antibiotic concentrations in surface water (Morgan Creek) around the OWASA WWTP (2/6/2006) (nd=not detected).....	83
Table 3.13: Comparison of the aqueous and sediment concentrations in surface water (Morgan Creek) around the OWASA WWTP (ppt) (2/6/2006) (nd = not detected).....	83
Table 3.14: Sediment antibiotic concentrations of sediments extracted from date of collection and one month later (na = not applicable; LVX was not included in the February 16 analysis).....	84

LIST OF FIGURES

	Page
Figure 1.1: Major photodegradation product of fluoroquinolones in aqueous solutions (Burhenne, Ludwig <i>et al.</i> 1999)	13
Figure 1.2: Photodegradation products of ciprofloxacin exposed to simulated sunlight (Turiel, Bordin <i>et al.</i> 2005)	13
Figure 1.3: Combined photodegradation products of sulfamethoxazole in LGW and natural waters from both natural and simulated sunlight (Zhou and Moore 1994; Boreen, Arnold <i>et al.</i> 2004)	14
Figure 1.4: Photodegradation products of tetracycline in LGW under various conditions (Morrison, Olack <i>et al.</i> 1991).....	14
Figure 2.1: GPS marking the points in relation to the WWTP and United States Geological Survey (USGS) stream gauge 02097517.....	24
Figure 2.2: Emission of the Noblelight 718 Z4 825W medium pressure mercury lamp before and after Pyrex filtration	28
Figure 2.3: Emission of Good Earth Lighting Growlight 18W “high UV” plant lamp.....	29
Figure 2.4: Emission of Phillips T20W UVB lamp before and after Pyrex filtration	29
Figure 2.5: Batch reactor (BR) setup.....	31
Figure 2.6: Second reactor design (FT).....	32
Figure 2.7: Final reactor design.....	33
Figure 3.1: Stability of SMX in LGW held at two temperatures (4°C and 22°C) over 27 days (analyzed with HPLC-PDA at 271 nm).....	40
Figure 3.2: Comparison of filtered LGW containing 0.05 mg/L SMX with the unfiltered solution (analyzed with HPLC-PDA at 271nm).....	40
Figure 3.3: Effect of filtration of a humic water on the stability of SMX (C ₀ = 1 mg/L, temperature at 4°C) analyzed with HPLC-PDA at 271 nm.....	41
Figure 3.4: Example of forced pseudo first order degradation of SMX (C ₀ = 10 mg/L) in LGW in the BR reactor	44

Figure 3.5:	Example of forced pseudo first order degradation of SMX ($C_0 = 1$ mg/L) in LGW in the BR reactor	45
Figure 3.6:	An example of pseudo first order degradation results of SMX in LGW ($C_0=1$ mg/L; pH=5.5) in the FT reactor	47
Figure 3.7:	Pseudo first order degradation of SMX in the FT reactor in LGW in the presence of Chapel Hill soil ($C_0=1.15$ mg/L; pH=5.7)	48
Figure 3.8a:	Persistence of SMX in LGW ($C_0 = 0.93$ mg/L) control.....	49
Figure 3.8b:	Persistence of SMX in LGW ($C_0 = 1$ mg/L; pH = 5.5) in the ER with Growlight visible lamp	49
Figure 3.9a:	SMX ($C_0 = 0.9$ mg/L, pH = 5.6) with LGW/Chapel Hill soil in the Control Reactor	49
Figure 3.9b:	SMX ($C_0 = 0.9$ mg/L, pH = 5.6) with LGW/Chapel Hill soil in the ER with the Growlight plant lamp	49
Figure 3.9c:	SMX ($C_0 = 0.9$ mg/L, pH = 5.6) with LGW/Chapel Hill soil in the ER with the Growlight plant lamp	49
Figure 3.10a:	SMX ($C_0 = 0.9$ mg/L, pH = 5.6) with LGW in the Control Reactor.....	51
Figure 3.10b:	SMX ($C_0 = 0.9$ mg/L, pH = 5.6) with LGW in the ER with the Phillips T20W lamp	51
Figure 3.10c:	First order degradation of SMX in LGW ($C_0 = 0.9$ mg/L; pH = 5.6) from exposure to the Phillips T20W UVB Lamp	51
Figure 3.11:	Photodegradation of 10 ng/L of SMX in LGW (ER)	52
Figure 3.12a:	SMX ($C_0 = 1$ mg/L, pH = 5.6) with LGW/Ottawa sand in the Control Reactor	53
Figure 3.12b:	SMX ($C_0 = 0.9$ mg/L, pH = 5.6) with LGW/Ottawa sand in the ER with the Phillips T20W lamp	53
Figure 3.12c:	First order degradation of SMX in LGW with 300 g of Ottawa sand under the Phillips T20W UVB lamp	53
Figure 3.13a:	SMX ($C_0=0.9$ mg/L, pH=5.7) with LGW/ Chapel Hill soil in the Control Reactor	54

Figure 3.13b: SMX ($C_0=0.9$ mg/L, pH=5.7) with LGW/ Chapel Hill soil in the Control Reactor	54
Figure 3.14a: SMX ($C_0=2.6$ mg/L, pH=5.5) with LGW/ Eastern NC agricultural soil in the ER with the Phillips T20W lamp	54
Figure 3.14b: SMX ($C_0=2.6$ mg/L, pH=5.5) with LGW/ Eastern NC agricultural soil in the ER with the Phillips T20W lamp	54
Figure 3.15: UV absorbance spectra of the ER and CR (4 L of LGW equilibrated with 300 g of Morgan Creek Sediment; pH = 6.7 - 6.8, TOC: 2.07 mg/L C).....	55
Figure 3.16: UV absorbance spectra of Morgan Creek sampling points (11/14/2005, 0.45um filtered) (UPS = upstream, TOC = 3.00mg/L C; DS = downstream, TOC = 5.24 mg/L C; E = effluent, TOC = 5.52mg/L C).....	56
Figure 3.17: Pseudo first order degradation of SMX ($C_0=0.10$ mg/L, pH = 6.7, TOC = 2.05 mg/L C) in the LGW/Morgan Creek sediment system.....	56
Figure 3.18a: HPLC-PDA chromatogram depicting the original response of SMX (1mg/L in LGW FT) at 0 hrs	57
Figure 3.18b: HPLC-PDA chromatogram after 9 hrs depicting the loss of SMX (1mg/L in LGW FT) and the formation of byproducts detectable at 271 nm	57
Figure 3.19: Molar absorptivity of sulfamethoxazole and predicted byproducts.....	58
Figure 3.20: Absorbance spectrum of the major unknown SMX photolysis byproduct extracted from an HPLC-PDA chromatogram	58
Figure 3.21: LC/MS full scan spectrum of SMX from 50-300 amu	59
Figure 3.22: LC/MS full scan spectrum of the major byproduct (50-300 m/z) from SMX ($C_0 = 1$ mg/L) in LGW exposed to the Phillips T20W lamp in the ER after 3 hrs exposure.....	60
Figure 3.23: Formation of SMX photoisomer in LGW ($C_0 = 1$ mg/L) in the ER with the Phillips T20W UVB lamp and the Pyrex filter after 32hrs of exposure.....	61
Figure 3.24: Formation of the SMX photoisomer ($C_0=10$ ng/L) in LGW exposed to the Phillips T20W lamp in the ER.....	62

Figure 3.25:	Production of the SMX photoisomer in the effluent of the OWASA WWTTP and downstream after the plant began low pressure UV treatment (2/14/06).....	64
Figure 3.26:	Comparison of extraction techniques for the recovery of SMX from the Eastern NC agricultural soil spiked with sulfamethoxazole (200 µg SMX/g soil) (n = 3)	66
Figure 3.27:	Three consecutive extractions of a spiked Eastern NC agricultural soil (200 µg SMX/g) with three different solvents	67
Figure 3.28:	Comparison of methanol with citric acid buffer (CAB): methanol extracting solvent extract concentrations of SMX from Eastern NC agricultural soil (15 µg/g) (n = 3)	68
Figure 3.29a:	Ciprofloxacin, Tetracycline and Sulfamethoxazole neat standards (1mg/L) in acetonitrile analyzed by HPLC with the Waters Series II 996 PDA detector.....	69
Figure 3.29b:	Ciprofloxacin, Tetracycline and Sulfamethoxazole neat standards (1mg/L) in LGW analyzed by HPLC with the Waters Series II 996 PDA detector.....	70
Figure 3.30a:	Calibration of SMX in reconstituted solvents.....	70
Figure 3.30b:	Calibration of TCC in reconstituted solvents.....	71
Figure 3.31:	Citric acid:methanol extraction of Eastern North Carolina agricultural soil	72
Figure 3.32:	Methanol extract of Eastern NC agricultural soil	72
Figure 3.33:	0.2M citric acid:methanol (1:1) extract spiked Eastern NC agricultural soil (15 µg SMX/g soil, 10 µg CPX/g soil; 24 µg TCC/g soil).....	73
Figure 3.34:	Methanol extraction of the spiked Eastern NC agricultural soil (15 µg SMX/g soil; 10 µg CPX/g soil; 24 µg TCC/g soil).....	73
Figure 3.35:	LCMS/MS chromatogram of a sediment extract illustrating the importance of the confirmation ion.....	74
Figure 3.36:	An LC-MS/MS example chromatogram of five different antibiotic separations.....	75

Figure 3.37:	Example of standard addition for Morgan Creek surface water and OWASA WWTP Effluent for SMX (2/6/2006). (UPS refers to upstream sample ($C_0 = 2$ ng/L); E refers to WWTP effluent ($C_0 = 328$ ng/L); DS refers to downstream sample ($C_0 = 192$ ng/L)).	77
Figure 3.38a:	Ciprofloxacin standard addition of a Morgan Creek sediment downstream extraction	77
Figure 3.38b:	Ciprofloxacin relative standard addition of a Morgan Creek sediment downstream extraction	77
Figure 3.39a:	Calibration curve illustrating the linearity of the sulfamethoxazole response (LC/MS/MS)	81
Figure 3.39b:	Linearity of ciprofloxacin calibration curve in LGW analyzed by LC/MS/MS	81
Figure 3.39c:	Linearity of levofloxacin calibration curve in LGW analyzed by LC/MS/MS	81

LIST OF ABBREVIATIONS AND SYMBOLS

A	absorbance
A_λ	total absorbance of the system
ASE	automated solvent extraction
b	pathlength
BR	batch reactor
c	speed of light in a vacuum
°C	degrees Celsius
[C]	concentration
C_0	initial concentration
C_e	concentration at equilibrium
CAB	citric acid buffer
CaCl_2	calcium chloride
CAFO	confined animal feeding operation
CDOM	colored dissolved organic matter
cm	centimeters
CO_3^{2-}	carbonate
$\text{C}_2\text{O}_4^{2-}$	oxalate
CPX	ciprofloxacin
CR	dark control
E	energy
e^-	electron
E_H	one electron reaction potential
eins	einstein (one mole of photons)
ER	exposure reactor

ESI	electrospray ionization
F_c	fraction of total absorption due to concentration
f_λ	fraction of total intensity
Fe^{2+}	ferrous iron (II)
Fe^{3+}	ferric iron (III)
ft	feet
FT	fish tank
g	grams
GC	gas chromatography
gps	global positioning system
h	Planck's constant
$h\nu$	photon
Hg	mercury
HLB	hydrophilic lipophilic balance
H_2O	water
HO^-	hydroxide ion
HO_2^-	hydroperoxide ion
HPLC	high performance liquid chromatography
hr	hour
I	intensity of light
I_0	incident intensity
I_λ	intensity of light at wavelength λ
in	inches
k	rate constant
K_d	sorption coefficient

k_{direct}	photodegradation rate constant of direct photolysis
L	liters
LC/MS/MS	liquid chromatography with tandem mass spectrometry
LGW	laboratory grade water
LOD	limit of detection
LOQ	limit of quantitation
LVX	levofloxacin
m	meters
M	molarity (moles/L)
MCX	mixed mode exchange
MgCl ₂	magnesium chloride
MGD	million gallons per day
MS	mass spectrometry
mW	milliwatts
m/z	mass to charge ratio
N	nitrogen atom
na	not applicable
nd	not detected
NC Ag	North Carolina agriculture
ng	nanograms
NH ₄ ⁺	ammonium ion
nm	nanometers
NO ₃ ⁻	nitrate ion
NOM	natural organic matter
¹ O ₂	singlet oxygen

O ₂ ^{*-}	superoxide
O ₃	ozone
OC	organic content
OWASA	Orange Water and Sewer Authority
ppt	parts per trillion
pB-10	IncP-1β antibiotic resistance plasmid
PDA	photodiode array
q _e	concentration of analyte sorbed to solid phase
RR	relative response
RSD	relative standard deviation
s	seconds
SAX	strong anion exchange
SMX	sulfamethoxazole
SPE	solid phase extraction
Stdev	standard deviation
TCC	tetracycline
TMP	trimethoprim
TOC	total organic carbon
UHP	ultra high purity
USDA	United States Department of Agriculture
USGS	United States Geological Survey
UV	ultraviolet
v/v	volume to volume ratio
VIS	visible
WWTP	wastewater treatment plant

ϵ	absorption coefficient or molar absorptivity constant
λ	wavelength
ν	frequency
Φ	quantum yield

CHAPTER 1

BACKGROUND AND LITERATURE REVIEW

1.1 Introduction

Human and veterinary antibiotics are important pharmaceuticals for the treatment of bacterial infections. Antibiotics are used in livestock as a preventive measure (“preemptive strike”) and as a growth measure (Hirsch, Ternes *et al.*, 1999). Total production in Germany of antibiotics in 1994 was 1831 tons (Hirsch, Ternes *et al.*, 1999). In Switzerland, during 1997, human consumption of antibiotics exceeded 30 tons per annum; sulfonamides accounting for 20% and fluoroquinolones 13% (Gobel, Thomsen *et al.*, 2005 a). A total of 10,000 tons were produced in the European Union in 1997, of which half was used for veterinary purposes and the other half for human medicinal purposes (Kummerer, 2001). In comparison, Levy (1998) noted that 23,000 tons were produced in the United States, over 40% of which was used in animals. Of that, more than 80% was used at subtherapeutic levels for growth promotion as opposed to therapeutic reasons (Levy, 1998).

Antibiotics reach the environment through several different pathways, primarily stemming from human and animal excretion. As much as 20-90% of the prescribed antibiotic passes through the human body unmetabolized, entering wastewater treatment plants (WWTPs) and are found in surface waters into which the WWTP effluents are discharged (Lindsey, Meyer *et al.*, 2001; Golet, Xifra *et al.*, 2003; Yang and Carlson, 2003; Kolpin, Skopec *et al.*, 2004; Lindberg, Wennberg *et al.*, 2005). Manure containing antibiotics may be applied to agricultural fields for fertilization leading to either runoff or groundwater exposure from leaching through the soil (Yang and Carlson, 2003) and since these chemicals can be environmentally stable, they can persist for a long time in soils, sediments, and water.

Determining the fate of antibiotics is imperative to aid in discovering what the impacts

of persistent low levels of antibiotics in environmental waters and sediments have on both public health and the environment. Other public health concerns include the development of antibiotic resistance in bacteria and its occurrence outside the clinical environment.

Of particular interest to this research was exploring the effects of natural photolysis and absorption of antibiotics to sediments as they move downstream of WWTP discharges. Antibiotics are normally prescribed for oral consumption and are generally resistant to hydrolysis (Kummerer, 2001). Many antibiotics are photolabile and phototoxic in humans (Drexel, Olack *et al.*, 1990; Spratt, Schultz *et al.*, 1999). In the natural environment, they may be susceptible to direct and indirect photolysis (Lunestad, Samuelsen *et al.*, 1995; Andreozzi, Raffaele *et al.*, 2003; Doll and Frimmel, 2003; Latch, Stender *et al.*, 2003; Boreen, Arnold *et al.*, 2004; Lam and Mabury, 2005). There are many photosensitizers present in streams, such as nitrates and humic materials that generate oxidation species, such as hydroxyl radicals and singlet oxygen under solar radiation. The products generated from photolysis may retain antimicrobial activity and be toxic to aquatic organisms (Hayashi, Nakata *et al.*, 2004). Sorption of antibiotics to soils and sediments could reduce their concentration in the water column, thereby decreasing the amounts freely available to photodegradation and possibly biodegradation (Hirsch, Ternes *et al.*, 1999). However, such partitioning may also act as a reservoir for selective pressure on microorganisms that could transfer resistance to pathogens (Kummerer, 2004).

1.2 Target Antibiotics

Tetracyclines, fluoroquinolones, sulfonamides, and trimethoprim are classes of synthetic antibiotics used extensively in human and veterinary medicine (Lorian, 1996; Kummerer, 2001; Thiele-Bruhn, 2003). Chemically relevant information is provided for common antibiotic classes in Table 1.1. The chemicals chosen for this study are among the top 200 prescribed drugs in the US: tetracycline, sulfamethoxazole (sulfonamide), trimethoprim, ciprofloxacin and levofloxacin (fluoroquinolones). Refer to Tables 1.2a and 1.2b for chemical structures of the target antibiotics.

Tetracyclines are broad spectrum antibiotics used for the treatment of a variety of infections, including typhus fever, upper respiratory infections, pneumonia, conjunctivitis,

gonorrhea, amoebic and urinary tract infections. They are commonly applied in agriculture and aquaculture for growth promotion and disease treatment (Witte, 1998; Chelossi, Vezzulli *et al.*, 2003; Le, Munekage *et al.*, 2005). Tetracycline is produced naturally by the streptomyces bacterium, a Gram positive actinobacteria found commonly in soil and decaying organic matter (Madigan, Martinko *et al.*, 2002).

Sulfonamides are synthetic compounds commonly applied in treatment for respiratory tract, urinary tract and enteric infections. Sulfamethoxazole and trimethoprim are commonly prescribed together (Renew and Huang, 2004). The ratio is generally fixed at 1:5 TMP:SMX (co-trimoxazole) to produce a bactericidal effect comparable to the bacteriostatic effect of the single components (Gobel, Thomsen *et al.*, 2005a). Sulfamethoxazole has been shown to be resistant to biodegradation (Al-Ahmad, Daschner *et al.*, 1999).

Fluoroquinolones are another common class of synthetic broad spectrum antibiotics used for multiple infections. Considerable amounts are utilized in animal husbandry, particularly with chickens, cows and pigs (Burhenne, Ludwig *et al.*, 1999). Quinolones are chemotherapeutic gyrase inhibiting chemicals that are particularly effective against enteric Gram-negative bacilli and to a lesser extent, nonenteric Gram negative bacilli, staphylococci and streptococci. Quinolone carboxylic acids are last resort pharmaceuticals against persistent infections (Hooper and Wolfson, 1993). Resistant to both biodegradation and hydrolysis, ciprofloxacin and levofloxacin can persist in the environment (Thiele-Bruhn, 2003; Turiel, Bordin *et al.*, 2005). Quinolones have been measured in hospital waste ranging from 3 to 87 µg/L (Hartmann, Alder *et al.*, 1998).

A significant portion of the antibiotic dosage passes through the body unmetabolized and thus enters into sewage treatment plants intact (See Table 1.3). Hydroxylation, cleavage and glucuronation are typical metabolic processes; however, it is possible that certain byproducts could be converted back into the parent compound (Lorian, 1996; Gobel, Thomsen *et al.*, 2005a).

Table 1.1: Chemical information regarding commonly used classes of antibiotics (Thiele-Bruhn, 2003).

Antibiotic Class	MW (g/mol)	Water solubility (mg/L)	Log Kow	pKa	Henry's Law Constant (pa L/mol)
Tetracyclines	444.5-527.6	230- 52000	-1.3- 0.05	3.3/ 7.7/ 9.3	1.7×10^{-23} - 4.8×10^{-22}
Sulfonamides	172.2-300.0	7.5- 1500	-8.1- 0.05	2-3/ 4.5- 10	1.3×10^{-12} - 1.8×10^{-8}
Fluoroquinolones	229.5-417.6	3.2- 17790	-1.0- -1.6	5.4-5.5/ 7.1 - 7.7	5.2×10^{-17} - 3.2×10^{-8}
Macrolides	687.9-916.1	0.45- 15	1.6- 3.1	7.7- 8.9	7.8×10^{-36} - 2.0×10^{-26}
Imidazoles	171.5-315.3	6.3- 407	-0.02- 3.9	2.4	2.3×10^{-13} - 2.7×10^{-10}
β -lactams	334.0-470.3	22- 10100	0.9- 2.9	2.7	2.5×10^{-19} - 1.2×10^{-12}

Table 1.2a: Structure and some physical properties of target antibiotics.

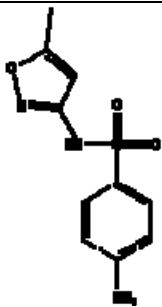
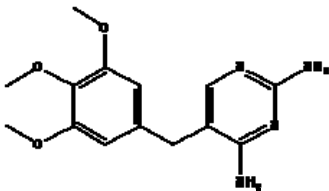
	Sulfamethoxazole (SMX) $C_{10}H_{11}N_3O_3S$	Trimethoprim (TMP) $C_{14}H_{18}N_4O_3$
Chemical Structure		
Molecular Weight	253	290
pKa ₁	1.6	
pKa ₂	5.7	

Table 1.2b: Structures and some physical properties of target antibiotics.

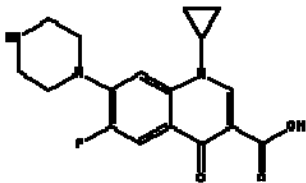
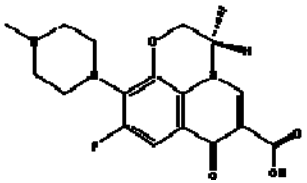
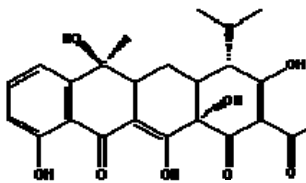
	Ciprofloxacin (CPX) $C_{17}H_{18}FN_3O_3$	Levofloxacin (LVX) $C_{18}H_{20}FN_3O_4$	Tetracycline (TCC) $C_{22}H_{24}N_2O_8$
Chemical Structure			
Molecular Weight	331	361	444
pKa ₁	5.5	5.4	2.7
pKa ₂	7.7	7.1	8.7

Table 1.3: Daily prescribed human dose and metabolism of the target antibiotics (Lorian, 1996).

Antibiotic	Daily Dose (mg)	% Excretion Unchanged
Sulfamethoxazole	2000	20-40
Trimethoprim	160	25-60
Ciprofloxacin	200	25-50
Levofloxacin	100	-
Tetracycline	500	80-90

1.3 Environmental Occurrence Data of Antibiotics

1.3.1 Wastewater Treatment Plants

A large variety of pharmaceuticals are found in WWTP effluent. Although the removal rates of antibiotics through the treatment process generally range from 60-90%, concentrations have been detected as high as 5µg/L in the final effluent (Ternes, Bonerz *et al.*, 2005). The release of low microgram per liter levels indicates that WWTPs are important point sources in surface waters. Gobel, Thomsen *et al.* (2005b) found that removal of sulfamethoxazole occurred mainly during activated sludge secondary treatment (55%). Trimethoprim was not significantly removed until sand filtration (tertiary). Based on the mass transfer throughout the treatment process, results also indicated the possibility that N⁴-acetylsulfamethoxazole (a human metabolite) retransformed to sulfamethoxazole in the activated sludge (Gobel, Thomsen *et al.*, 2005a). Spiking N⁴-acetylsulfamethoxazole into activated sludge resulted in an increase of sulfamethoxazole concentration with the simultaneous loss of the metabolite. No change occurred when the metabolite was spiked into silica sand only. Fluoroquinolones were more efficiently removed by activated sludge; 88-92% based on mass balance (Golet, Xifra *et al.*, 2003; Xia, Bhandari *et al.*, 2005).

1.3.2 Streams

Antibiotics have been detected in streams across the European Union and the United States. The United States Geological Survey (USGS) measured the concentration of 95 different organic wastewater contaminants, among them 23 antibiotics, in 139 different streams across the United States between 1999 and 2000 (Kolpin, Furlong *et al.*, 2002). The stream sampling sites were selected based on close proximity to urban, industrial, and agricultural waste point sources and represented a wide range of geography, land use, climate, and basin size. Levels were less than 1µg/L and were detected in approximately 50% of the samples. Sulfamethoxazole was found at maximum concentrations of 500 ng/L, trimethoprim at 700 ng/L, and ciprofloxacin 30 ng/L. Tetracycline was only detected in one stream at a concentration of 110 ng/L.

A similar study by the USGS in 2001 collected 76 aqueous samples upstream and

downstream of urban centers in Iowa (Kolpin, Skopec *et al.*, 2004). Sulfamethoxazole, trimethoprim, tetracycline, and ciprofloxacin were only detected in samples collected at low flow at levels of 70 ng/L, 80 ng/L, 300 ng/L, and 30 ng/L respectively. Sulfamethoxazole was detected the most frequently of all monitored antibiotics in both studies.

A study in the mountains of Colorado evaluated the effect of point (municipal plants) and nonpoint (contaminant runoff) sources of tetracyclines and sulfonamides discharge into the Cache la Poudre river (Yang and Carlson, 2003). Tetracycline concentrations fluctuated from sample site to site (50-320 ng/L), increasing after impacts from both agricultural and wastewater treatment plant sources. While sulfonamides are also used in animal husbandry, they were only detected downstream of municipal WWTP discharge at 120-160 ng/L levels.

1.4 Photochemistry

Light is characterized as having both wave and particle properties and is considered to be a combination of oscillating electric and magnetic fields that generates energy which is emitted, transmitted, and absorbed in discrete units (photons/quanta) according to equation 1.1.

$$E = h\nu = (hc)/\lambda \quad (1.1)$$

E = energy (J)

h = Planck's constant (6.63×10^{-34} J·s)

c = speed of light in a vacuum (3.0×10^8 m/s)

ν = frequency (hz)

λ = wavelength (nm)

The unit for one mole of light is called an einstein; 1 einstein = 6.02×10^{23} photons/mol.

The first law of photochemistry, otherwise known as the Grotthus-Draper law, states that a chemical must absorb radiation for a photochemical change to occur within its structure (Liefer, 1988). The absorption coefficient, also known as molar absorptivity constant (ϵ), is a measure of a molecule's ability to absorb a photon of a specific wavelength, as described in equation 1.2.

$$\text{Abs} = (I/I_0) = b\epsilon[C] \quad (1.2)$$

I = intensity of light transmitted

I_0 = incident intensity

b = pathlength (cm)

ϵ = absorption coefficient ($\text{L mol}^{-1} \text{cm}^{-1}$)

$[C]$ = concentration of absorbing species (mol/L)

Absorbance is measured using a spectrophotometer that contains a photometer cell of pathlength b (cm) and is a function of the incident wavelength due to the change in irradiance, which in turn, is a measure of the energy source. The rate of direct photolysis can be expressed as shown in equation 1.3.

$$-d[C]/dt = I_0 \Phi F_c (1 - e^{-bA}) \quad (1.3)$$

I_0 = incident intensity

Φ = quantum yield

A_λ = total absorbance of the system

F_c = fraction of total absorption due to concentration

Total absorption is equal to the sum of the absorbance coefficients of a species multiplied by the concentration for all absorbing species as described in equation 1.4.

$$A_\lambda = \sum \epsilon_n [C_n] = (\epsilon_1 [C_1] + \epsilon_2 [C_2] \dots \epsilon_n [C_n]) \quad (1.4)$$

Fraction absorbed by C_1 is

$$F_{1\lambda} = (\epsilon_1 [C_1]) / A_\lambda \quad (1.5)$$

In a system with only one photoactive species the equation reduces to

$$-d[C]/dt = I_0 \Phi (1 - e^{-b\epsilon[C]}) \quad (1.6)$$

When the absorption of the system is high ($Abs > 2$)

$$-d[C]/dt = I_0 \Phi \quad (1.7)$$

When the absorption of the system is low ($Abs < 0.1$)

$$-d[C]/dt = I_0 \Phi b \epsilon [C] \quad (1.8)$$

The intensity and pathlength of a system are determined by varying the concentration if the absorption coefficient and quantum yield are known. Once the intensity and pathlength are known, the quantum yield of an unknown compound can be calculated according to equation 1.9.

$$\Phi = (-d[C]/dt) / I_0 \quad (1.9)$$

Effective pathlength and quantum yields are usually determined with monochromatic sources due to the complexity of multi-wavelength photolysis. Quantum yields can be wavelength dependent (Liefer, 1988). Chemical actinometers and radiometers are used to estimate total intensity of light in a given system. The intensity at each wavelength is constant and normalized to a total of 1. The fraction of light absorbed by each species varies with wavelength and changes as reactions progress.

The quantum yield expresses the fraction of excited molecules of a given compound that react by a particular physical or chemical pathway. When a molecule has been energized to an excited state by light absorption, there are multiple pathways of releasing that energy. Physical processes include heat transfer, luminescence, and photo-sensitization. Chemical processes include fragmentation, intramolecular rearrangement, isomerization, hydrogen abstraction, dimerization, and electron transfer (Murov, 1973; Liefer, 1988; Schwarzenbach, Geschwend, *et al.*, 1993; Larson and Weber, 1994).

Two forms of photodegradation occur in natural waters: direct and indirect photolysis. In direct photolysis, the target analyte absorbs the radiation that causes transformation as discussed previously. Indirect photolysis proceeds through reactive intermediates that absorb light. A chemical not subject to direct photolysis may be transformed indirectly instead. Intermediates include singlet oxygen, aqueous electrons and hydroxyl, carbonate, alkyl peroxide radicals (Schwarzenbach, Geschwend *et al.*, 1993). Nitrate and dissolved organic matter absorption of radiation can be the source of many transient photooxidants in environmental waters. Indirect photolysis also proceeds through photosensitization, the transfer of energy from a photolabile compound to an organic compound at ground state. The hydroxyl radical, a highly electrophilic and nonselective intermediate, is one of the most reactive photooxidant species (see Table 1.4). Typical reactions include hydrogen abstraction and double bond addition. Second order rate constants of the hydroxyl radical with xenobiotics often approach diffusion-limited values of 10^7 - $10^{10}\text{M}^{-1}\text{s}^{-1}$ (Buxton, Greenstock *et al.*, 1988). Due to the high reactivity of the photooxidants, environmental concentrations are at low levels. For example, levels of hydroxyl radical in surface waters have been reported at 10^{-14} to 10^{-18}M (Brezonik and Fulkerson-Brekken, 1998). The low concentrations could limit environmental significance, despite high reaction rate constants with organic contaminants (Schwarzenbach, Geschwend *et al.*, 1993).

The role of humics in the photodegradation of chemicals is complex. Humics have the ability to exert two opposite effects on degradation rate of organics in the aqueous environment (Stangroom, Macleod *et al.*, 1998). Their capability of absorbing a broad range of wavelengths can reduce the available energy, acting as an inner filter. However, by absorbing light, the humics are promoted to a higher energy state (triplet state) and can either generate other transient photooxidants or photosensitize the target analyte (Gao and Zepp, 1998). The net sum on the phototransformation rate of organic substances depends on the balance of the two possible processes.

Table 1.4: Environmentally relevant photooxidants (* denoting free radical) and standard one electron reaction potentials (E_H) (Schwarzenbach, Geschwend *et al.*, 1993).

Oxidant	Reaction in Water			E_H (V)
HO*	HO*	+ e-	= OH ⁻	1.9
O ₃	O ₃ *	+ e-	= O ₃ ⁻	1.0
¹ O ₂	¹ O ₂	+ e-	= O ₂ ^{*-}	0.83
HO ₂ */O ₂ ^{*-}	HO ₂ *	+ e-	= HO ₂ ⁻	0.75
³ O ₂	³ O ₂	+ e-	= O ₂ ^{*-}	-0.16
ArO*	ArO*	+ e-	= ArO ⁻	0.79
RO*	RO*	+ e-	= RO ⁻	1.2
ROO*	ROO*	+ e-	= ROO ⁻	0.77
CO ₃ ^{*-}	CO ₃ ^{*-}	+ e-	= CO ₃ ²⁻	1.6
NO ₃ *	NO ₃ *	+ e-	= NO ₃ ⁻	2.3

1.4.1 Actinometry

An actinometer is defined as a chemical system with a well studied quantum yield that undergoes a photoinduced reaction and from which the absorbed photon flux can be calculated based on the reaction rate. Photon flux is synonymous with photon irradiance, calculated in units of Einsteins per unit time per unit area. Chemical actinometers are best used in experiments involving complex irradiation geometry to measure the absolute radiation accurately. Limitations of chemical actinometry include interfering absorption of actinometer photoproducts, the optical density of the actinometer solution, temperature changes, and quantum yield wavelength dependence (specifically for polychromatic light sources) (Kuhn, Braslavsky *et al.*, 2004). Temperature variations may influence the actinometer results if the solution density or quantum yield are temperature dependent.

1.4.2 Light Sources

Environmental photochemistry is sunlight driven. A continuous input of sunlight energy (1.3 kW/m^2) reaches the earth's upper atmosphere, where 50% is reflected back into space. The UV spectral portion of light that reaches the earth's surface ranges from 290-400 nm. Shorter wavelengths are removed by atmospheric constituents, mainly ozone (Larson and Weber, 1994). Visible light ranges from 400-760 nm. A number of artificial light sources are used in laboratory experiments to simulate natural photolysis, such as mercury vapor lamps, deuterium lamps, and xenon arc lamps (Liefer, 1988).

Mercury vapor lamps are quartz tubes containing a few torr of argon gas and liquid mercury. As voltage is applied across the electrodes, the cathode emits electrons that excite the argon gas. The excited argon ionizes the mercury through collision. After a sufficient population of mercury ions is established, current flows through the lamp and mercury relaxes from its excited state, with photons emitted (Phillips, 1983). As the vapor pressure increases above 10^{-2} torr, the mercury atoms absorb photons emitted from other mercury atoms and release longer wavelengths. Low pressure mercury lamps primary wavelength emissions are 185 and 254 nm (Phillips, 1983). Medium pressure lamps (10^2 - 10^4 torr) require higher current (more power), produce a higher photon flux and more discrete wavelength emissions. However, medium pressure lamps operate at high temperatures (600-900°C) (Hatchard and Parker, 1956).

1.4.3 Photolysis of Antibiotics

Fluoroquinolones, sulfonamides, and tetracyclines are susceptible to direct and indirect photolysis depending on reaction conditions such as pH. Fluoroquinolones share a common photodegradation product (Figure 1.1). Ciprofloxacin undergoes phototransformation by means of dealkylation, defluorination, and hydroxylation (See Figure 1.2) (Turiel, Bordin *et al.*, 2005).

Quantum yields and photolytic rates of sulfamethoxazole have been thoroughly studied under laboratory conditions (see Table 1.5). The rate constant in this class of drugs depends significantly on the pH and heterocyclic moiety. Figure 1.3 provides detected degradation products for sulfamethoxazole in laboratory grade water (LGW) (Zhou and Moore, 1994; Boreen, Arnold *et al.*, 2004; Lam and Mabury, 2005). Laboratory studies of

tetracycline in aqueous and organic media reveal that direct photolysis yields lumitetracycline and dimethylamine at pH<7.5. At higher pHs, the formation of anhydrotetracycline is favored (Morrison, Olack *et al.*, 1991). Figure 1.4 illustrates the major reported tetracycline photoproducts.

Table 1.5: Direct rate constants for sulfamethoxazole in various buffered solutions measured under natural sunlight (Boreen, Arnold *et al.*, 2004).

pH	K_{direct} ($\times 10^{-5}$) (s^{-1})	Stdev Of k_{direct} ($\times 10^{-5}$) (s^{-1})	$\Sigma \epsilon_{295-340\text{nm}} L_{\lambda}$ ($\text{mE cm}^{-3} \text{M}^{-1} \text{d}^{-1} \text{nm}^{-1}$)	$k_{\text{direct calc}}$ ($\times 10^{-5}$) (s^{-1})	Φ	Stdev of Φ
2.6	5.1	0.9	0	<0.3	0	0
4.1	6	1				
5.3	5.1	0.8	7.8	6	0.5	0.09
6.9	1.3	0.3				
10.8	0.6	1	4.6	0.8	0.09	0.01

k_{direct} is the photodegradation rate constant of direct photolysis, $\Sigma \epsilon_{295-340\text{nm}} L_{\lambda}$ is the wavelength weight sunlight exposure, $k_{\text{direct calc}}$ is the calculated component direct photolysis rate constant based on ionic speciation, Φ is the calculated quantum yield.

Published results regarding the influence of humics on photolysis degradation rates vary based on the specific pharmaceutical. A study by Andreozzi, Raffaele *et al.* (2003) reported that in the presence of 5mg/L C (commercial humate sodium salt) and 10mg/L nitrate, the half life of sulfamethoxazole decreased. This finding indicated that sulfamethoxazole was susceptible to indirect photolysis. However, in surface water results, direct photolysis was determined to be the major pathway of sulfamethoxazole degradation (Boreen, Arnold *et al.*, 2004; Lam and Mabury, 2005). Direct photolysis of fluoroquinolones is also the major pathway for degradation and the addition of humic acid decreased the kinetic rate, acting as a filter instead of a sensitizer (Lam, Tantuco *et al.*, 2003; Turiel, Bordin *et al.*, 2005).

Photoproducts have been detected under natural conditions. Sulfanilic acid and sulfanilamide were detected in Lake Josephine and Lake Superior waters spiked with sulfonamides and exposed to natural sunlight (Boreen, Arnold *et al.*, 2004). Photo-decomposition of tetracycline spiked into fish pond water exposed to simulated sunlight produced lactone and hydroxyl carboxylic acid derivatives (Oka, Ikai *et al.*, 1989).

Sulfamethoxazole and trimethoprim have been reported to be stable in marine

environments. In a study where eight antibiotics were dissolved in sea water, submerged in a quartz sphere, held at a depth 1m below the sea surface and exposed to natural sunlight, oxytetracycline degraded and lost antibacterial activity in 21 days, while sulfamethoxazole and trimethoprim were stable and maintained their antimicrobial activity (Lunestad, Samuelsen *et al.*, 1995).

Figure 1.1: Major photodegradation product of fluoroquinolones in aqueous solutions (Burhenne, Ludwig *et al.*, 1999).

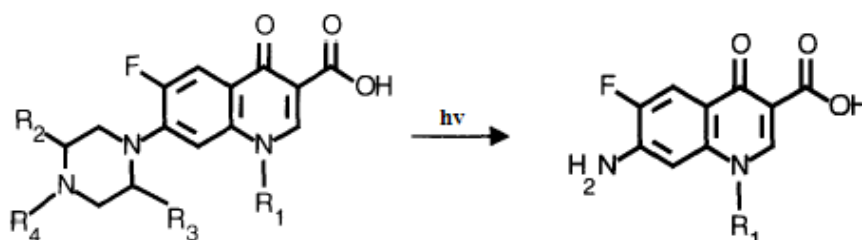


Figure 1.2: Photodegradation products of ciprofloxacin exposed to simulated sunlight (Turiel, Bordin *et al.*, 2005).

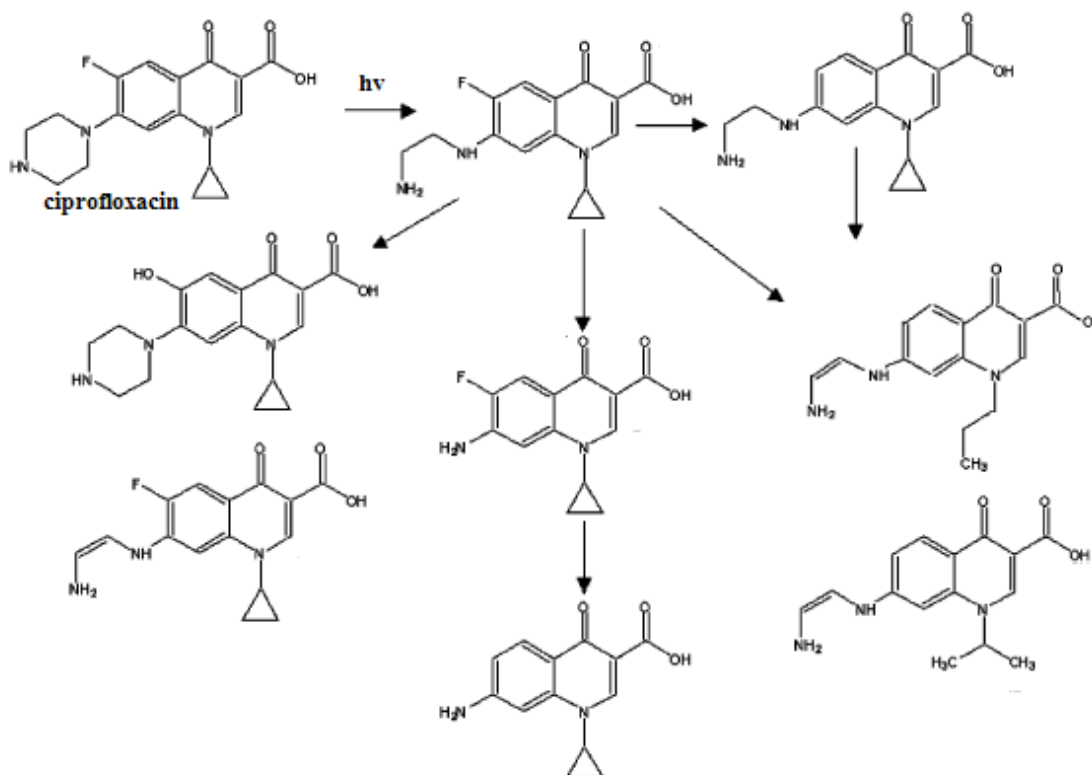


Figure 1.3: Combined photodegradation products of sulfamethoxazole in LGW and natural waters from both natural and simulated sunlight (Zhou and Moore, 1994; Boreen, Arnold *et al.*, 2004).

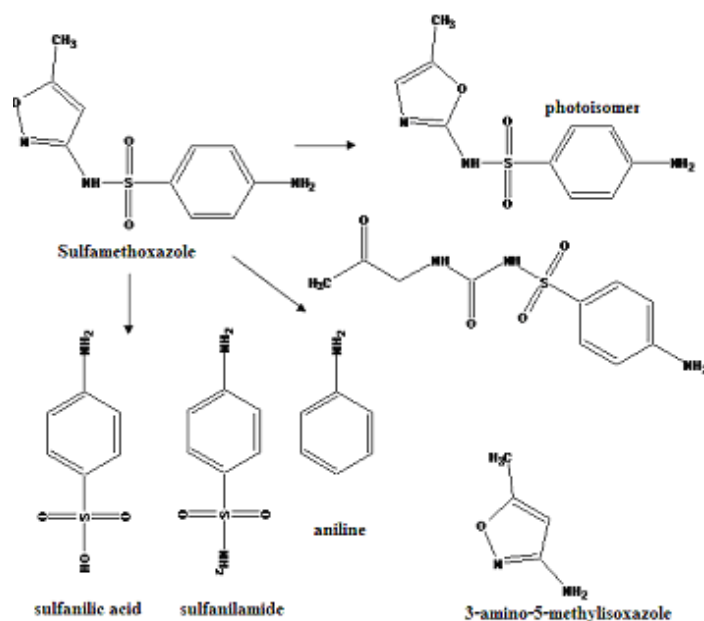
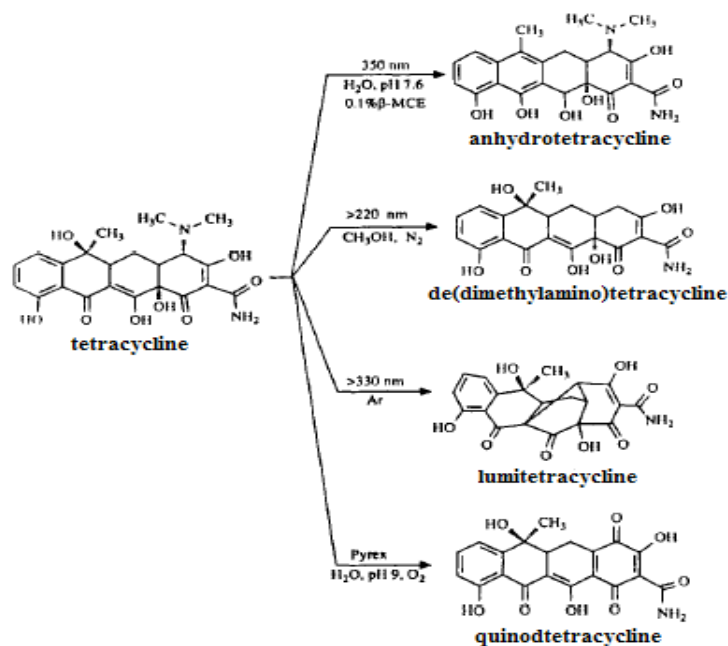


Figure 1.4: Photodegradation products of tetracycline in LGW under various conditions (Morrison, Olack *et al.*, 1991).



1.5 Sorption of Antibiotics

Antibiotics are mostly water soluble, polar compounds that ionize depending on the environmental pH. Clay minerals and humic substances are the primary soil components where absorption of xenobiotics occur (Schwarzenbach, Geschwend *et al.*, 1993).

Sorption mechanisms for polar chemicals include hydrophobic partitioning, cation exchange, bridging, surface complexing, or hydrogen bonding (Thiele-Bruhn, 2003).

Sorption is influenced by pH since many of the antibiotics have multiple ionic states.

Cation and zwitterion forms greatly affect sorption to clays.

Fluoroquinolones sorb readily to soils, sediments, and dissolved organic matter. From batch studies, 95-99% of the fluoroquinolones were removed from the aqueous phase by soil, soil clay fractions, and layer silicates. Desorption by 0.01M CaCl₂, used to extract loosely bound and exchangeable analytes from sediment and soil samples, was less than 2.6% (Nowara, Burhenne *et al.*, 1997).

Tetracycline detection in the aquatic environment is complicated by hydrolysis and binding to free ions and sediments (Figuerola, Leonard *et al.*, 2004). Substitutions on the basic tetracycline structure had little effect on the sorption of the tetracyclines to clays. Zwitterion sorption was more favorable on acidic clays. Calcium salts promoted tetracycline sorption on alkaline clays via surface bridging. Tetracyclines have been reported to be persistent in sediment and soils. Extraction of Pocomake river sediments (located in Maryland, USA) with 1M MgCl₂ (used to remove loosely bound and bioavailable compounds from soils) quantified 0.6-1.2 µg/g oven dry weight of oxytetracycline (Simon, 2005). Tetracycline concentrations as high as 4 mg/kg have been detected in sediments below fish farms (Thiele-Bruhn, 2003).

Results of the sulfamethoxazole isotherms indicated that sorption to soil organic matter was preferential, decreasing mobility in the aqueous phase. However, sorption was based on weak hydrogen bonding, indicating that sulfonamides would easily be susceptible to desorption processes. Sulfamethoxazole did not adsorb as readily to soils as other antibiotics, such as ciprofloxacin and tetracycline (Thiele-Bruhn, Seibicke *et al.*, 2004).

Literature reported values for the adsorption of the antibiotics to soil, sludge, and aquatic sediments are summarized in Table 1.6. The sorption coefficient can be calculated using the following equation:

$$K_d = q_e / C_e \quad (1.10)$$

K_d = sorption coefficient (L/kg)

q_e = concentration of analyte sorbed to solid phase (mol/kg)

C_e = equilibrium aqueous concentration of the analyte (mol/L)

Table 1.6: Sorption coefficients of antibiotics determined from batch sorption and isotherm experiments.

Antibiotic	Soil Sample Description	K_d (L/kg)	Reference
Tetracycline	Drummer, pH 7.5, 2.9% OC	3102	(Sassman and Lee, 2005)
	Raub, pH 6.0, 1.35% OC	287	(Sassman and Lee, 2005)
	Toronto, pH 4.2, 1.34% OC	104601	(Sassman and Lee, 2005)
	EPA-14, pH 3.8, OC 0.47%	312447	(Sassman and Lee, 2005)
	Eustis, pH 5.4, OC 0.47%	12.8	(Sassman and Lee, 2005)
	activated sludge	8400	(Kim, Eichhorn <i>et al.</i> , 2005)
Sulfamethoxazole	clay loam, pH 6.8, 0.37% OC	0.23	(Drillia, Stamatelatou <i>et al.</i> , 2005)
	silt loam, pH 4.3, 7.1% OC	37.8	(Drillia, Stamatelatou <i>et al.</i> , 2005)
	activated sludge	256	(Gobel, Thomsen <i>et al.</i> , 2005a)
Trimethoprim	activated sludge	208	(Gobel, Thomsen <i>et al.</i> , 2005a)
Ciprofloxacin	sludge, pH 6.5, 37% OC	417	(Thiele-Bruhn, 2003)
	sludge, pH 7.5-8.4	19952	(Golet, Xifra <i>et al.</i> , 2003)
	loamy sand, pH 5.0, 1% OC	398	(Golet, Xifra <i>et al.</i> , 2003)
	loamy sand, pH 5.3, 0.7% OC	427	(Nowara, Burhenne <i>et al.</i> , 1997)

1.6 Water Sediment Systems

Experiments have been designed to model the fate of xenobiotics in water/sediment systems. Löffler, Rombke *et al.* (2005) modeled water/sediment systems for pharmaceuticals based on a pesticide protocol from the Organization for Economic Co-operation and Development guideline 308. A series of 500 mL amber glass vials were filled with 200 g of sediment and 300 mL of creek water. Carbon dioxide traps with 30 g of granulated soda lime sealed the flask. The water/sediment flasks were equilibrated for seven days at 20°C prior to pharmaceutical spiking. Samples were taken immediately after spiking, and at 0.25, 1, 2, 7, 14, 28, 56, and 100 days later. The water, sediment and soda lime were collected for analysis at each sampling time. The reaction vessels were static and did not allow for incorporating other processes, such as photolysis. In comparison, Kalsch (1999) used glass aquaria (50 x 50 x 35 cm) filled with 3 cm of sediment and 80 L of water, spiked with X-ray contrast media (mg/L levels), and allowed incubation of the system for 209 days. The aquaria were exposed to sunlight 12 hrs/day and aqueous samples were taken at various intervals for high performance liquid chromatography (HPLC) analysis.

Other studies have created large scale reactors (microcosms) (Ronnefahrt, Traub-Eberhard *et al.*, 1997; Kalsch, 1999; Brain, Johnson *et al.*, 2004). Brain, Johnson *et al.* (2004) had access to a facility containing 30 outdoor artificial ponds; 1.2 m deep, 3.9 m diameter, holding approximately 12000 L of water. The bottoms of the ponds were covered with 45 plastic trays containing sediments. Ronnefahrt, Traub-Eberhard *et al.* (1997) designed a pond containing 800 L of water with a 15 cm sediment layer located inside a green house (20°C with lighting). Samples were regularly taken from the water and top layer of sediment.

Many studies utilize ¹⁴C-labeled standards to track the fate of the target compounds through the gaseous, aqueous and sediment phase (Brain, Johnson *et al.*, 2004; Löffler, Rombke *et al.*, 2005). The labeled surrogates allow differentiation between transformation, mineralization, and the formation of bound residues.

1.7 Current Analytical Methods

Methods for the detection of antibiotics in aqueous, soil, and biosolids matrices are numerous (Hirsch, Ternes *et al.*, 1998; Lindsey, Meyer *et al.*, 2001; Andreozzi, Raffaele *et al.*, 2003; Löffler and Ternes, 2003; Jacobsen, Halling-Sorensen *et al.*, 2004; Renew and Huang, 2004; Himmelsbach and Buchberger, 2005; Ye, 2005; Gobel, Thomsen *et al.*, 2005b). A majority of the methods analyze samples by liquid chromatography with tandem mass spectrometry (LC/MS/MS). Other methods incorporate ultraviolet (UV) or fluorescence detection. Detection limits in the aqueous phase are often less than 1 ng/L for LC/MS/MS analysis. Aqueous and solid extraction methods rely on pre-concentration techniques such as solid phase extraction (SPE). SPE resins that separate analytes based on hydrophobic as well as hydrophilic properties are most commonly used, such as HLB (hydrophilic lipophilic balance cartridges), MCX (mixed mode HLB-cation exchange cartridges), and Strata-X (brand equivalent to HLB) (Thiele-Bruhn, 2003).

Extraction of contaminants from solid phases (soils, biosolids, and sediments) has typically revolved around solvent extraction techniques such as sonication, mechanical shaking, microwave extraction, and accelerated/automated solvent extraction (ASE) (Jacobsen, Halling-Sorensen *et al.*, 2004). ASE has been found to be the most efficient tool for pharmaceutical extraction.

Multiple antibiotic structures comprise a nonpolar core with polar functional groups. Extraction with very polar and nonpolar solvents yields poor results (Holten Lutzhoft, Vaes *et al.*, 2000). Thiele-Bruhn (2003) recommended the use of weakly acidic buffers in combination with organic solvents. Calcium chloride solutions were not recommended to extract mobile, nonadsorbed fractions of antibiotics from the soil because tetracyclines form insoluble complexes with the calcium (Wessels, Ford *et al.*, 1998).

Limits of detection (LOD, S/N = 3) for soil extraction methods include 0.6-5.6 ng/g for oxytetracycline and 0.9-2.9 ng/g sulfadiazine (Jacobsen, Halling-Sorensen *et al.*, 2004). Limits of quantitation (LOQ, S/N = 10) have been reported as 3-41 ng/g for sulfonamides, macrolides and trimethoprim from sewage sludge water/methanol (1:1, v/v). LODs ranging from 40-80 ng/g and LOQs of 150-250 ng/g have been reported for quinolones and fluoroquinolones (Turiel, Martin-Esteban *et al.*, 2006). These methods either use ASE or microwave extraction. The advantages of ASE include minimal solvent usage, automation

which enables simultaneous extraction for a high number of samples, and high pressure and temperature, which enhances solubility and mass transfer of target analytes (Gobel, Thomsen *et al.*, 2005b). A simple and reliable method for multiple antibiotic class extraction was needed that did not require the use of either ASE or microwave-assisted extraction methods, which were unavailable.

1.8 Public Health Related Issues

Essential antibiotics are becoming less effective against bacterial infections. Overprescription, misuse, and improper dosing have created environments where selective pressure for resistance has occurred (Levy, 1998). Hospitals provide optimal conditions for resistance with the close proximity of pathogens and antibiotics. Indications of increased bacterial resistance in hospital and pharmaceutical plant waste have been reported (Guardabassi, Petersen *et al.*, 1998; Goni-Urriza, Capdepuy *et al.*, 2000). Confined animal feeding operations (CAFOs) provide continuous subtherapeutic exposure of antibiotics in livestock, 25-75% of which passes through the animal unmetabolized and can persist in the soil after land application of the manure (Chee-Sanford, Aminov *et al.*, 2001). These agricultural sources of antibiotics have been correlated with increased resistance and as sources of resistant genes (Witte, 1998; Chee-Sanford, Aminov *et al.*, 2001). Prominent examples of resistant strains include vancomycin-resistant enterococci, methicillin-resistant *Staphylococcus aureus* and multiresistant pseudomonads (Kummerer, 2004). Drug resistance infections increase a patient's risk of death.

There is concern regarding resistance propagation via mobile genetic elements, such as transposons and conjugated plasmids that transfer resistance genes to other bacteria (Ohlsen, Ternes *et al.*, 2003). Antibiotic resistance plasmids isolated from both clinical and environmental (including sewage) bacteria have shown that the plasmids serve as vectors for horizontal mobility of encoded genes (Kummerer, 2002). Schuller, Heuer *et al.* (2003) isolated the nucleotide sequence of the IncP-1 β antibiotic resistance plasmid (pB10) from wastewater treatment plants in Germany. The pB-10 gene load specifically mediates resistance against amoxicillin, streptomycin, sulfonamides and tetracyclines. The IncP-1 β appeared to undergo recombination in the environment, which could facilitate greater

bacterial adaptability (Schluter, Heuer *et al.*, 2003). Ohlsen, Ternes *et al.* (2004) reported that while plasmid transfer of *Staphylococcus aureus* occurred in a bioreactor containing dewatered sludge and liquid sewage, the low levels of antibiotics present were not sufficient to increase resistance plasmid transfers.

Aquaculture is a source of sufficiently high sediment concentration of antibiotics (Chelossi, Vezzulli *et al.*, 2003; Thiele-Bruhn, 2003; Le, Munekage *et al.*, 2005). Sulfamethoxazole and trimethoprim resistant *Bacillus* and *Vibrio* were isolated from Vietnamese shrimp farms (Le, Munekage *et al.*, 2005). *Bacillus* strains producing antimicrobial compounds were extracted in the Mediterranean not only from fish farm sediments, but from the surrounding areas as well. This finding indicated a widespread migration effect (Chelossi, Vezzulli *et al.*, 2003).

Toxicity is another concern. Accumulation of antibiotics in soils may significantly reduce soil bacteria populations by exerting temporary selective pressure on soil microorganisms (Thiele-Bruhn and Beck, 2005). On the other hand, it was estimated that there was low probability of toxic effects on aquatic life from the low ng/L levels of antibiotics in streams (Golet, Alder *et al.*, 2002). While acute toxicity associated with antibiotics is associated with mg/L levels, the effects of chronic low doses at environmental levels are unknown.

1.9 Research Overview

To understand the natural fate of antibiotics once they are released into streams from point sources, a reactor was created to simulate a controlled stream environment. This reactor, equipped with recirculating water and baffles to distribute the flow, was placed under lamps with ultraviolet-A, ultraviolet-B, and visible light output to simulate natural sunlight. Characterized soils and sediments were added to the reactor; target antibiotics were added into the aqueous phase, and rates of photolysis that were a function of varying water quality were measured. In addition, the fate of antibiotics released from a WWTP partially fed by hospital waste was studied after evolving quality assured analytical methodologies for the compounds in the aquatic and sediment columns.

CHAPTER 2

MATERIALS AND METHODS

2.1 Materials

All chemicals were obtained from commercial sources and were used without further purification. Acetonitrile (Optima), methanol (HPLC, GC Resolv), concentrated sulfuric acid, and ferric sulfate were purchased from Fisher Scientific (Pittsburgh, PA). Formic acid (99%), p-nitracetophenone (97%), 1,10-phenanthroline (99%), aniline (98%), and sulfanilic acid (99%) were purchased from Acros Organic (Morris Plains, NJ). Sulfamethoxazole (95-99%) and ciprofloxacin hydrochloride were purchased from MP Biomedicals (Aurora, Ohio). Levofloxacin (98%) and tetracycline hydrochloride (95%) were purchased from Fluka Biochemika (St. Louis, MO). Sulfanilamide was obtained from Kodak (Rochester, NY). Citric acid monohydrate was purchased from Sigma-Aldrich (St. Louis, MO). Potassium acetate, potassium oxalate (99%), isoamyl alcohol, pyridine (99.9%), dimethyldichlorosilane, toluene, methanol (ACS grade; for rinsing glassware), and disodium ethylenediamine tetraacetate (Na_2EDTA , ACS grade) were purchased from Mallinkrodt Chemicals (Paris, Kentucky). Simatone standard solutions (100 $\mu\text{g/mL}$ in methanol) were obtained from Accustandard (New Haven, CT). Solutions of $^{13}\text{C}_6$ -sulfamethoxazole (100 $\mu\text{g/mL}$ in acetonitrile), $^{13}\text{C}_3$ -ciprofloxacin (100 $\mu\text{g/mL}$ in methanol) and $^{13}\text{C}_6$ -sulfamethazine (88 $\mu\text{g/mL}$ in methanol) were obtained from Cambridge Isotope Laboratories (Andover, MA). Laboratory grade water (LGW) was obtained from a water purification system, leased from Pure Water Solutions (Hillsborough, NC), containing activated carbon resin, mixed bed ion exchange resins, and a 0.2 μm filter. The 18 Mohm water contained less than 0.2ppm total organic carbon.

For solid phase extraction (SPE), Oasis HLB cartridges (200 mg, 6 cc, hydrophilic lipophilic balance resin [copolymer poly(divinylbenzene)-co-N-vinylpyrrolidone]) were purchased from Waters Inc. (Milford, MA); Strata-X (200 mg, 6 cc, mixed bed resin, under

patent) and SAX cartridges (500 mg, 3cc, strong anion exchange, under patent) were purchased from Phenomenex (Torrence, CA).

2.2 Glassware Cleaning Procedure

Glassware was detergent washed, soaked in a 10% nitric acid bath, rinsed three times with chloraminated tap water, and three times with LGW, and then placed in a drying oven at 110°C. Volumetric glassware and polypropylene bottles (Nalgene, Rochester, NY) were rinsed with methanol and air dried at room temperature.

2.3 Autosampler Vial Deactivation

Analyte loss to glassware by sorption from solvent was minimized by silanizing the gas chromatography vials (Lab Supply Distributors, Mt Laurel, NJ) with 5% dimethyldichlorsilane in toluene for 24 hrs before thoroughly rinsing with toluene and methanol to remove residual silanizing agent, then rinsing with LGW and drying with methanol before use.

2.4 Standards

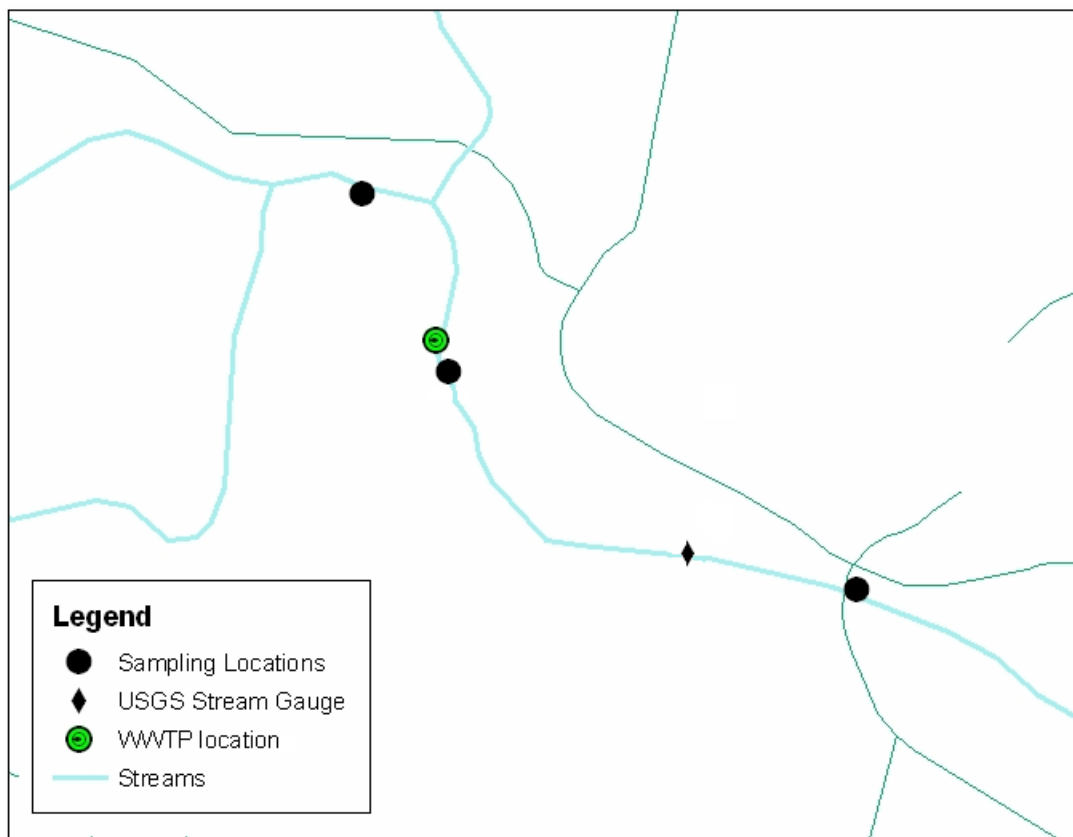
Stock solutions were prepared from the neat standards in either methanol (HPLC or GC Resolv grade) or acidic methanol (0.1% formic acid in methanol (HPLC or GC Resolv grade) at 500-2000 mg/L concentrations and stored at 4°C for up to 3 months. Working solutions were prepared fresh each time as needed.

2.5 Sampling Site

A wastewater plant (WWTP) was chosen that serviced a large town (population 50,000) that included a full service hospital, university, and multiple residential nursing homes. The full treatment process at the plant included preliminary screening, primary and secondary sedimentation, activated sludge, nutrient removal, and chlorination. The plant has a maximum daily flow of 12 million gallons per day (MGD), but typical releases ranged from 8-9 MGD. The average chlorine dose was approximately 3 mg/L. As of January 2006, the plant replaced the chlorination process with UV treatment (low pressure

mercury lamps). Other self reported parameters were as follows: typical ammonia release values were in the range of 0.3-4 mg/L $\text{NH}_4^+\text{-N}$; phosphorus 0.4-0.6mg/L; and total suspended solids 7-30 mg/L. Three sampling sites chosen for this study were collected upstream of the WWTP discharge, at the point of effluent discharge, and downstream of discharge as shown in Figure 2.1. The figure is a global positioning system (gps) map illustrating sampling points in relation to the WWTP and United States Geological Survey (USGS) stream gauge 02097517. Sampling points were marked with a Garmin (Olathe, KS) eTrex Legend personal navigator (accuracy ranges from 4-40 ft). The upstream was located 343 m from the point of effluent discharge and was minimally affected by agricultural non-point sources. The downstream sampling site was located 725 m from the effluent discharge. Effluent was taken directly from the plant discharge. Sediment effluent samples were collected approximately 1m from the point of plant discharge with flow rates ranging from 1-4 MGD, but mostly unaffected by the upstream dilution. The plant effluent feeds into Morgan Creek, accounting for 70-90% of downstream flow depending on the seasonal conditions.

Figure 2.1: GPS marking the points in relation to the WWTP and United States Geological Survey (USGS) stream gauge 02097517.



2.6 Surface Water Extraction

The surface water extraction method was developed by Ye (2005) with only minor adjustments made as follows: The surface water extraction volume was changed from 250 mL to 230 mL because the target antibiotic concentrations were high enough to be detected even with an 8% sample volume loss; thus it was possible to add the sample water, antibiotic and surrogate spikes, the EDTA and formic acid solutions into a 250mL amber bottle without spilling; ^{13}C -labeled sulfamethoxazole and ciprofloxacin were used as surrogates; a 2% formic acid solution was used to acidify the samples; and LGW was used to rinse the bottles and sample lines before the cartridges were dried.

2.6.1 Sample Collection and Storage

The WTP effluent, plus the upstream and downstream Morgan Creek water were collected in acid washed 1 L and 4 L amber borosilicate glass bottles and stored at 4°C in the dark.

2.6.2 Sample Preparation

Aqueous samples were passed through a 0.7 µm glass fiber filter (Millipore, Billerica, MA), followed by a 0.45 µm nylon filter (Pall Corp, Ann Arbor, MI) to obtain at least 2 L of filtrate. The filtered water was divided into 230 mL portions and poured into 250 mL amber bottles. After the samples were bottled, each filtrate portion was spiked with a ¹³C-labeled surrogate (¹³C₆-sulfamethazine or a combination of both ¹³C₆-sulfamethoxazole and ¹³C₃-ciprofloxacin at concentrations of 88 ng/L). Samples designated for standard addition were then spiked with the target antibiotics. Na₂EDTA (2 mL of a 2.5 g/L stock solution) was added to the solution, then adjusted to pH 6 by the addition of a 2% formic acid solution. The mixture was then solid-phase extracted through either HLB or Strata-X cartridges connected to a 24-port vacuum manifold (Fisher, Pittsburg, PA). Prior to extraction, the HLB or Strata-X cartridges were conditioned with 6mL of methanol (HPLC grade), followed by 6 mL of LGW. Flow through the solid phase was maintained at 5 mL/min or less. After the entire sample volume of surface water passed through the cartridge but before drying out, the sample bottles were rinsed three times with 10 mL of LGW and these rinses added to the cartridge. The SPE columns were dried for 1hr under maximum vacuum (- 20" Hg), after which the analytes were then eluted from the resin with two 4 mL rinses of acidic methanol (0.1% formic acid in methanol (GC Resolv grade) into 13 mL conical glass test tubes. The extracts were blown down to approximately 20 µL under a gentle stream of UHP nitrogen (National Welders Supply Welders Co, Charlotte, NC) at 45°C using a Pierce Reacti-Vap Model 18780 (Rockford, IL). The 20 µL blow down volume was approximated by comparison with 13mL glass conical test tubes containing measured volumes of 10, 20, 30 and 40 µL of water using a 50 µL Digital Microdispenser. The extracts were reconstituted to 250 µL with 0.1% formic acid and spiked with 10 µL of a 1.25 mg/L simatone in methanol (Fisher,

HPLC grade) solution and mixed using a Thermolyne Maxi-Mix vortexer (Dubuque, IO) for 30 sec. The precise extract volumes were measured with a 500 μ L gas-tight Teflon luer-lock syringe (Hamilton, Reno, NV), then pushed through 0.45 μ m cellulose syringe filters (Lab Supply Distributors, Mt Laurel, NJ) into 250 μ L glass inserts placed inside 2mL amber autosampler vials. The vials were capped with polypropylene screw thread closures containing rubber/Teflon, polytetrafluoroethylene (PTFE) septa (Lab Supply Distributors, Mt Laurel, NJ), prior to storage at 4°C, until analysis. Maximum holding time was one week.

2.7 Sediment Extraction

The sediment extraction method was developed using a combination of methods (Jacobsen *et al.*, 2004;Ye 2005) with adjustments.

2.7.1 Sample Collection and Storage

Morgan Creek sediment was collected in acid-washed high density polypropylene bottles (Nalgene, Rochester, NY). Samples were brought back to the laboratory for immediate water removal and storage in the dark at 22°C, once dried. The wet sediments were transferred into a Büchner filter apparatus, containing an LGW prewetted 0.7 μ m glass fiber filter (Millipore, Billerica, MA), covered with aluminum foil (Harris Teeter, Mathews, NC) and allowed to dry under vacuum for 24 hrs.

2.7.2 Sample Preparation

The dry sediments were sieved through a 2 mm brass mesh (Forestry Supply Distributors, Raleigh, NC) and then divided into 40 mL amber vials in 10 g portions. Each vial was spiked with an isotopically labeled surrogate (150 μ L of 88 μ g/L $^{13}\text{C}_6$ -sulfamethazine

(1.3 ng/g soil) in HPLC grade methanol or a combination of both $^{13}\text{C}_6$ -sulfamethoxazole (250 μ L of a 200 μ g/L solution in HPLC grade methanol; 5 ng/g soil) and $^{13}\text{C}_3$ -ciprofloxacin (250 μ L of a 1 mg/L solution in HPLC grade methanol; 25 ng/g soil). Designated sediment portions were also spiked with the target antibiotics for

standard addition, concentrations ranging from 1 to 50 ng/g, and allowed to mix with soil by the addition of solvent. The sediments were extracted by adding 25 mL of 1:1 0.2 M citric acid buffer (pH 4.7): methanol (HPLC or GC Resolv) and shaken for 30 min with a Burrell wrist action shaker (Pittsburgh, PA). The sample vials were centrifuged at 2500 rpm for 12 min at 22°C on the Beckman Coulter Allegra 6 centrifuge (Palo Alto, CA). The supernatant was collected using a graduated glass pipet (typically 20-22mL recovered) and diluted to 250 mL with LGW in a 250 mL glass amber bottle in preparation for clean-up and concentration by solid phase extraction (a combination of SAX and Strata-X). The SPE columns were conditioned separately prior to sample addition. The SAX cartridge was first washed with 3 mL of methanol (HPLC grade), followed by a 3 mL wash of 20 mM citric acid buffer (pH = 4.7). The Strata-X cartridge was conditioned with 6 mL of methanol (HPLC grade) and then washed with 6 mL of LGW. After conditioning, the two cartridges were connected in series, with sample first passing through the SAX resin. The sample loading flow rate was maintained at 5 mL/min or less. Following the sample loading, the sample bottle and lines were rinsed three times with 10 mL of 20 mM citric acid buffer. The final cartridge rinse consisted of 0.1M potassium acetate (2 mL), and then the SAX column was removed from the system and discarded. The Strata-X columns were dried for 1 hr under maximum vacuum (- 20" Hg) prior to the analyte elution with two 4 mL aliquots of acidic methanol (0.1% formic acid in GC Resolv grade methanol), which were collected in 13 mL conical glass test tubes. The tubes were placed in a water bath at 45°C. Temperature was measured with a test tube containing water and a Fisher mercury thermometer. Extracts were blown down to approximately 20 µL under a stream of UHP nitrogen (National Welders Supply Welders Co, Charlotte, NC) in a Pierce Reacti-Vap Model 18780. The extracts were reconstituted to 250 µL with 0.1% formic acid using a 500 µL Teflon luer-lock syringe and spiked with 10 µL of a 1.25 mg/L simatone solution in methanol (Fisher, HPLC grade). Each sealed test tube was vortexed using a Thermolyne Maxi-Mix vortexer (Dubuque, IO) for 30 sec, after which the supernatant liquid was removed via a 500 µL Teflon luer-lock syringe (Hamilton, Reno, NV) and subsequently pushed through a 0.45 µm cellulose syringe filter (Lab Supply Distributors, Mt Laurel, NJ) into an amber autosampler vial fitted with 250 µL glass inserts. Samples were stored at 4°C until analysis with a maximum holding time of one week.

2.8 Photolysis

2.8.1 Artificial Light Sources

Three different lamps were used as artificial light sources. The first was a Heraeus Noblelight (Kleinostheim, GER) TQ 718Watt Z4 medium pressure mercury lamp. The main features of emission spectrum from this lamp were a continuum from 200 to 245 nm and a discrete line spectrum from 270 nm to 700 nm as shown in Figure 2.2. A Pyrex borosilicate pan was used as a filter to remove wavelength emissions less than 300 nm. The second lamp was a Good Earth Lighting (Wheeling, IL) 18 watt Growlight fluorescent plant lamp whose emission spectra is shown in Figure 2.3. The third lamp utilized was the Phillips (Atlanta, GA) T20W UVB. The main feature of this lamp was the continuous emission from 270 nm to 400 nm as shown in Figure 2.4. The change in intensity before and after filtration using a Pyrex borosilicate pan is listed in Table 2.1. The lamp spectra from 200 to 500 nm were measured using an Ocean Optic, Inc. (Dunedin, FL) 52000 fiber optic spectrometer. The lamp intensities were measured with an International Light (Peabody, MA) IL1400 radiometer.

Figure 2.2: Emission of the Noblelight 718 Z4 825W medium pressure mercury lamp before and after Pyrex filtration.

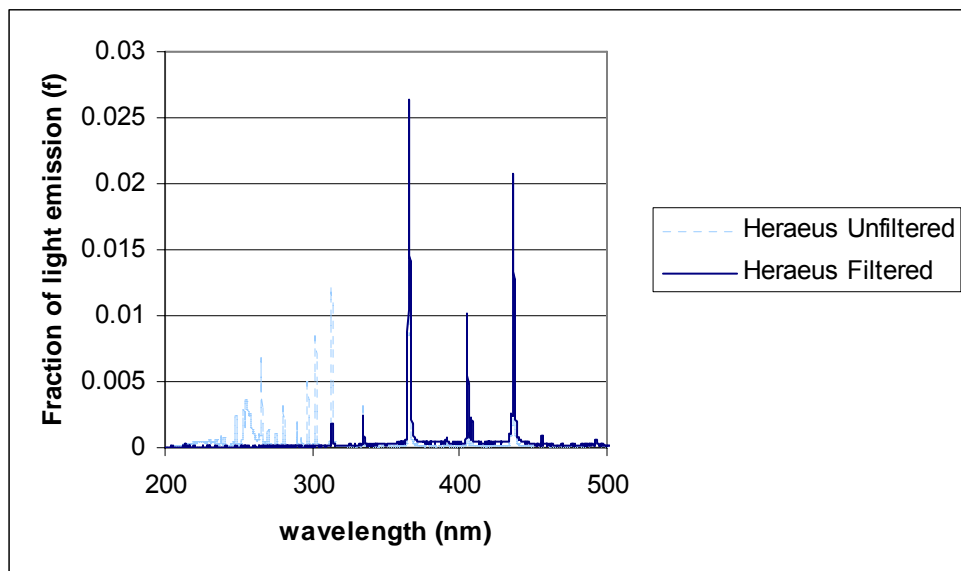


Figure 2.3: Emission of Good Earth Lighting Growlight 18W “high UV” plant lamp.

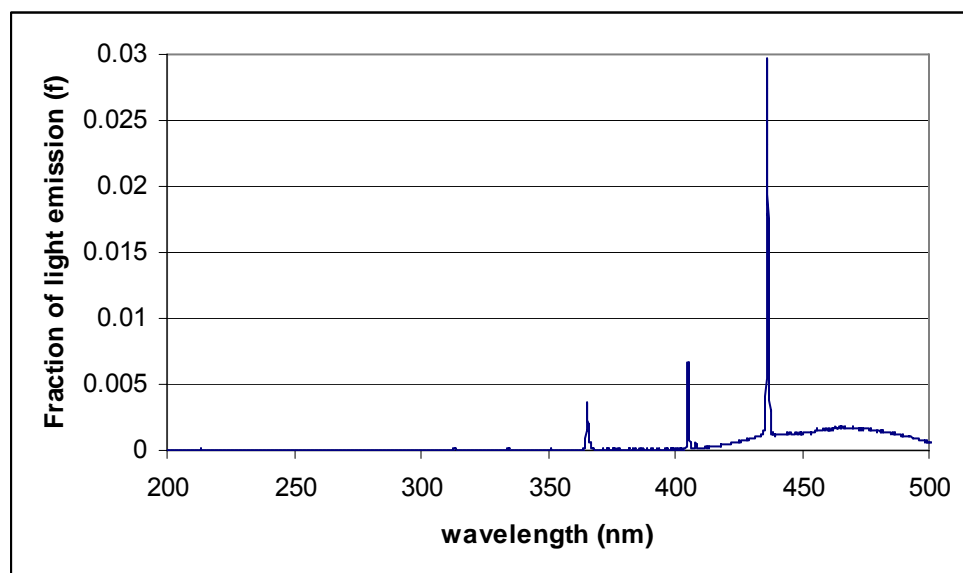


Figure 2.4: Emission of Phillips T20W UVB lamp before and after Pyrex filtration.

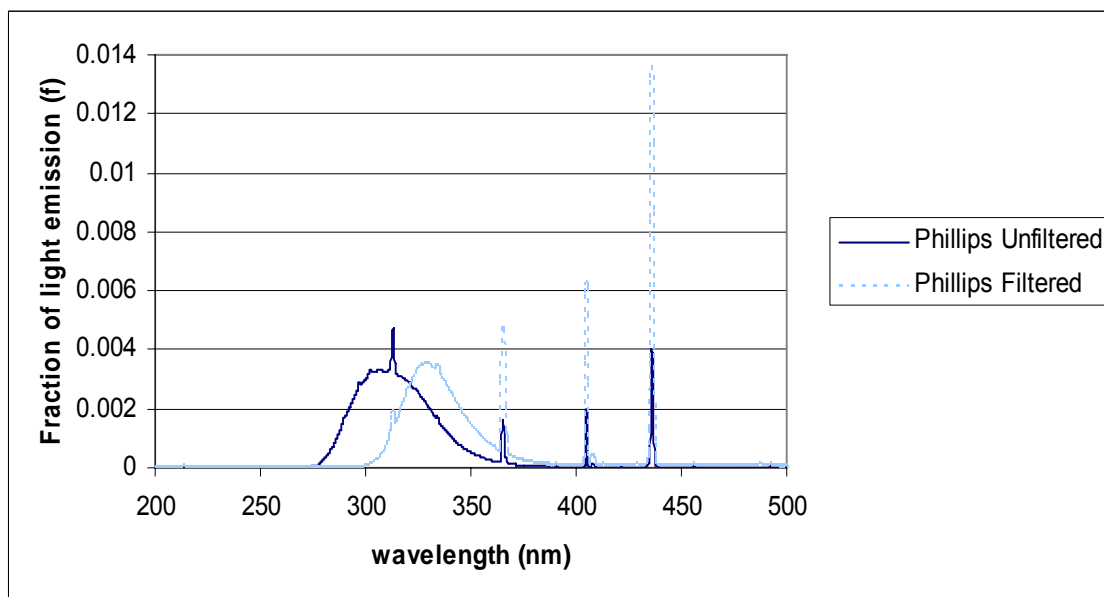


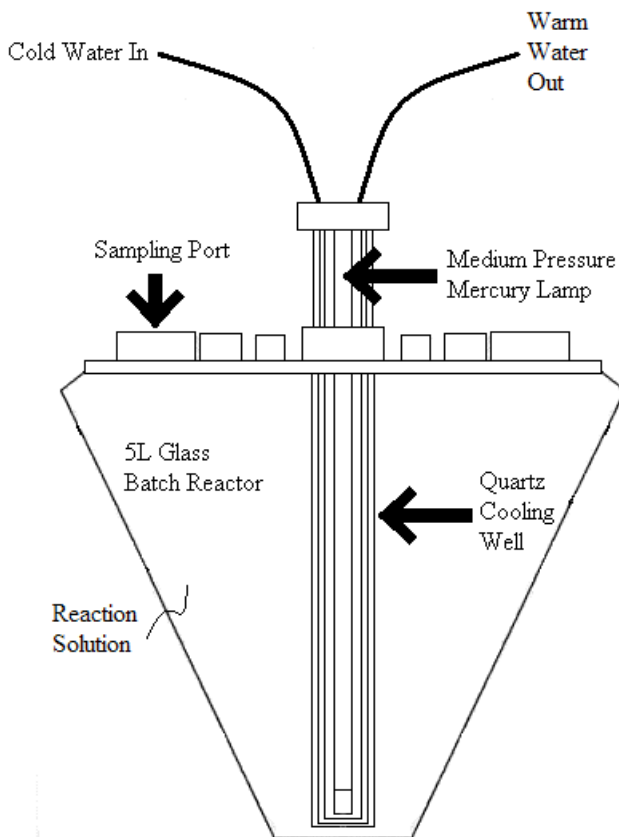
Table 2.1: Effects of the Pyrex filter on the Phillips T20W lamp intensity.

	Distance of radiometer from Lamp (in)	Intensity 200- 350nm (mW/cm ²)	Intensity 350- 1000nm (mW/cm ²)
no Pyrex filter	10.4	2.81E-02	8.5
	12.4	2.21E-02	7.7
with Pyrex filter	10.4	1.27E-03	6.0
	12.4	1.20E-03	5.8

2.8.2 Reactor Design Evolution

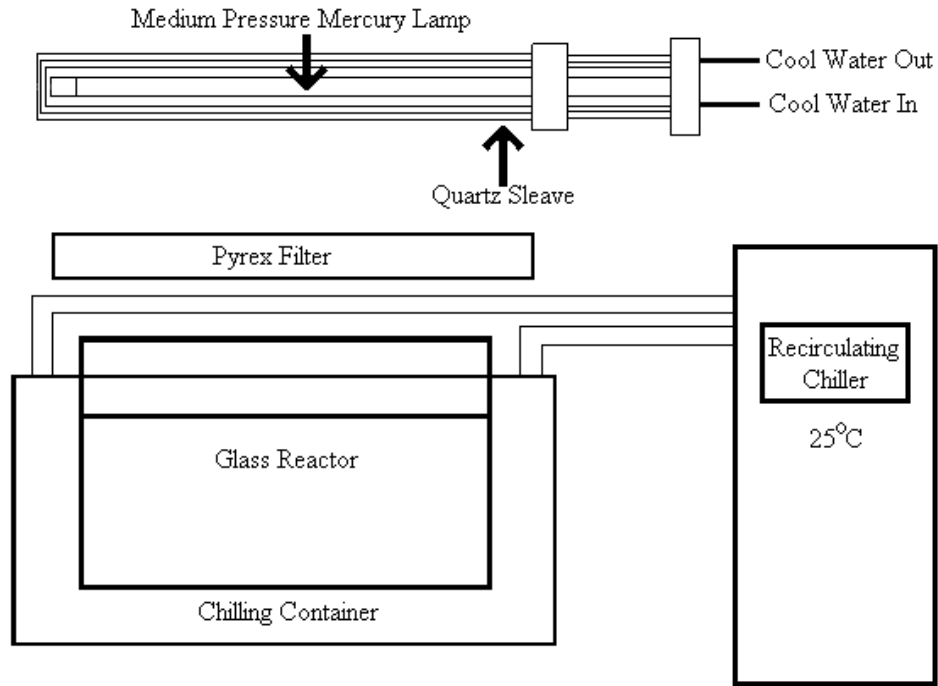
The early batch reactor (BR) experiments were carried out in a 5.5 L conical Pyrex photochemical reactor from Ace Glass (Vineland, NJ), covered with aluminum foil. The Heraeus medium pressure mercury lamp was placed inside the BR but prevented from reaching the solution by a water-cooled double walled quartz sleeve positioned in the center of the reactor (See Figure 2.5).

Figure 2.5: Batch reactor (BR) setup.



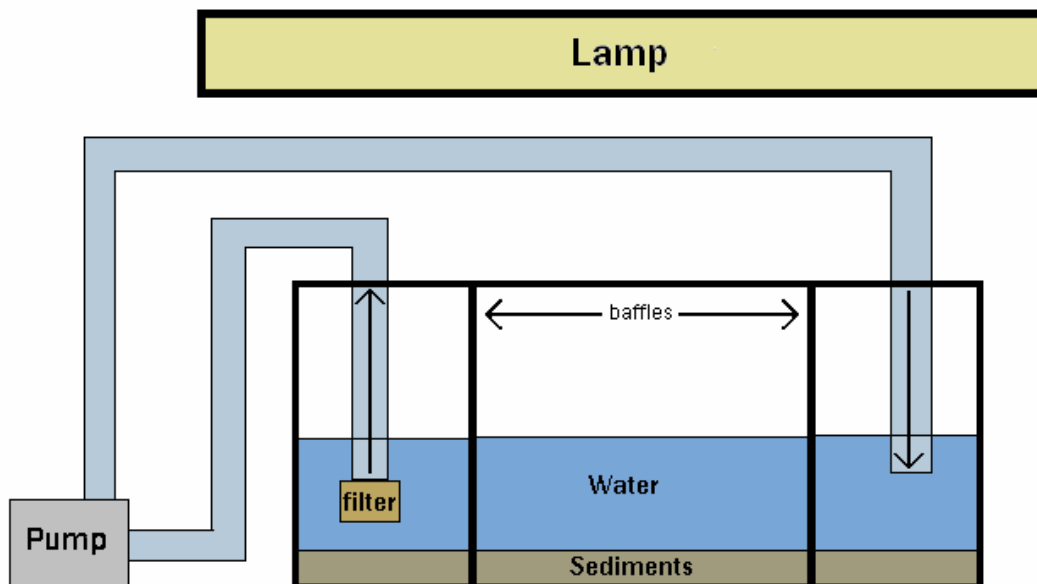
In the second phase of reactor design (refer to Figure 2.6), the Heraeus medium pressure lamp was located in the quartz cooling sleeve, positioned 4 in. above a Pyrex (borosilicate) baking pan, used to filter out wavelengths less than 290 nm, running parallel to the reactor length. The lamp was 17 in. above an open rectangular borosilicate glass reactor (11.6 in. x 8.63 in. x 9.13 in.), referred to as the fish tank (FT). The FT reactor was placed inside a small cooler through which flowing water was circulated by a Neslab NFT 33 recirculator/chiller (Waltham, MA) set at 21°C to provide a water bath. The sample volumes were 5 L. The surface of the water was 3.89 in. from the bottom of the FT and 24.7 in. from the lamp.

Figure 2.6: Second reactor design (FT).



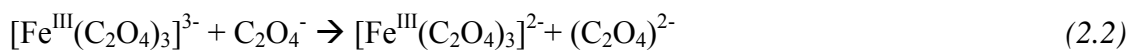
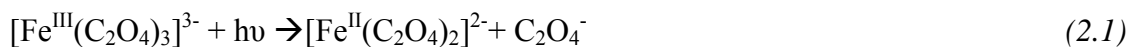
The final design was used in duplicate. One reactor was used as a dark control (CR) to run simultaneously with the exposure reactor (ER). Two borosilicate glass aquaria (12in x 6in x 8in) were designed to contain both aqueous and sediment samples. The water was recirculated throughout the reactors with the aid of Marineland (Mentor, OH) Maxi-jet 400 and 1200 pumps. Sponge filters (Aqua Clear, Mansfield, MA) were placed at the pump influent to protect the pump from natural debris that became waterborne from the sediments and soil added to reactors. Flow from the pumps ranged from 1-2 L/min. Both reactors were divided into three compartments by the placement of two baffles to distribute the flow (refer to Figure 2.7). The artificial light sources for the ER reactor were the Good Earth Lighting Growlight and the Phillips T20W UVB lamp.

Figure 2.7: Final reactor design.



2.8.3 Actinometry

The intensity of the Heraeus medium pressure mercury lamp in the BR and FT reactors was measured by chemical actinometry using a potassium ferrioxalate method as described by Murov (1973). Potassium ferrioxalate is a sensitive, high optical density actinometer in which the iron is photochemically reduced from ferric to ferrous form upon absorbing wavelengths less than 500 nm, as shown in equations 2.1 to 2.3. The net reaction is shown in equation 2.4. The concentration of ferrous iron is determined by complexation with 1,10-phenanthroline [Fe^{II} (phen)]. The resulting complex has an absorption maximum at 510 nm.



The reactors were filled with the pure actinometer solution only and run without the addition of any matrix components. The initial ferrioxalate solutions of approximately

0.006 M in 5 L batches were made from combining a 0.2 N solution of ferric sulfate with equal volumes of a 1.2 M potassium oxalate solution and diluting with LGW. Stored separately, the ferric sulfate and potassium oxalate solutions are stable for one month (Murov, 1973). From the BR and FT reactors, 1 mL samples were taken at specific times including at time zero (blank) and added to a 25 mL volumetric flask containing a buffer (0.5 mL of sodium acetate solution) and 1,10-phenanthroline (2 mL of 0.2% in water), which was then diluted to the mark with LGW. After stoppering and inverting three times, a 2 mL aliquot was placed in 1 cm quartz cuvette and the absorption at 510 nm was measured with the Hitachi (Mountain View, CA) U-330 spectrophotometer.

2.8.4 Final Reactor Procedure

The following procedure was used with the final reactor design. Both the CR and ER reactors were prepared in the same way. LGW (4.1 L) was first allowed to equilibrate with either Ottawa sand, Chapel Hill soil, Eastern North Carolina Agricultural soil or Morgan Creek sediment (200-300 g) in a 5 L Erlenmeyer flask for 48 hrs exposed to ambient room light. A 100 mL aliquot of this equilibrated unspiked water was taken for characterization (pH, UV-Vis spectrometry, total organic carbon (TOC)). The supernatant water was then removed into another 5 L Erlenmeyer flask containing no sediments and spiked with 1 mg/L of sulfamethoxazole and the solution was allowed to mix. An aqueous sample was taken from the Erlenmeyer prior to use in the reactor for comparison to water concentrations immediately after addition to the reactor. The wet sediment was distributed across the bottom of the reactor as evenly as possible in each compartment. The spiked water was then added to the reactor slowly down the side of the glass to avoid major disturbance of the sediment layer. Fisher brand Ertco mercury thermometers were placed in the corners of both the ER and CR reactors to monitor the water temperature. Aqueous samples (250 μ L aliquots) were collected from all three baffle compartments in each reactor with a 500 μ L syringe, immediately filtered through a 0.45 μ m cellulose syringe filter (Lab Supply Distributors, Mt. Laurel, NJ) and stored in 2 mL amber glass autosampler vials fitted with 250 μ L glass inserts at 4°C until analysis for loss of sulfamethoxazole and formation of byproducts. The ER reactor was exposed to the Phillips T20W UVB lamp and the CR reactor was kept in the dark. Aqueous samples were

taken at various time intervals from both the ER and CR reactor. Sampling times varied from hours to days. With the addition of the pyrex pan filter, sampling time was increased from days up to two weeks. Upon termination of the photolysis and dark control experiments, sediment samples were collected from both reactors and extracted as described in Section 2.7.

2.9 HPLC Analysis

Liquid chromatography was performed on either a Varian (Walnut Creek, CA) 1200L triple quadrupole MS/MS system with a ProStar 210 LC pump, a modular Waters II (Milford, MA) High Pressure Liquid Chromatography 515 pump with a 996 Photodiode Array (HPLC-PDA) and 717 Autosampler, or a Waters 7695 separations module combined HPLC pump-autosampler-vacuum degasser inline with a 996 PDA detector. Mobile phase A for each instrument was 0.1% formic acid (by volume in LGW) and mobile phase B was Optima Grade acetonitrile. Several elution methods were employed, depending on the target analytes. An isocratic method of 80% 0.1% formic acid: 20% acetonitrile was used for LGW samples containing only sulfamethoxazole. Gradients were used for antibiotic mixtures and environmental samples. For sulfadugs and related byproducts, the starting condition was 20% mobile phase B, linearly increasing to 80% in 16 min, held for 2 min, linearly decreasing back to 20% in 2 min, and equilibrated to the starting condition for 15 min. The program for this gradient (run 1) is shown in Table 2.2.

Table 2.2: Gradient Run 1 for HPLC analysis of sulfamethoxazole and related photodegradation byproducts.

Time (min)	%Mobile Phase A (0.1 Formic Acid)	%Mobile Phase B (Acetonitrile)
0	80	20
16	20	80
18	20	80
20	80	20
35	80	20

A second gradient was used for mixed antibiotic samples extracted from surface waters

and sediments. Solvent B, initially at 10%, linearly increased to 30% over 15 min. The rate increased to 25% B/min for 2 min and was held at 80% for 1 min. The % Solvent B returned to starting conditions (10%) in 2 min and the column was allowed to equilibrate for 15 min for a total run time of 35 min (relate to Table 2.3).

Table 2.3: Gradient Run 2 for HPLC analysis of antibiotic mixtures.

Time (min)	% Mobile Phase A (0.1 Formic Acid)	% Mobile Phase B (Acetonitrile)
0	90	10
15	70	30
17	20	80
18	20	80
20	90	10
35	90	10

2.9.1 LC/MS Analysis

A Phenomenex (Torrence, CA) Luna 3 μ C₁₈ column (150 cm x 2.00 mm, 3 μ m) combined with a Varian (Walnut Creek, CA) Metaguard 2.00 mm Pursuit 3u C₁₈ guard column was used to chromatographically separate target analytes for mass spectrometric analysis. Flow was set at 0.2 mL/min. Injection volumes of 20 or 50 μ L of sample, (depending on concentration) were delivered by a partially filled 100 μ L sample loop.

Antibiotics were ionized by electrospray ionization (ESI) in positive mode. Optimized parameters were determined by direct infusion of each analyte separately (prepared at 1 mg/L in LGW) directly into the mass spectrometer at 20 μ L/min using a Harvard Apparatus syringe pump (Holliston, MA) and the Varian MS Workstation (v. 6.40) software. Daughter ions and optimum collision voltages were determined by the MS Breakdown tool in the software during direct infusion (See Table 2.4). The ESI manifold conditions were set as follows: Needle position = (15, 4.5, 27)(x, y, y'); needle voltage = 5000 V; dry gas temp = 250 °C; dry gas pressure = 20 psi; nebulizing gas pressure = 50 psi; shield voltage = 60V. During MS/MS breakdown, the Argon collision gas (HP, National/Specialty Gases, Durham, NC) was set at 2.8 mTorr.

Table 2.4: Target analytes and the MS/MS breakdown information.

Analyte	Parent Ion (m/z)	Daughter Ion (m/z)	Optimum Collision Voltage (V)
simatone ¹	198	128	-18
Sulfamethoxazole	254	108,156	-20,-12
¹³ C ₆ -sulfamethoxazole	260	114,162	-20,-14
sulfathiazole ¹	256	108,156	-20,-14
sulfamerazine ¹	265	108,156	-22,-12
sulfamethizole ¹	271	108,156	-19,-12
sulfachlorpyridazine ¹	285	108,156	-23,-15
¹³ C ₆ -sulfamethazine ¹	285	186	-18
Sulfadimethoxine ¹	311	108,156	-24,-19
trimethoprim ¹	291	123, 230	-21, 23
Ciprofloxacin	332	245, 288	-23, -17
¹³ C ₃ -ciprofloxacin	336	248, 291	-22, -18
Levofloxacin	362	318, 344	-16, -20
tetracycline ¹	445	410, 427	-18, -12
Aniline	94	51, 77	-26, -16
Sulfanilamide	173	93	-18
sulfanilic acid	174	93	-16

¹Conditions optimized by Ye (2005).

2.9.2 HPLC-PDA Analysis

The HPLC column used for the Waters PDA instruments was a Supelco (St. Louis, MO) Discovery C₁₈ (28 cm x 4.6 mm, 5 µm) fitted with a C₁₈ guard column. Flow rate was set at 1mL/min. Injection volumes were 300 µL with the Waters series II system and 50 µL for the Waters 7695. The diode array was set to scan wavelengths 230-400 nm. For samples containing sulfamethoxazole, the 271 nm results were extracted from the chromatograms.

2.10 Soil Characterization

Soil texture, organic matter content, water holding capacity, soil particle density and soil pH were analyzed according to standard methods (Klute and Page, 1982). A Fisher

Isotemp Senior Model oven (Pittsburgh, PA) was used to dry the soils at 110°C. The procedures are listed in Appendix A. A Linberg Heavy-Duty muffle furnace (Williamsport, PA) was used for organic matter content. A VWR ASTM soil hydrometer (West Chester, PA) and Omega 2252 Thermostar temperature probe (Stanford, CT) were used for the soil texture characterization procedure. Whatman #1 12cm diameter paper filters (Bentford, UK) were used in the water holding capacity experiments.

2.11 pH

pH was measured with a Fisher Scientific (Pittsburgh, PA) Accumet pH meter model 10 using an Accumet silver/silver chloride gel filled polymer single junction pH combination electrode. The meter was calibrated with fresh pH 4.00, 7.00, and 10.00 buffers (Fisher, Pittsburgh, PA) and corrected for temperature.

2.12 Total Organic Carbon (TOC) Analysis

TOC analysis was performed with a Shimadzu (Columbia, MD) 5000 series combustion oxidation instrument. The standard operating procedure, based on Standard Method 54310B (Clescerl, Greenberg *et al.*, 1999), is presented in Appendix B.

2.13 UV-VIS Spectrometry

UV-VIS spectra were obtained with a Hitachi (Mountain View, CA) U-3300 spectrophotometer. Standards of target analytes were prepared at concentrations ranging from 10^{-4} to 10^{-6} M to determine the molar absorptivity constants. Samples were loaded into rectangular quartz cells with a path length of 1 cm.

CHAPTER 3

RESULTS AND DISCUSSION

3.1 Stability of the Antibiotics during Analysis

Standards of sulfamethoxazole (SMX) at 0.05 and 1 mg/L in LGW were stable for at least one month when held in glass amber vials in the dark. There was no apparent difference between holding temperatures of 4°C and 22°C, as shown in Figure 3.1. The cellulose filters also had little effect on the UV response for SMX in LGW response (Figure 3.2). In samples containing both dissolved and suspended organics, the stability of the SMX was increased by removing suspended organic matter using syringe filtering through 0.45 µm filters, as soon as possible, rather than waiting until the day of analysis (see effects in Figure 3.3). Humic water was created by allowing 200 g of Eastern NC agricultural soil (described in *Section 3.2*) and 1 L of LGW to equilibrate for two weeks in a 2 L Erlenmeyer flask at room temperature, exposed to ambient room light. At the end of two weeks, the water color had changed from clear to yellow generating a UV detector response in the 200-700 nm range that was elevated from compared to the original LGW.

Figure 3.1: Stability of SMX in LGW held at two temperatures (4°C and 22°C) over 27 days (analyzed with HPLC-PDA at 271 nm).

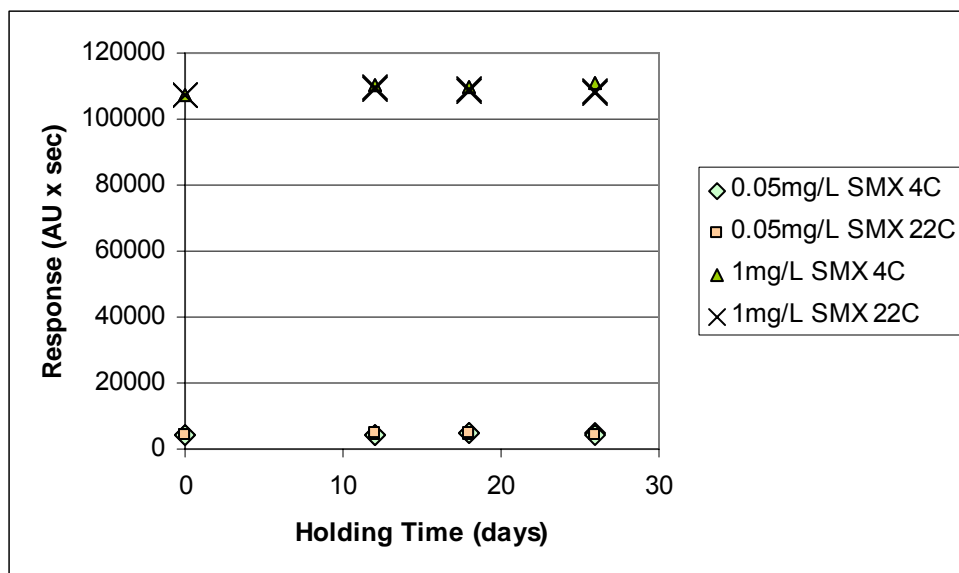


Figure 3.2: Comparison of filtered LGW containing 0.05 mg/L SMX with the unfiltered solution (analyzed with HPLC-PDA at 271 nm).

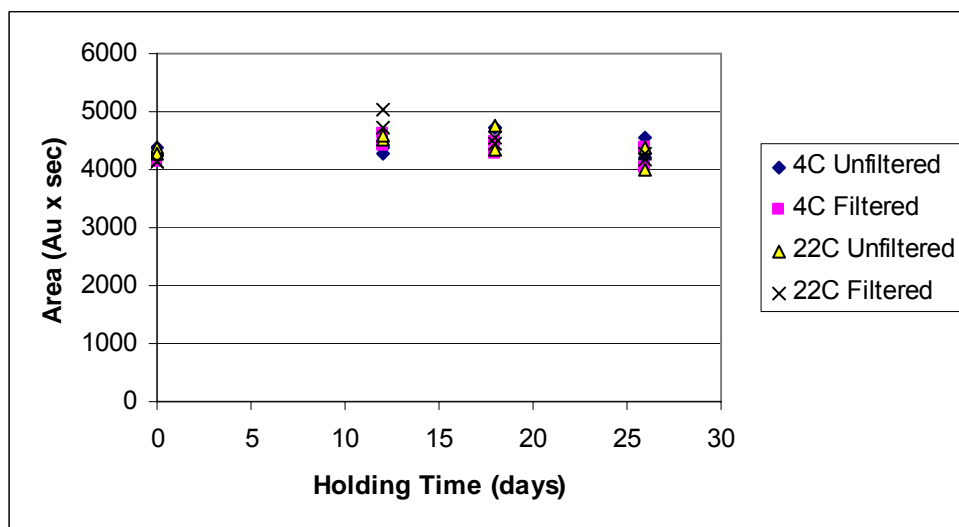
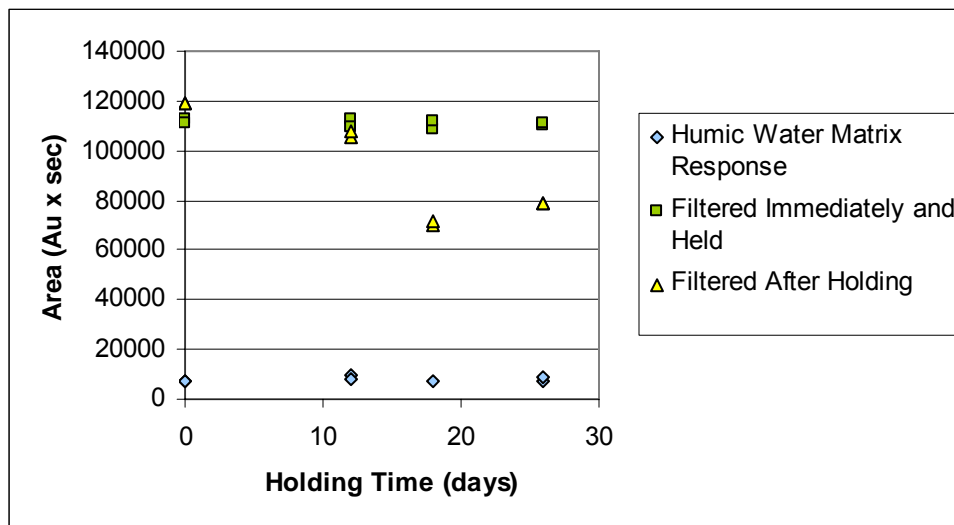


Figure 3.3: Effect of filtration of a humic water on the stability of SMX ($C_0=1\text{mg/L}$, temperature at 4°C) analyzed with HPLC-PDA at 271 nm.



The detector response of ciprofloxacin (CPX) decreased in LGW upon repeated injections from the same sample vial (see Table 3.1); however ciprofloxacin has been reported to be stable in LGW equivalent Milli-Q water (Turiel, Bordin *et al.*, 2005). To test whether the reduced detector response over time was due to sorption on the glassware surface, glass amber autosampler vials were deactivated by silanization. Silanization chemically converts the hydroxyl groups on the glass surface (that often act as adsorption sites) into inactive, neutral $-\text{O}-\text{SiR}_3$ functional groups, eliminating non-specific bonding. Standards of CPX (0.43 mg/L), tetracycline (TCC) (1.1 mg/L), and SMX (0.22 mg/L) were prepared in LGW, and injected on the LC/MS for analysis at different holding times (refer to Table 3.2 for results). The instrument response for both CPX and TCC was higher in the deactivated vials at each timed injection compared to the untreated vial. The difference of the initial response of TCC and CPX could be that in the normal vial, a fraction of the antibiotics sorbed quickly to the glass surface hydroxyl groups. The response still continued to decrease as each sample was reinjected at later times. Since SMX in LGW was previously shown to be stable, a standard of SMX in aqueous solution was reinjected multiple times between the vials of TCC and CPX to verify that the change in the instrument response was not due to the instrument itself.

It was decided that the benefits of deactivated glassware were minimal compared to the

toxicity of the deactivation reagents. In addition, while the decrease in response over 25 hrs holding times in the normal vials was 10, 12, and 1% for CPX, TCC, and SMX respectively, the change in response was much higher for the deactivated vials (24% CPX, 23% TCC, 8% SMX). Since the rate of degradation appeared to be lowest with 25 hrs (the maximum time a vial would be held before injection), a decision was made to analyze samples in a timely fashion to minimize the effects of degradation.

Table 3.1: Comparing the responses of consecutive injections of the same aqueous solutions of SMX, CPX, and TCC in LGW analyzed by HPLC-PDA at 271 nm.

Sample	Time (hr)	Area			Residual Concentration (µg/L)		
		TCC	CPX	SMX	TCC	CPX	SMX
Solution 1 TCC=24µg/L CPX=59µg/L SMX=92µg/L	0.0	49228	13474	130983	24	59	92
	0.5	42656	12829	130476	21	56	92
	1.0	41920	11683	132400	20	51	93
	1.5	39143	9087	132181	19	40	93
	2.0	37018	8469	132831	18	37	93
Solution 2 TCC=120 µg/L CPX=300 µg/L SMX=460 µg/L	0.0	728361	133167	1109128	118	295	460
	0.5	738092	129271	1107152	120	286	459
	1.0	747584	129568	1103638	121	287	458
	1.5	737276	119919	1110665	119	266	461
	2.0	740844	120005	1105749	120	266	459

Table 3.2: Comparing the LC-MS/MS response of aqueous solutions of CPX (0.43 mg/L), TCC (1.1 mg/L) and SMX (0.22 mg/L) in untreated and deactivated glass vials.

Time (hrs)	CPX		TCC		SMX	
	Deactivated Glass Vial	Normal Glass Vial	Deactivated Glass Vial	Normal Glass Vial	Deactivated Glass Vial	Normal Glass Vial
0	3.60E+08	2.67E+08	5.35E+08	3.57E+08	9.53E+08	9.43E+08
3	3.13E+08	2.83E+08	4.49E+08	3.91E+08	9.40E+08	9.35E+08
23	2.78E+08	3.29E+08	4.04E+08	3.45E+08	8.88E+08	9.28E+08
25	2.75E+08	2.40E+08	4.14E+08	3.15E+08	8.81E+08	9.43E+08

3.2 Soil and Sediment Characterization

Six different soils from North Carolina were collected and characterized. Each soil was assigned to its USDA (United States Department of Agriculture) textural class based on the clay, silt and sand content. Table 3.3 shows the soil texture, organic matter content, particle density, water capacity, and pH of each soil. The collected soils represent a range of texture and organic content. Understandably, the eastern North Carolina Agricultural (NC Ag) soil taken from an active farm had the highest organic content due to the application of fertilizers. The Morgan Creek sediments had the lowest organic matter, clay and silt content.

Table 3.3: Soil and sediment characterization from six different North Carolina locations.

Soil Sample	Eastern NC Ag.	Chapel Hill	Chatham County	Orange County 1	Orange County 2	Morgan Creek
USDA Textural Class	Sandy Loam	Sandy Loam	Sandy Loam	Silty Clay	Silty Loam	Sand
Clay (%)	9	14	10	50	23	2
Silt (%)	22	18	18	42	56	5
Sand (%)	69	68	72	8	21	93
Organic Matter Content (%)	23	12	4	16	12	0.8
Particle Density (Dp) (g/cm³)	1.2	2.6	2.4	2.4	2.3	2.6
Water Holding Capacity (%)	112	44	42	63	59	35
pH	4.6	6.2	6.2	5.2	5.2	7.0

3.3 Photolysis of SMX

3.3.1 Batch Reactor Results

The Batch Reactor (BR) was the most difficult among the reactor designs for controlling temperature, exposure time, continuous mixing, and efficiency of sample removal. The Heraeus medium pressure mercury lamp was partially submerged in 1 L of 10 mg/L and 1 mg/L solutions of SMX. Even with the cooling quartz sleeve and water bath, the temperature of the irradiated solution changed. The solutions were exposed to the full spectrum of the medium pressure lamp. Also, since ozone was generated by the lamp (which did not have a filter in place for the 180 nm emission of medium pressure mercury

lamps), the results are skewed. The reaction kinetics of SMX were forced to pseudo-first order conditions because direct photolysis fits this model (see Figure 3.4 and Figure 3.5); but given the limitations of the reactor design, these conditions were most probably not achieved. The half-life of sulfamethoxazole in the BR was less than half a minute (see Table 3.3) for 10 mg/L solutions of SMX in LGW. While the half-life for the 1mg/L SMX solutions were on average 0.5 min. different from the 10 mg/L solutions (see Table 3.4), precision for the 1 mg/L data was substantially lower and fewer sample points were taken.

This batch reactor was more suitably designed to simulate water treatment processes, where water comes directly in contact with the lamps. These results indicate that medium pressure lamps could be effective in removing sulfamethoxazole from treated waters. HPLC-PDA chromatograms of the BR solutions showed degradation of the SMX below detection limits after 5 min. During the 5 min. of sampling, other peaks that absorbed at 271 nm appeared, indicating the formation of byproducts, but these also eventually disappeared from the chromatogram. If the flux were sufficient during a treatment process, SMX and some of its photoproducts could be photochemically broken down as well.

Figure 3.4: Example of forced pseudo first order degradation of SMX ($C_0 = 10$ mg/L) in LGW in the BR reactor.

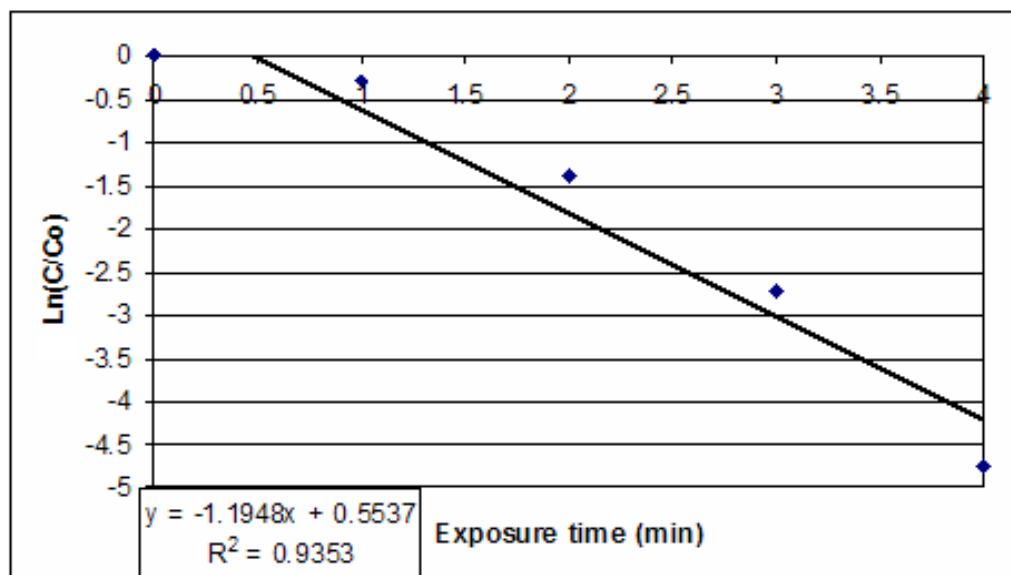


Figure 3.5: Example of forced pseudo first order degradation of SMX ($C_0 = 1$ mg/L) in LGW in the BR reactor.

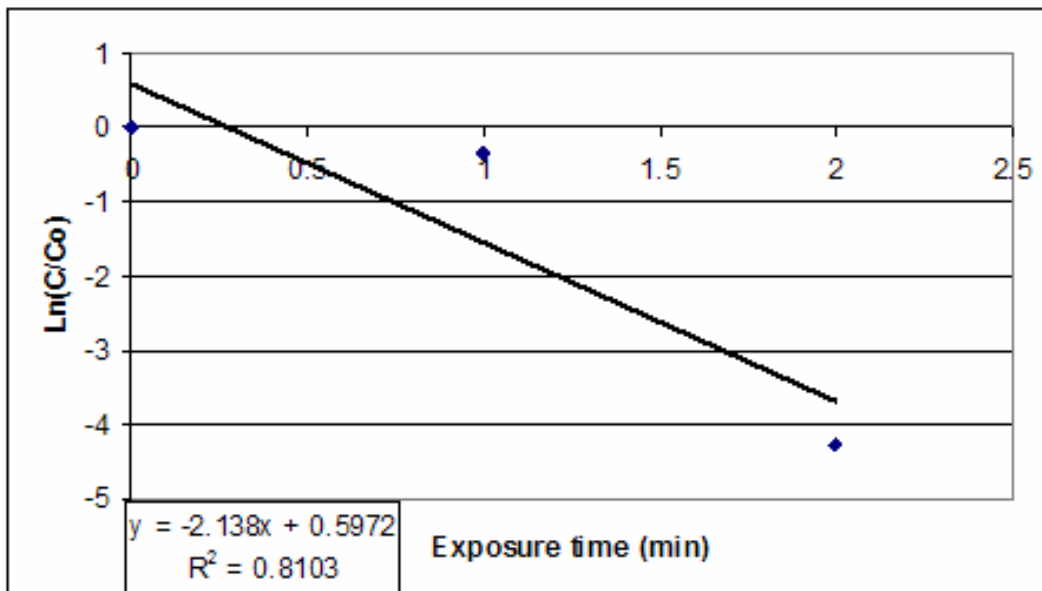


Table 3.4: Summary of kinetics for 10 mg/L SMX in BR assuming pseudo first order degradation ($n = 3$).

Average k (min^{-1})	Stdev (min^{-1})	%RSD	Average half-life (min)	Stdev (min)	%RSD
2.11	0.02	1	0.33	0.0033	1

Table 3.5: Summary of kinetics information for 1 mg/L SMX in BR assuming pseudo first order degradation ($n = 2$).

Average k (min^{-1})	Average half-life (min^{-1})	%Relative Difference
1.38	0.51	27

3.3.2 Second Reactor Design

The second reactor design (FT) was flawed in a similar fashion to the BR, in that the 14 L reactor was static (no form of continuous mixing) and the medium pressure mercury lamp was still forming ozone due to the lamp emission at 180 nm. However, because the

lamp was not submerged in the solution, solution temperature was easier to control. It was also easier to withdraw samples at various timed intervals with more precision. Due to the distance of the lamp from the liquid surface and the use of the Pyrex filter, the fluence was less compared to the BR reactor. The addition of the Pyrex filter removed wavelengths less than 290 nm. The reaction rate of SMX in LGW in this reactor at $C_0 = 1 \text{ mg/L}$ is shown in Figure 3.6 with a corresponding half-life of $2.9 \pm 0.2 \text{ hr}$ (refer to Table 3.5). The half-life of SMX in the FT increased compared to the BR due to the fact the wavelengths less 290 nm were removed and the fluence was decreased compared to direct contact with the lamp (1×10^{-5} vs $3 \times 10^{-4} \text{ ein/s}$).

When 300 g of Chapel Hill soil, a sandy loam with a 12% organic matter content, (refer to Table 3.3) was placed in the bottom of the reactor, the half-life of SMX in the aqueous phase increased to 28 hrs (refer to Table 3.6). The comparison of photodegradation rates can be made between the LGW and Chapel Hill soil system because the pH of each system was similar. In LGW, solutions of sulfamethoxazole had pH values of approximately 5.5 without the addition of acids or buffers. The pH of the Chapel Hill soil water in the reactor was 5.7. As reported by Boreen, Arnold *et al.*, (2004), the quantum yield of sulfonamides and rate of degradation in water are pH dependent due to speciation (see Table 1.5). The absorbance of sulfamethoxazole shifted depending on whether the major species in aqueous solution was cationic, neutral or anionic. The dominant species of SMX in pH range of 5.5 - 5.7 would be the neutral and anionic forms.

The reaction rate of SMX ($C_0 = 1.15 \text{ mg/L}$) in LGW in the presence of Chapel Hill soil in the FT reactor is shown in Figure 3.7. The slower photodegradation rate is most likely the result of optical filtering due to the presence of organic and particulate matter. The leaching of organics and increased particulate matter from the soil could competitively absorb light. Colored dissolved organic matter (CDOM) decreases absorbance, particularly in the most important photochemical spectral range of 280 - 320 nm for sulfamethoxazole (UVB) (Gao and Zepp, 1998). Suspended particulate matter (such as sediment particles) scatter incident light and reduce the penetration of light below the surface of the water. The sediment particles could act as a shield from photolysis as the analyte binds into regions of the particle where the light does not reach. The CDOM and particles may also quench the excited states of the analyte through a transfer of energy

(Larson and Weber, 1994). The increased persistence of sulfamethoxazole in complex matrixes is similar to other published results (Lam, Tantuco *et al.*, 2003).

Figure 3.6: An example of pseudo first order degradation results of SMX in LGW ($C_0 = 1 \text{ mg/L}$; $\text{pH} = 5.5$) in the FT reactor.

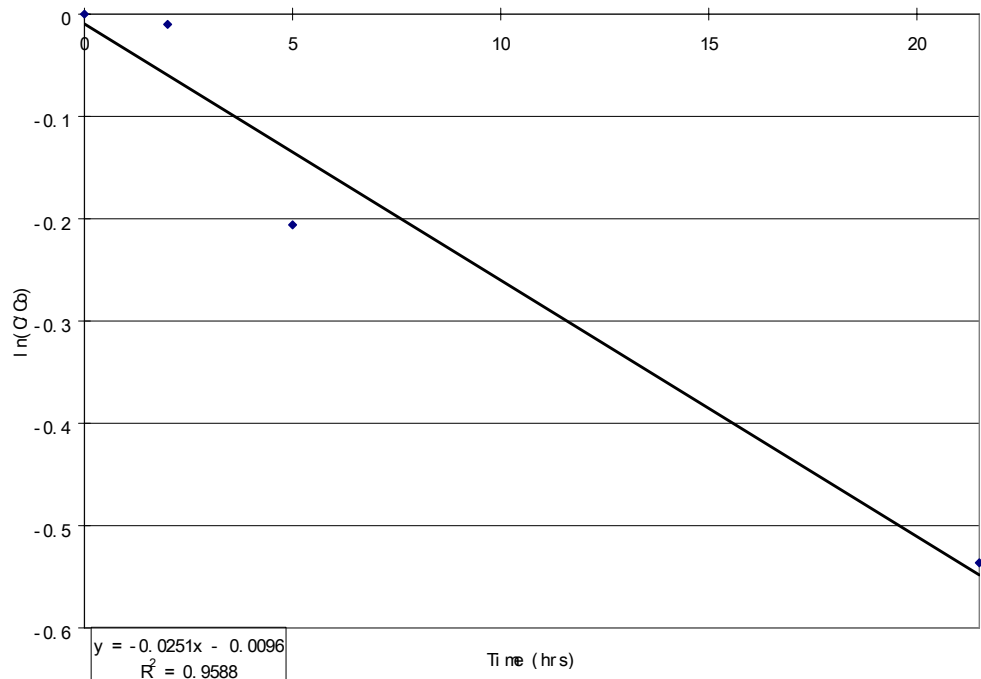
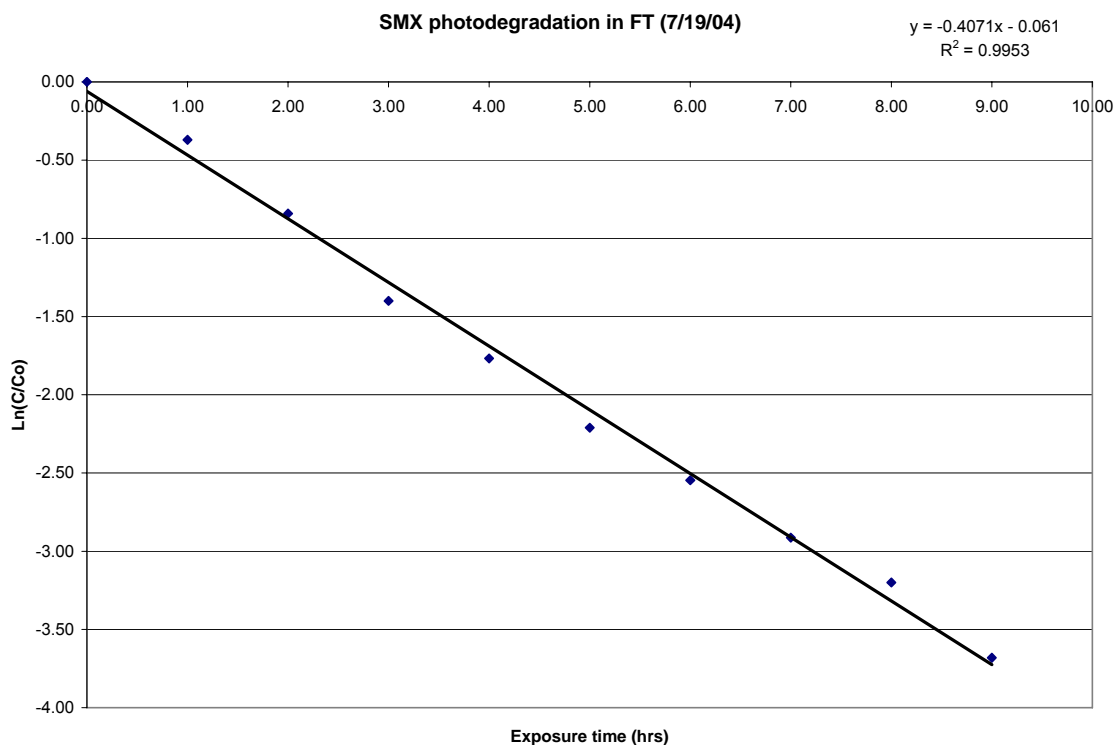


Table 3.6 Summary of kinetics information for 1mg/L SMX in BR assuming pseudo first order degradation ($n = 5$).

Average $k \text{ (hr}^{-1}\text{)}$	Stdev $\text{(hr}^{-1}\text{)}$	%RSD	Average half-life (hr)	Stdev (hr)	%RSD
0.236	0.016	7	2.94	0.20	7

Figure 3.7: Pseudo first order degradation of SMX in the FT reactor in LGW in the presence of Chapel Hill soil ($C_0 = 1.15$ mg/L; pH = 5.7).



3.3.3 Final Reactor Design

In the final reactor design, the lamp was changed, the glassware was modified, and pumps were added to the system to add flow to the system (refer to *Section 2.8.2*). A 0.93 mg/L solution of sulfamethoxazole in LGW was recirculated through the entire reactor to ensure that there were no adsorbing surfaces that could act as a sink for the target analyte (Figure 3.8a). Two lamps, the Growlight and Phillips, were used as artificial light sources in the exposure reactor (ER). The Growlight plant lamp produces emissions mainly in the UVC and visible region (see Figure 2.3). The Phillips T20W UVB lamp, in comparison to the medium pressure mercury lamp used in earlier versions of the reactor and plant lamp, emitted a broad spectrum from 270-400 nm (UVB and UVA) and did not produce ozone (see Figure 2.4). No significant changes in sulfamethoxazole concentration ($C_0 = 1$ mg/L, pH = 5.5) occurred in the recirculating LGW solution after 8 hrs of exposure to the Growlight lamp (Figure 3.8b). The aqueous concentration of sulfamethoxazole in the presence of Chapel Hill soil in the control reactor (CR), in which no lamps were used, also

did not change (Figure 3.9a). Increasing the exposure time of sulfamethoxazole to the Growlight lamp in the ER from 8 hrs to 90 hrs (Figure 3.9b) and even 160 hrs (Figure 3.9c) did not affect the aqueous concentration of sulfamethoxazole in the LGW solution. The light intensity from the Growlight plant lamp was clearly not sufficient to cause a change in the concentration of sulfamethoxazole, indicating that sulfamethoxazole was not sensitive to UVA and visible light.

Figure 3.8a: Persistence of SMX in LGW ($C_0 = 0.93$ mg/L) control.

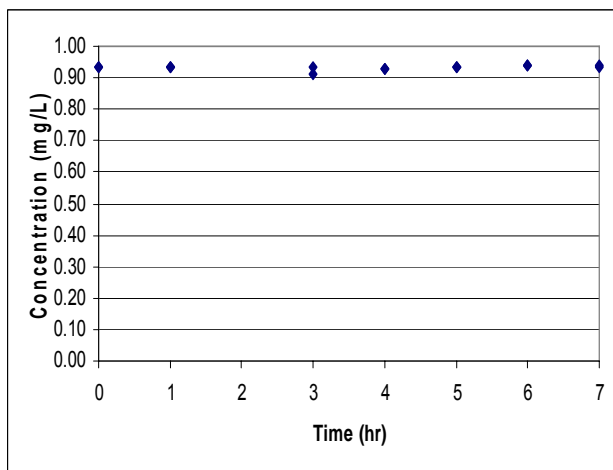


Figure 3.8b: Persistence of SMX in LGW ($C_0 = 1$ mg/L; pH = 5.5) in the ER with Growlight visible lamp.

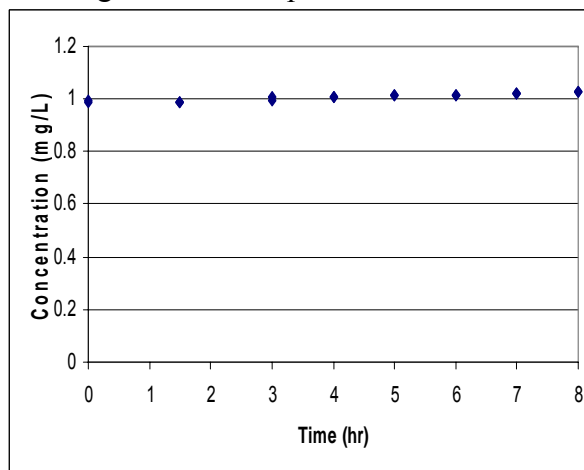


Figure 3.9a: SMX ($C_0 = 0.9$ mg/L, pH = 5.6) with LGW/Chapel Hill soil in the Control Reactor.

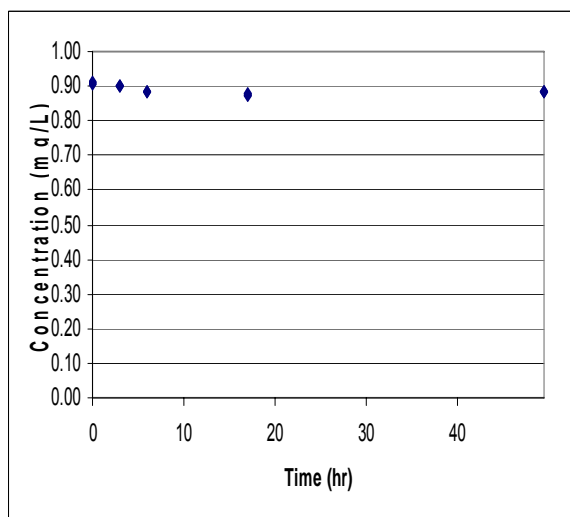


Figure 3.9b: SMX ($C_0 = 0.9$ mg/L, pH = 5.6) with LGW/Chapel Hill soil in the ER with the Growlight plant lamp.

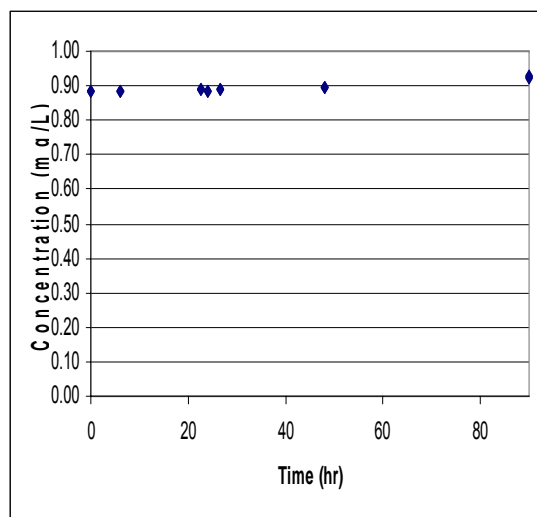
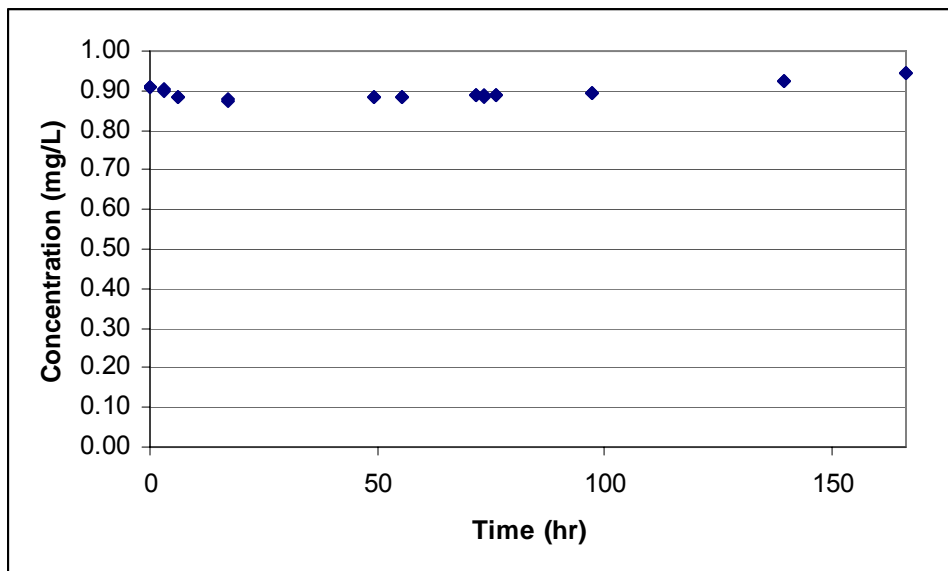


Figure 3.9c: SMX ($C_0 = 0.9$ mg/L, pH = 5.6) with LGW/Chapel Hill soil in the ER with the Growlight plant lamp.



When using the Phillips T20W UVB lamp as the artificial light source in the ER, the rate of sulfamethoxazole degradation increased compared to the static experiments in the FT reactor using the medium pressure mercury lamp, with a measured half-life of 0.8 hrs compared to 2.9 hours (Figures 3.10a, 3.10b, 3.10c). This result was expected due to the 270-300 nm emission range of the Phillips lamp and the fact that the sulfamethoxazole absorbance maximum (λ_{max}) is in the range of 268-271 nm (see Figure 3.19). The change in half-life also illustrates the importance of calculating the kinetic rate constant of polychromatic light based on fluence instead of time, if comparisons are to be made from laboratory to laboratory. The rate of degradation of a 10 ng/L SMX solution in LGW (a more environmentally relevant concentration) exposed to the Phillips 20W UVB lamp was comparable to that observed in the 0.1 mg/L and 1 mg/L solutions, with the half-life ranging from 0.80-0.97 hr (Figure 3.11).

Figure 3.10a: SMX ($C_0=0.9$ mg/L, pH=5.6) with LGW in the Control Reactor.

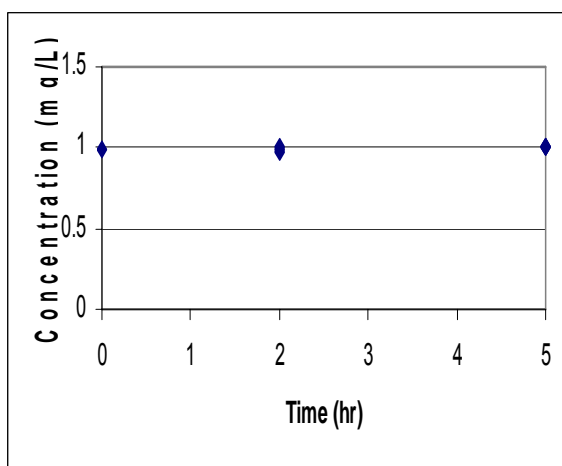


Figure 3.10b: SMX ($C_0=0.9$ mg/L, pH=5.6) with LGW in the ER with the Phillips T20W lamp.

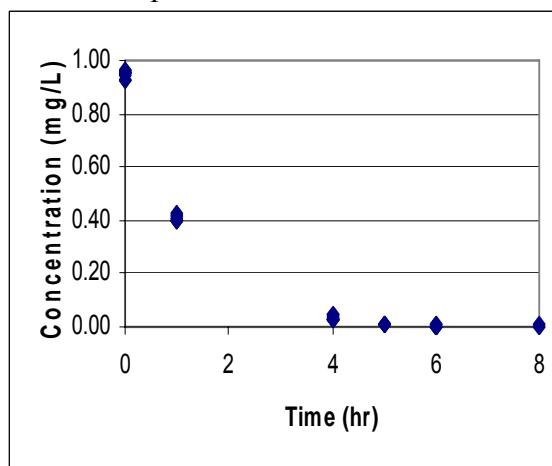


Figure 3.10c: First order degradation of SMX in LGW ($C_0 = 0.9$ mg/L; pH = 5.6) from exposure to the Phillips T20W UVB Lamp.

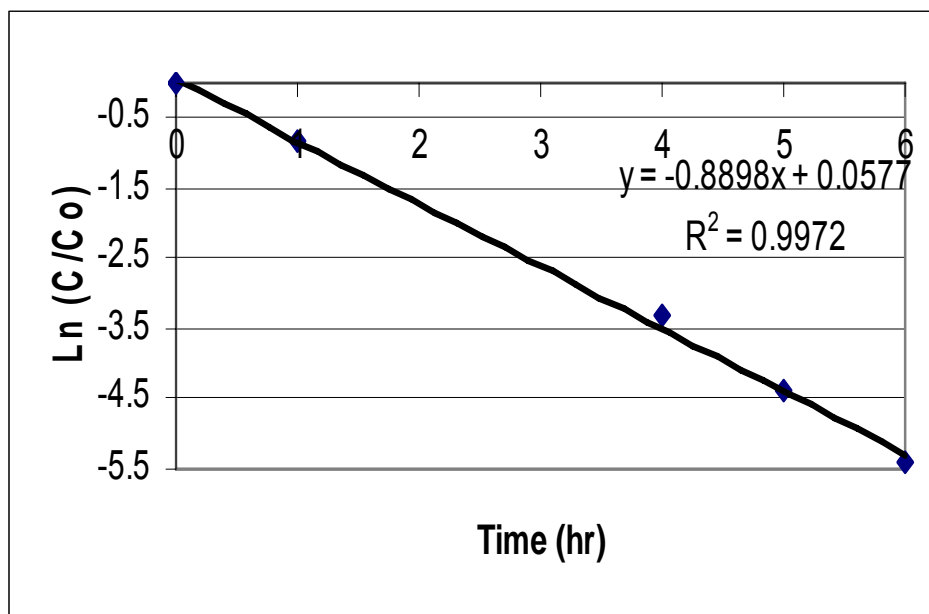
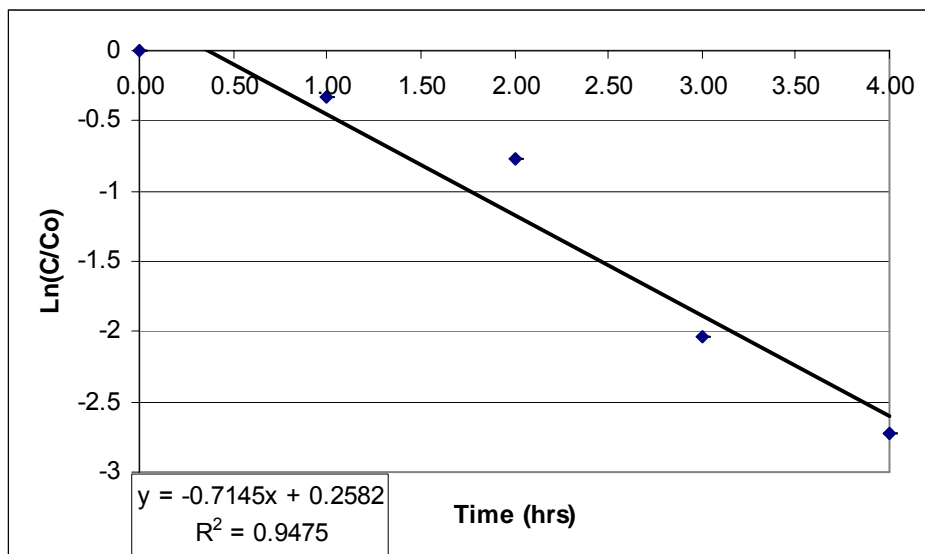


Figure 3.11: Photodegradation of 10 ng/L of SMX in LGW (ER).



The addition of Ottawa sand to the CR and ER reactor systems decreased the SMX degradation rate in comparison to the LGW solutions, increasing the half-life of sulfamethoxazole in solution from 0.8 hrs to 4 hrs (Figure 3.12c). In the control reactor, if absorption was occurring in the sand, this was not discernible (Figure 3.12a). Results were similar with the Chapel Hill soil (Figure 3.13a). This could be due to the relatively short sampling time of hours/days in this experiment compared to days and months in other studies (Ronnefahrt, Traub-Eberhard *et al.*, 1997; Kalsch, 1999; Löffler, Rombke *et al.*, 2005). With the addition of Eastern NC Ag soil, a higher organic content soil (see Table 3.3), to the reactor, the loss of sulfamethoxazole was noticeable in the control reactor (Figure 3.14a) as well as during exposure (Figure 3.14b). After 20 hrs of contact time with the soil in the CR, the concentration of sulfamethoxazole changed from 2.6 mg/L to 2.2 mg/L (a 0.4 mg/L loss). Assuming the change in the aqueous concentration was not due to biotic degradation in the CR, this finding would indicate a concentration of 2 µg/g in the soil. The combined effect of sorption and photolysis resulted in 77% removal of sulfamethoxazole from the water after 20 hrs of exposure to both UVB light and soil. The Eastern NC Ag soil was characterized with a 23% organic matter content compared to the 0.7-1.3% in sediments from a local creek which received treated wastewater. The Ottawa sand and Chapel Hill sandy loam were more comparable to the sediments in terms of physical soil characteristics and because sorption of sulfamethoxazole from the aqueous

phase to the sandy soil was not detectable, it might be expected that stream sediments with low organic content will have low concentrations of sulfamethoxazole even if it is present in the aqueous phase of the stream.

Figure 3.12a: SMX ($C_0 = 1\text{mg/L}$, $\text{pH} = 5.6$) with LGW/Ottawa sand in the Control Reactor.

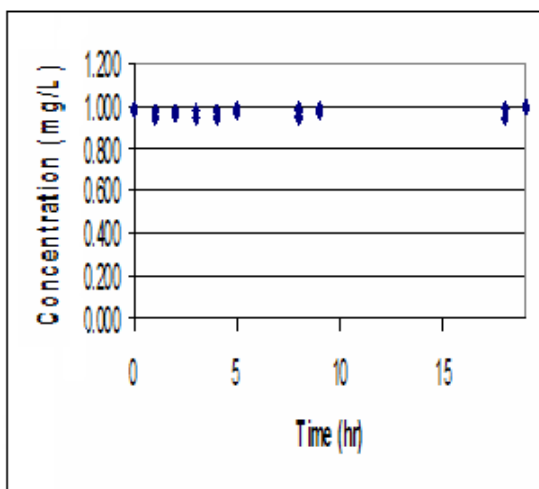


Figure 3.12b: SMX ($C_0 = 0.9\text{mg/L}$, $\text{pH} = 5.6$) with LGW/Ottawa sand in the ER with the Phillips T20W lamp.

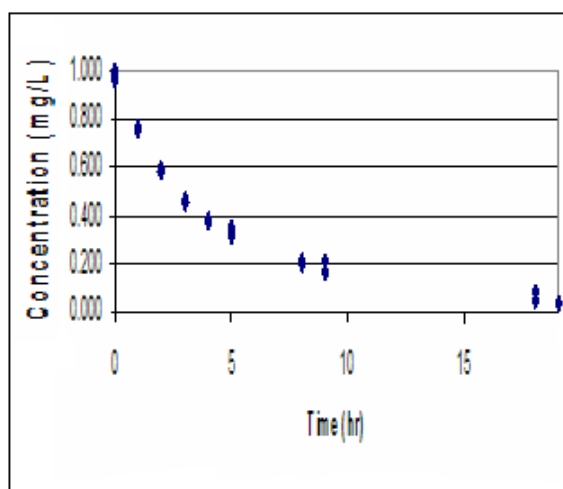


Figure 3.12c: First order degradation of SMX in LGW with 300 g of Ottawa sand under the Phillips T20W UVB lamp.

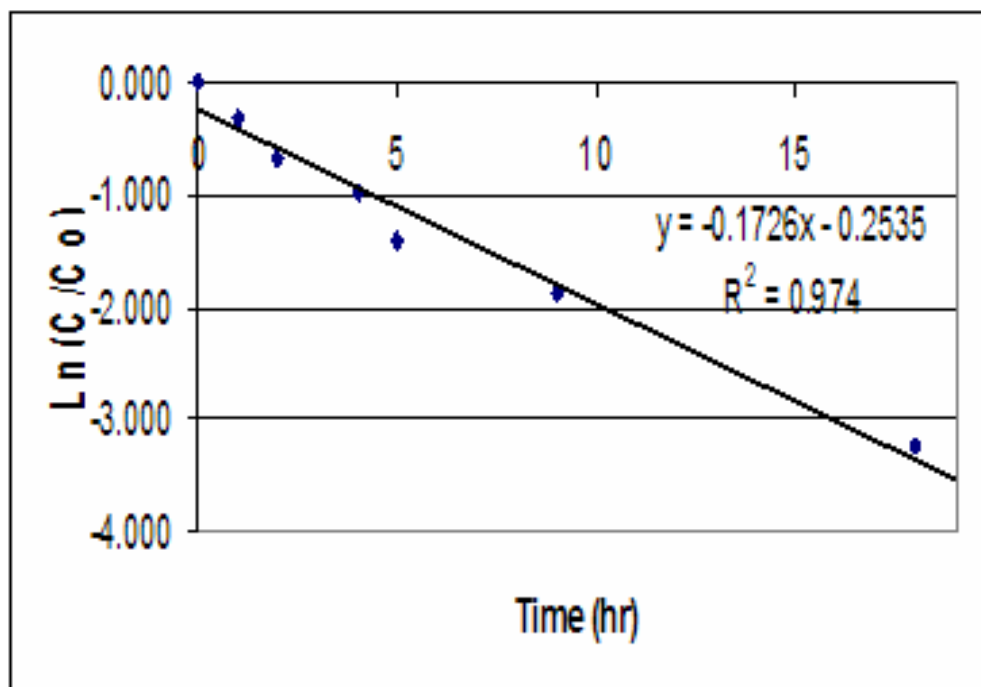


Figure 3.13a: SMX ($C_0=0.9\text{mg/L}$, $\text{pH}=5.7$) with LGW/Chapel Hill soil in the Control Reactor

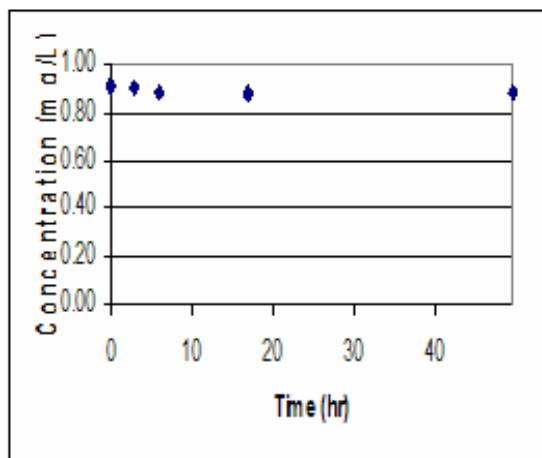


Figure 3.13b: SMX ($C_0=0.9\text{mg/L}$, $\text{pH}=5.7$) with LGW/Chapel Hill soil in the ER with the Phillips T20W lamp

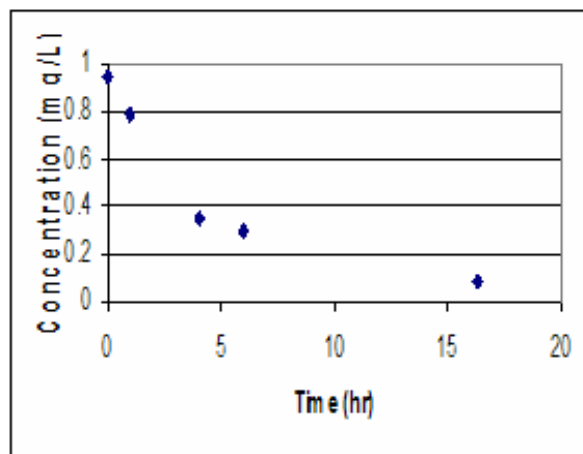


Figure 3.14a: SMX ($C_0=2.6\text{ mg/L}$, $\text{pH}=5.5$) with LGW/ Eastern NC agricultural soil in the Control Reactor

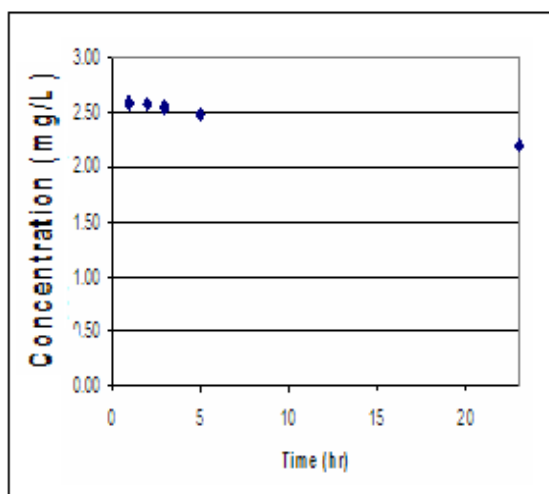


Figure 3.14b: SMX ($C_0=2.2\text{ mg/L}$, $\text{pH}=5.5$) with LGW/ Eastern NC agricultural soil in the ER

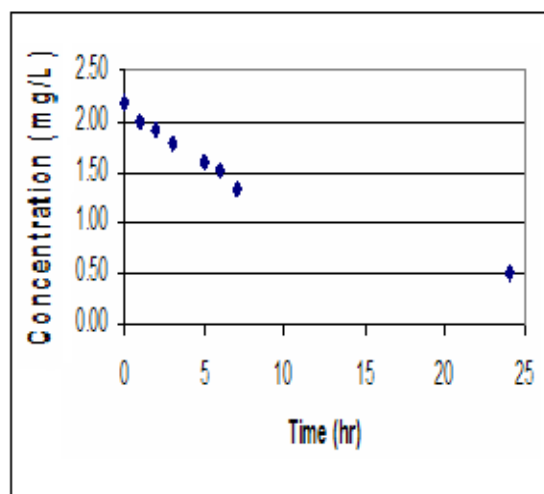


Figure 3.15 includes absorbance spectra of LGW that was allowed to equilibrate with 300 g of Morgan Creek sediment, illustrating not only the differences of background matrix and the changes in water quality, but the leaching of materials from the soil that competitively absorb in the 270-315 nm range. Figure 3.16 provides examples of Morgan Creek and OWASA WWTP effluent, respectively, for comparison. The rates of

degradation in the Morgan Creek water/sediment system (Figure 3.17) were decreased compared to LGW, sand, Chapel Hill, and Eastern NC Ag soil, but the results are not directly comparable to the LGW due to the pH change (pH = 6.7 - 6.8 compared to 5.5 - 5.7). The primary state of sulfamethoxazole in reactors and in the stream environments would be anionic, which has a lower quantum yield than the neutral states, and therefore, the direct photodegradation rates would be less.

Figure 3.15: UV absorbance spectra of the ER and CR (4 L of LGW equilibrated with 300 g of Morgan Creek Sediment; pH = 6.7-6.8, TOC: 2.07 mg/L C).

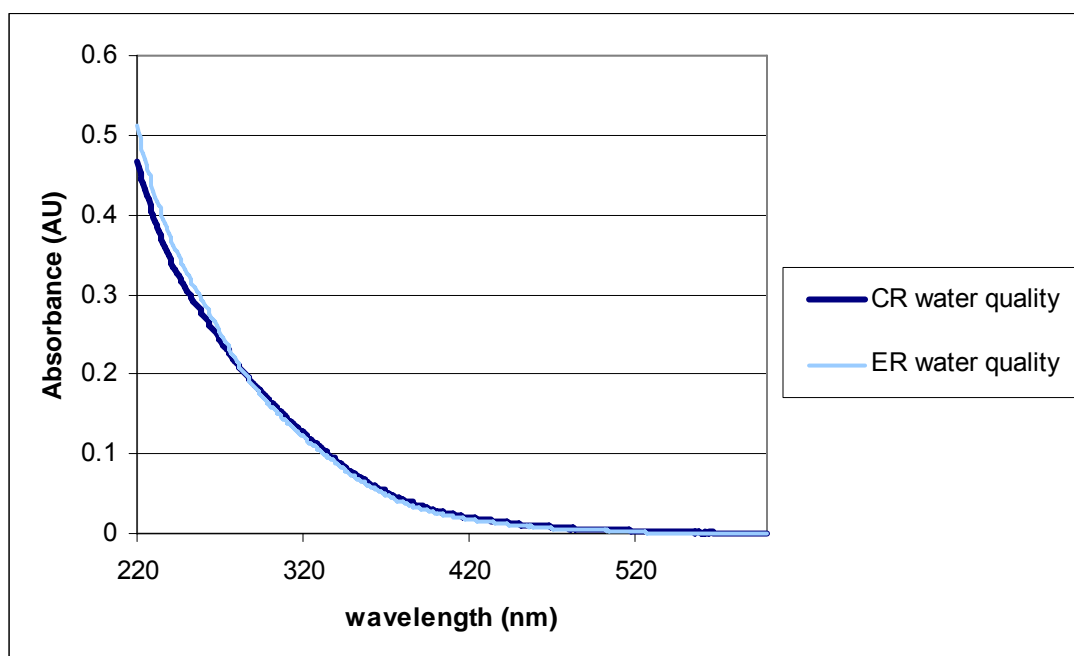


Figure 3.16: UV absorbance spectra of Morgan Creek sampling points (11/14/2005, 0.45 μm filtered) (UPS = upstream, TOC = 3.00mg/L C; DS = downstream, TOC = 5.24 mg/L C; E = effluent, TOC = 5.52mg/L C).

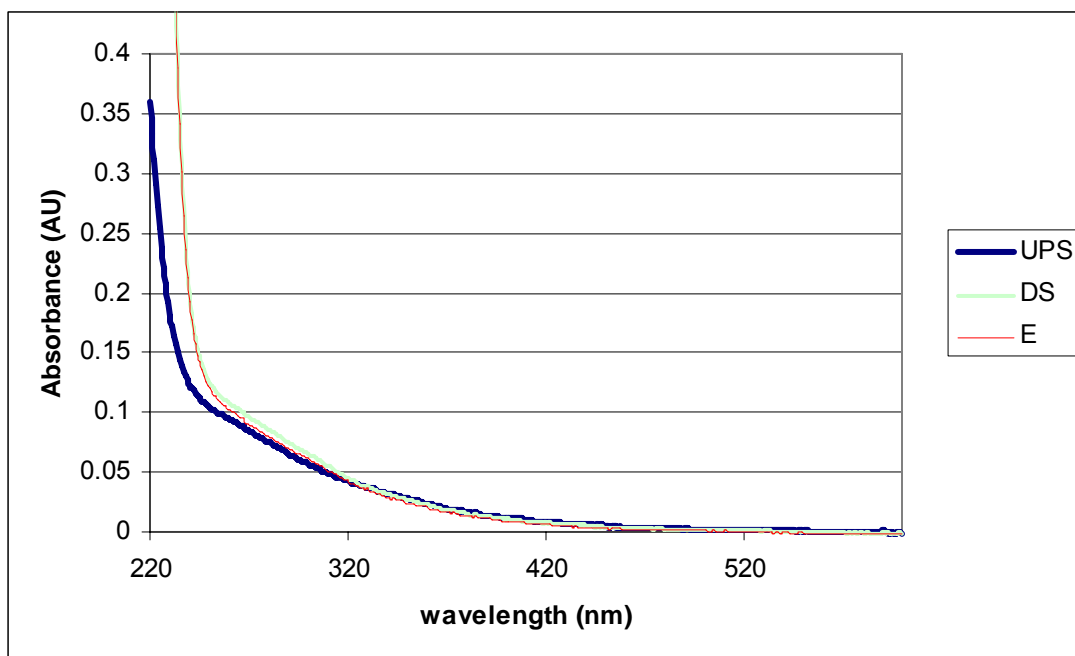
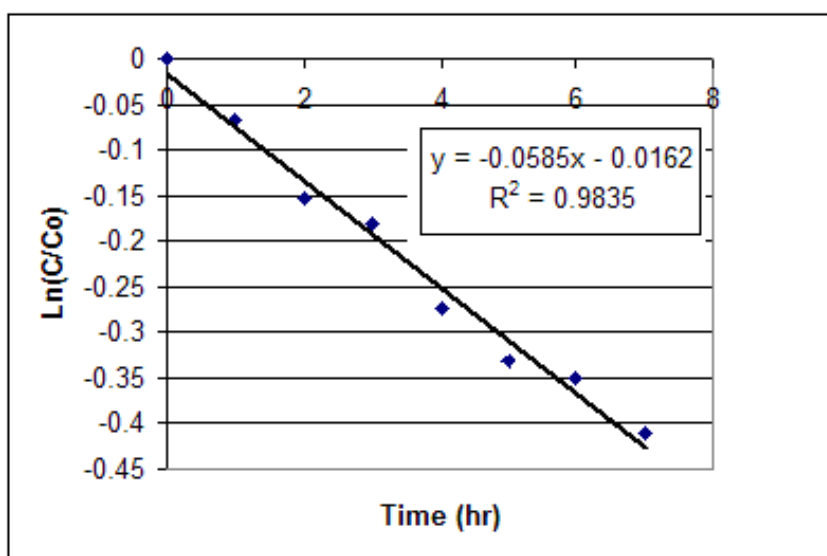


Figure 3.17: Pseudo first order degradation of SMX ($C_0 = 0.10 \text{ mg/L}$, pH = 6.7, TOC = 2.05 mg/L C) in the LGW/Morgan Creek sediment system.



3.3.4 Photolysis Byproducts

As the parent compound, sulfamethoxazole, was removed from the reactor systems, byproducts were simultaneously being formed (example HPLC-PDA chromatograms shown in Figures 3.18a and 3.18b). Photodegradation products of sulfamethoxazole in laboratory systems have been identified by Zhou and Moore (1994), as illustrated in Figure 1.4. Figure 3.19 shows the absorbance spectrum of these byproducts with available standards. Figure 3.20 is an absorbance spectrum extracted from an HPLC-PDA chromatogram of an unidentified photolysis product generated from an LGW solution of SMX ($C_0 = 1$ mg/L, pH = 5.5, 25°C) in the FT. Both figures indicate that the products may in turn be photolabile due to the absorbance maxima in the UV-B region. As exposure time in the reactor increased, the byproduct intensity also decreased. The loss was most noted in the batch reactor, as expected based on the high UV dose given, the exposure to the full spectral emission of the medium pressure lamp which includes the λ_{max} of the initial byproducts, and perhaps high temperature and ozone formation.

Figure 3.18a: HPLC-PDA chromatogram depicting the original response of SMX (1mg/L in LGW FT) at 0hrs.

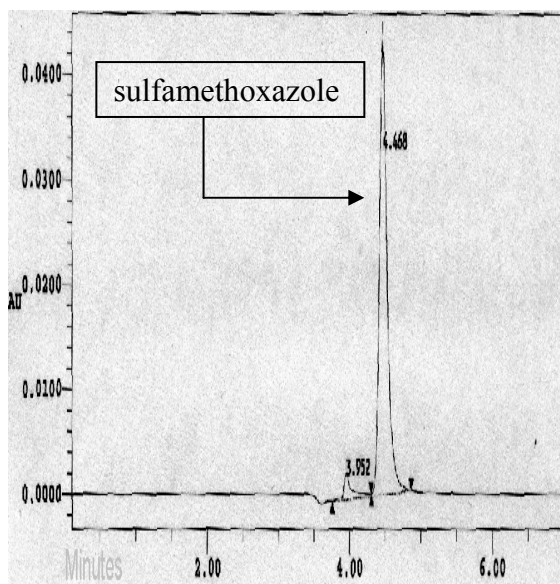


Figure 3.18b: HPLC-PDA chromatogram after 9hrs depicting the loss of SMX (1 mg/L in LGW FT) and the formation of byproducts detectable at 271 nm.

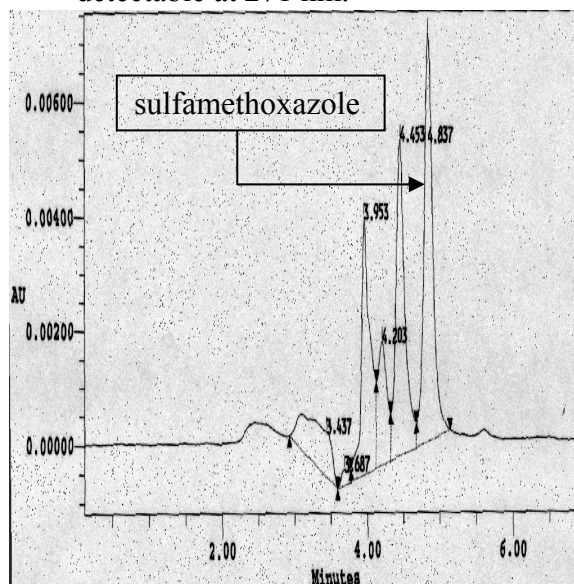


Figure 3.19: Molar absorptivity of sulfamethoxazole and predicted byproducts.

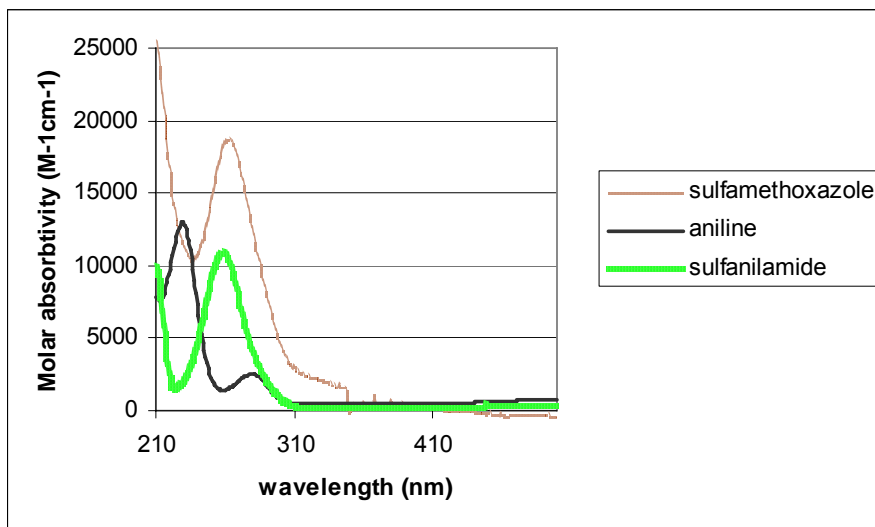
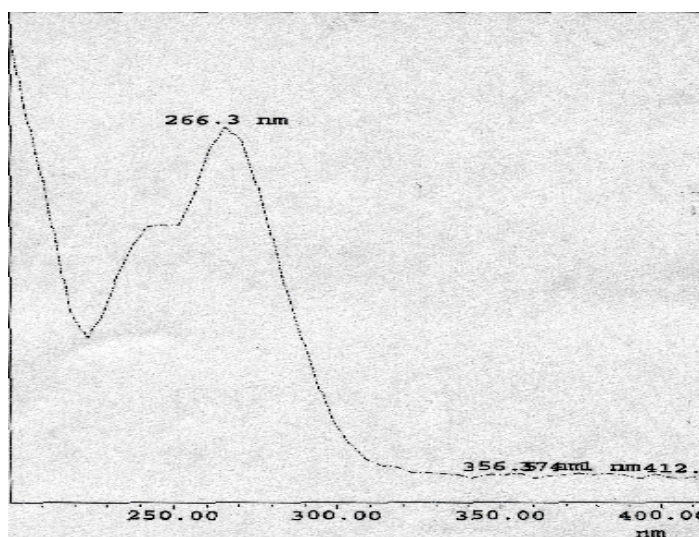


Figure 3.20: Absorbance spectrum of the major unknown SMX photolysis byproduct extracted from an HPLC-PDA chromatogram.



Of particular interest was the formation of a product of the same mass and fragmentation as sulfamethoxazole (Figure 3.21), but of a shorter chromatographic retention time, indicating a more polar compound (Figure 3.22). Its fragmentation pattern and daughter ions were the same as those of SMX, pointing to a possible photoisomerization process. This product developed only as a result of photolysis in either the control reactor or in the neat standard. The isomer was detected in the aqueous phase when exposed to the Phillips T20W lamp both with and without the Pyrex filter (Figure

3.23), indicating it could be formed during exposure to sunlight. It was also detected in the reactor after exposure of the 10ng/L solution of SMX after sample pre-concentration through solid phase extraction (Figure 3.24).

In comparing the LC/MS/MS response of the photoisomer to SMX in Figure 3.24 to Figure 3.23, there appears to be a greater conversion ratio of SMX for Figure 3.24. After 3 hrs, the response of photoisomer is almost equal to the response of the SMX ($C_0=10$ ng/L), while for the 1 mg/L solution of SMX show in Figure 3.23, only fraction of SMX has been converted into the photoisomer. The contributing factor to this difference in the rate of transformation is the characteristics of the light used for exposure. For the 1mg/L solution of SMX, the pyrex filter was in place, filtering out wavelengths less than 290 nm. The filter was not present in the 10 ng/L SMX experiments. Therefore, not only was the intensity of light between 200-350 nm 20 times greater for the 10 ng/L concentration of SMX than the 1 mg/L solution, but the absorption maxima of SMX at 270 nm was present in the unfiltered lamp spectra. As expected, the transformation of SMX into photo-byproducts is increased when the light source includes wavelengths that SMX strongly absorbs.

Figure 3.21: LC/MS full scan spectrum of SMX from 50-300 amu.

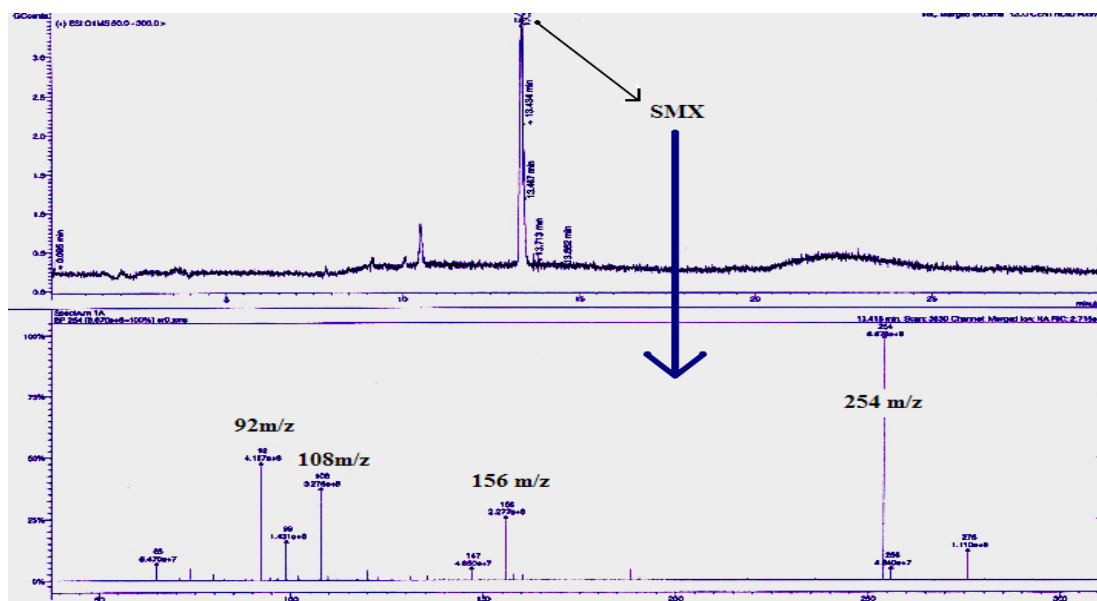


Figure 3.22: LC/MS full scan spectrum of the major byproduct (50-300 amu) from SMX ($C_0=1\text{mg/L}$) in LGW exposed to the Phillips T20W lamp in the ER after 3 hrs exposure.

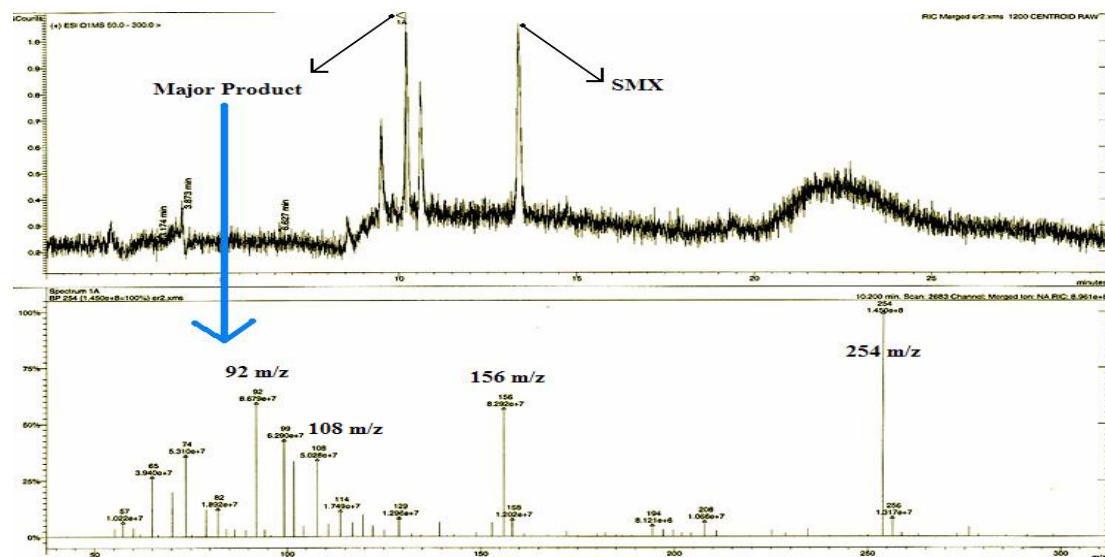


Figure 3.23: Formation of SMX photoisomer in LGW ($C_0 = 1$ mg/L) in the ER with the Phillips T20W UVB lamp and the Pyrex filter after 32 hrs of exposure.

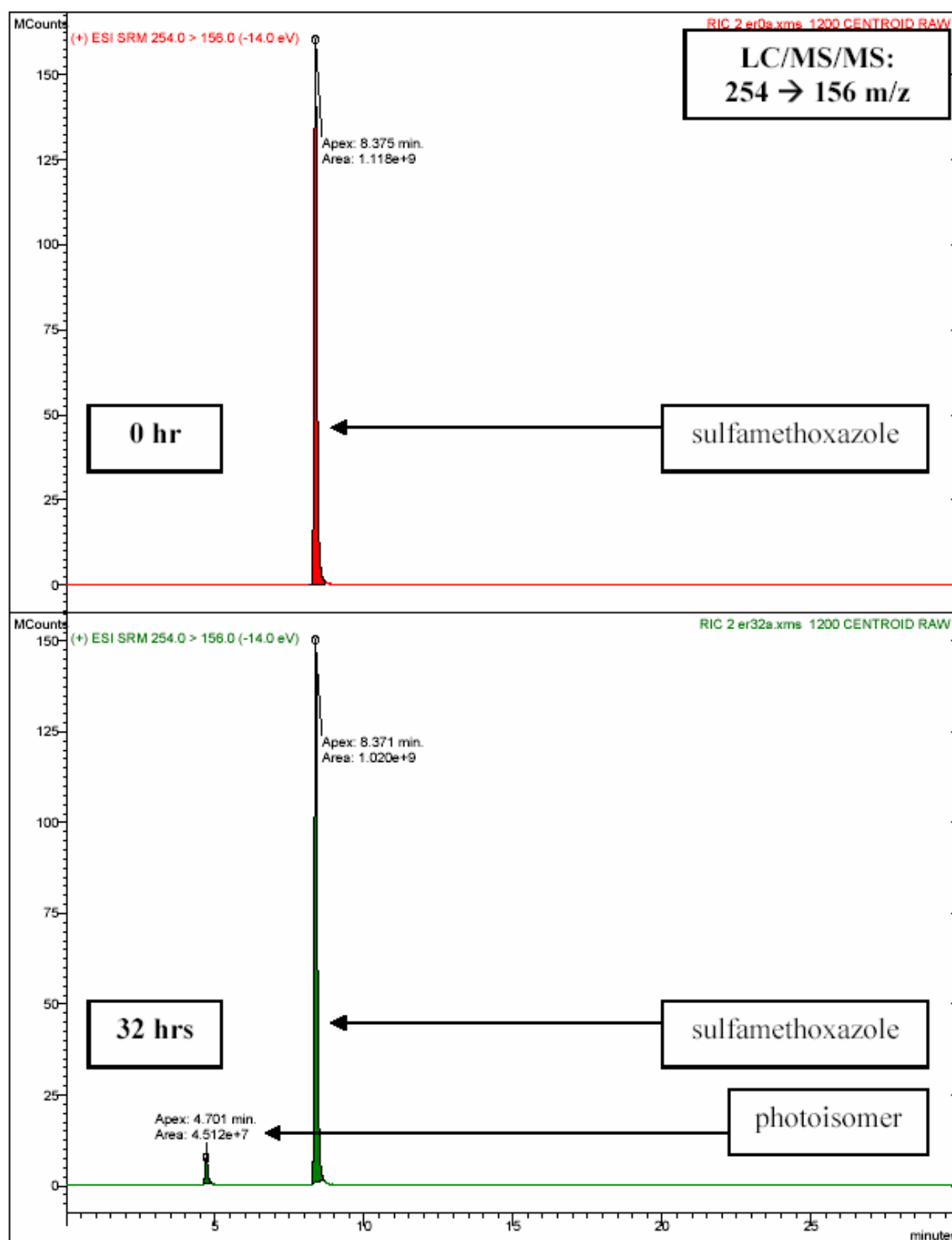
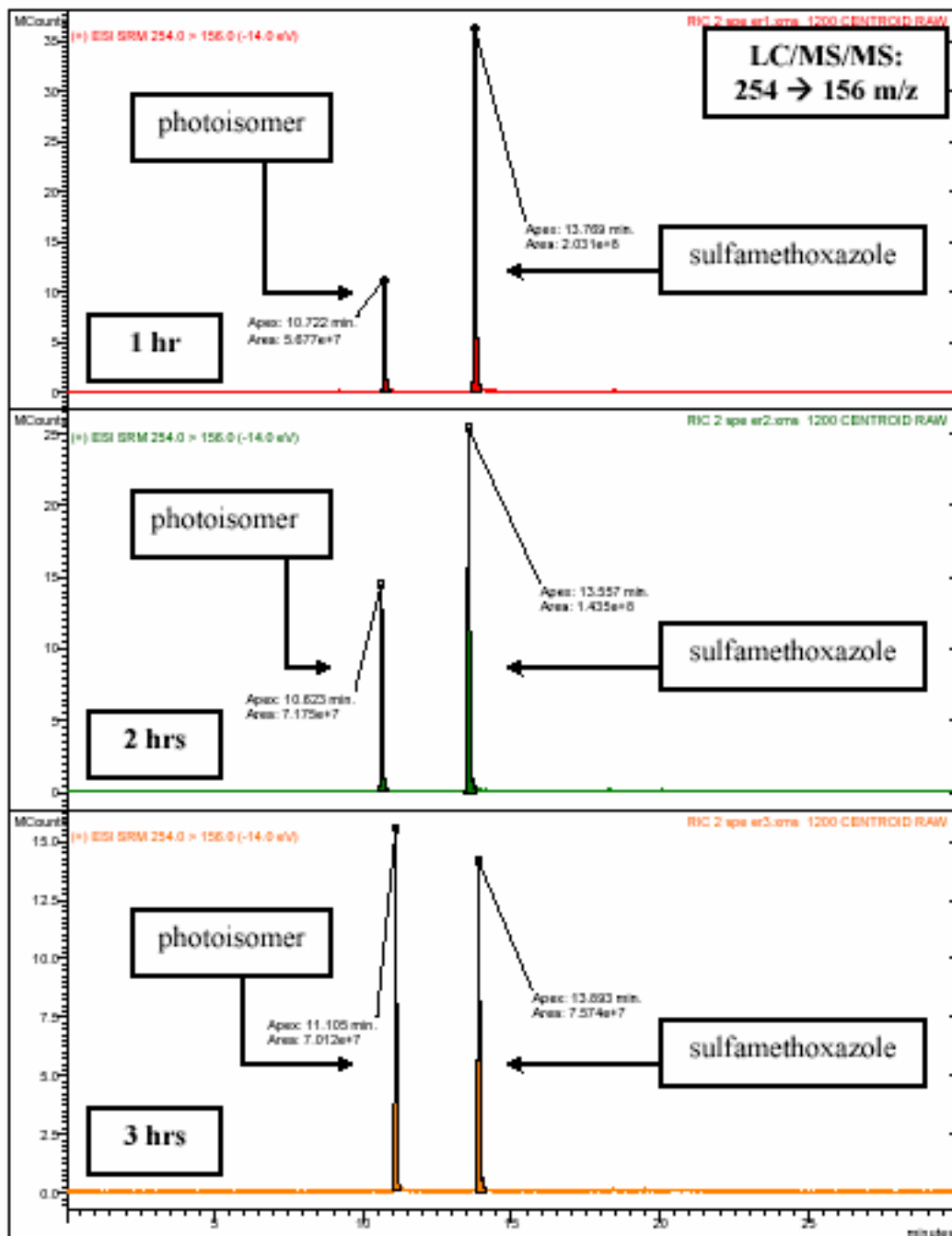


Figure 3.24: Formation of the SMX photoisomer ($C_0 = 10 \text{ ng/L}$) in LGW exposed to the Phillips T20W lamp in the ER.

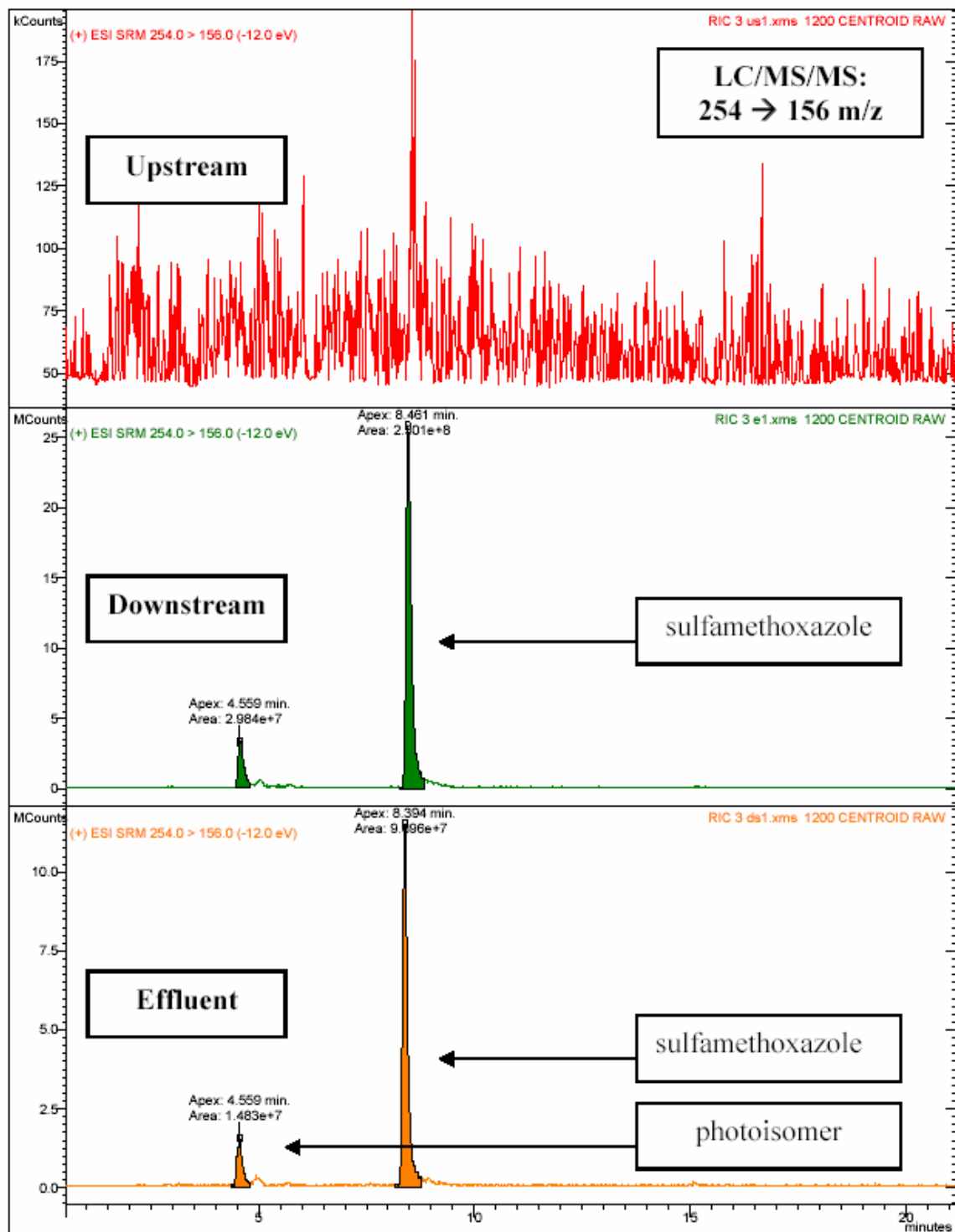


The product was formed by a rearrangement of the isoxazole function group (ring contraction-ring expansion mechanism) of sulfamethoxazole (Horspool and Song, 1994). This product was also found by Zhou and Moore (1994) and Lam and Mabury (2005) in LGW. The change in polarity was caused by a shift in the dipoles, the change in the

structural relationship between the isoxazole oxygen, the sulfamic acid oxygens, and the nitrogen. This isomer, due to its structural similarity to the parent compound, could retain antimicrobial effects. The second product identified in the exposure reactor was sulfanilic acid using LC/MS/MS by comparing the retention time and fragment ions to a standard solution. Sulfanilic acid was also detected by Boreen, Arnold *et al.* (2004) in lake water spiked with sulfonamides exposed to natural sunlight.

When the WWTP operating utility changed the disinfection process from chlorination to UV disinfection using low pressure mercury lamps, the photoisomer was detected in waters collected both from the effluent and half a mile downstream (Figure 3.25). The photo-isomer was not detected in Morgan Creek downstream samples (725 m from the effluent discharge) when chlorination was used at the treatment plant, but this could be due to the fact that downstream site did not provide enough sunlight exposure time from the point of discharge for product formation at detectable levels.

Figure 3.25: Production of the SMX photoisomer in the effluent of the OWASA WWTP and downstream after the plant began low pressure UV treatment (2/14/06).



3.4 Optimizing Soil and Sediment Extraction

3.4.1 Extraction Method

There are several methods for extracting chemicals from soils. Two options were readily available for this study: sonication and wrist-action shaking. Three common extraction solvents (methanol, acetonitrile, and ethyl acetate) were compared using both methods of extraction by spiking the Eastern NC agricultural soil with a known concentration of sulfamethoxazole (200 µg/g). Because ethyl acetate is not miscible with water, the ethyl acetate samples were blown down and reconstituted in an equal volume of methanol prior to analysis. Assuming 100% recovery, a 25 mL extract of 5 g of soil spiked at 200 µg SMX/g soil would generate a concentration of SMX in the extract of 40 mg/L. This concentration was too high for direct analysis by both the HPLC-PDA and LC/MS instruments, and so extracts were diluted. A 5 mL aliquot was diluted to 25 mL with LGW for a dilution factor of 5 and a theoretical concentration of 8 mg/L SMX. The results based on matrix calibration curves are shown in Figure 3.26 and the corresponding Table 3.7. The wrist-action shaking technique generated recoveries that were 4-10 times better than when using sonication. The difference between the solvent recoveries in the shaking technique was less than 1%, although ethyl acetate extracts had the greatest variability, possibly due to the extra reconstitution step.

Figure 3.26: Comparison of extraction techniques for the recovery of SMX from the Eastern NC agricultural soil spiked with sulfamethoxazole (200 µg SMX/g soil) (n = 3).

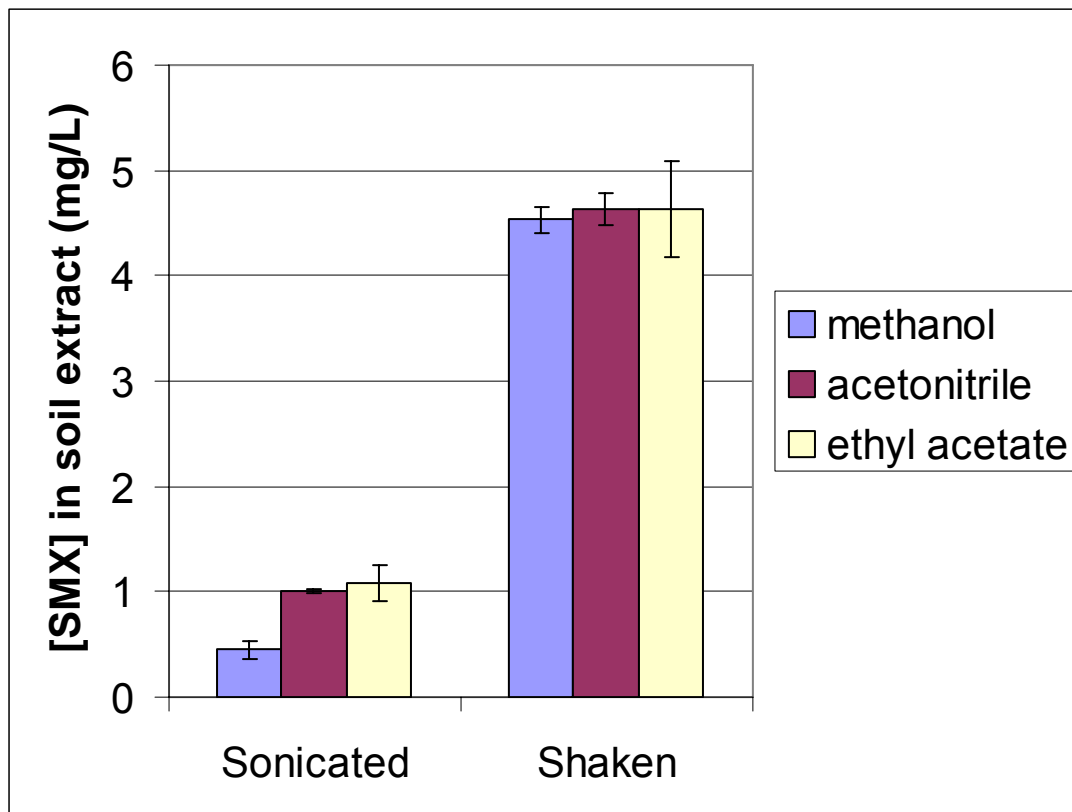


Table 3.7: Results of sonicated extracts compared to the shaken extracts of the Eastern NC agricultural soil spiked with sulfamethoxazole (200 µg SMX/g soil) (n=3).

	Sonicated			Shaken		
	Methanol	Acetonitrile	Ethyl Acetate	Methanol	Acetonitrile	Ethyl Acetate
Concentration (mg/L)	0.45	1.01	1.09	4.53	4.63	4.63
Stdev (mg/L)	0.09	0.02	0.17	0.16	0.19	0.6
% RSD	20	2	16	4	4	13
% Average Recovery	6	13	14	57	58	58

3.4.2 Soil Extraction Solvent

Almost 60% of sulfamethoxazole was extracted from the Eastern NC agricultural soil

spiked with 200 µg SMX/g soil with the first 25 mL portions of methanol, acetonitrile, and ethyl acetate (Figure 3.27). Total recovery from the sum of the three consecutive extractions ranged from 80 - 94% (Table 3.8). Acetonitrile had the highest overall extraction efficiency of the three and ethyl acetate the lowest. However, after a single extraction, differences were minimal.

Figure 3.27: Three consecutive extractions of a spiked Eastern NC agricultural soil (200 µg SMX/g) with three different solvents.

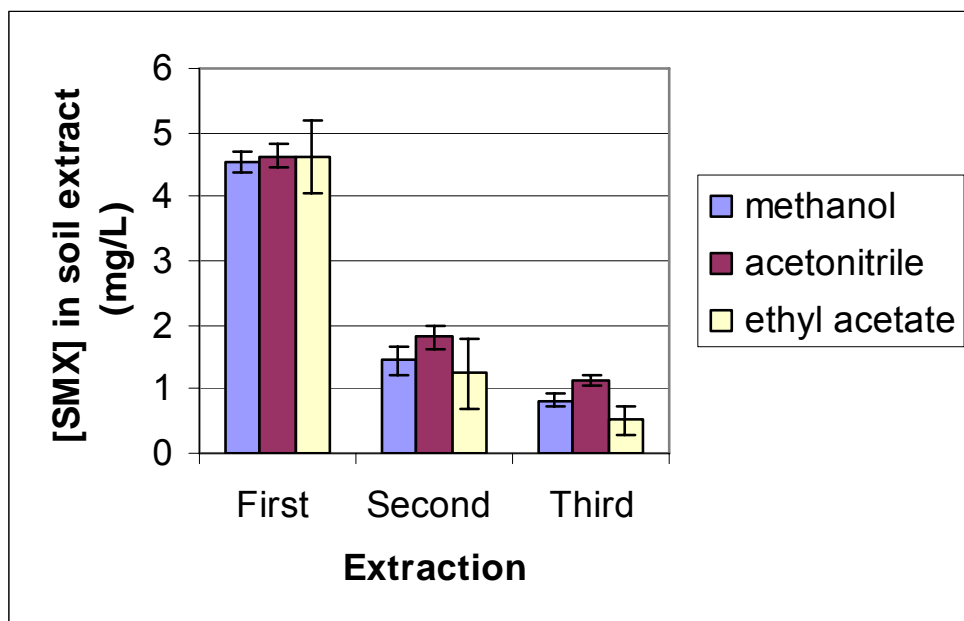
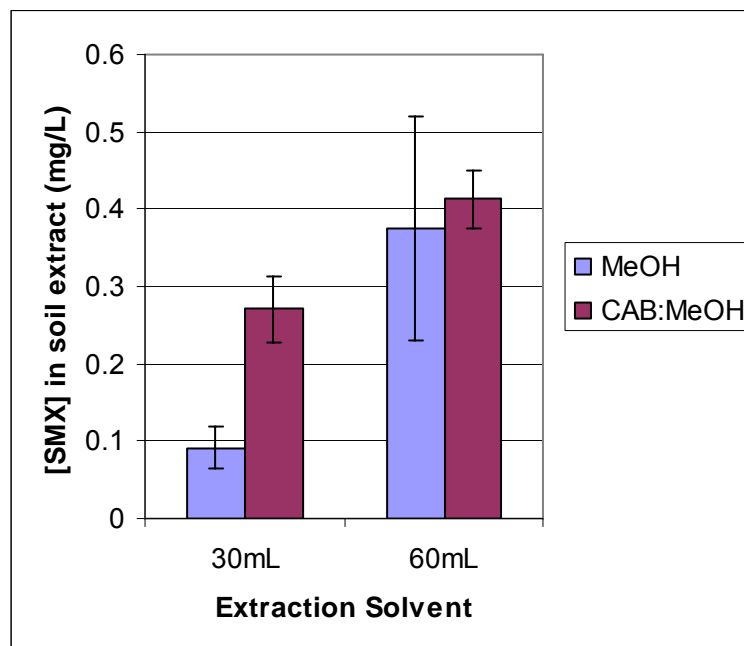


Table 3.8: Results of three consecutive extractions of the same soil sample with three commonly used solvents (200 µg/g) (n = 3).

Extraction	Solvent	Conc (mg/L)	Stdev (mg/L)	%RSD	%Average Recovery
First	Methanol	4.53	0.16	4	57
	Acetonitrile	4.63	0.19	4	58
	Ethyl Acetate	4.63	0.6	13	58
Second	Methanol	1.46	0.22	15	18
	Acetonitrile	1.81	0.18	10	23
	Ethyl Acetate	1.25	0.55	44	16
Third	Methanol	0.82	0.11	13	10
	Acetonitrile	1.11	0.08	7	14
	Ethyl Acetate	0.51	0.24	47	6
Total	Methanol	6.81	0.58	9	85
	Acetonitrile	7.55	0.41	5	94
	Ethyl Acetate	6.39	0.38	6	80

Single extraction recovery needed to be improved to balance maximum analyte recovery with sample processing time. Combinations of pH buffers and organic solvent can be used to extract polar compounds such as antibiotics from sediments. Jacobsen, Halling-Sorensen *et al.* (2004) successfully used a citric acid buffer (pH = 4.7): methanol solvent to extract sulfonamides, tetracyclines, and macrolides with the aid of an automated solvent extractor. Comparing a citric acid buffer (CAB): methanol extraction to pure methanol, the buffer mixture extracted sulfamethoxazole three times better than the methanol alone when using a 30 mL solvent volume to 5 g of soil ratio (Figure 3.28). The difference was not as obvious when using the 60 mL solvent volume for extraction. Results indicate that the extraction efficiency could be improved by increasing the methanol volume. There was less precision in the methanol extracts. The relative standard deviation of the 60 mL methanol extracts was as high as 39%. The poor precision could be exasperated by the variability in organic solvent recovery from the soil.

Figure 3.28: Comparison of methanol with citric acid buffer (CAB) :methanol extracting solvent extract concentrations of SMX from Eastern NC agricultural soil (15 $\mu\text{g/g}$) (n = 3).



3.4.3 Final Sample Solvent

For better antibiotic resolution in LC/MS, the solid phase extracts must be reconstituted

from acetonitrile or methanol to LGW. Figure 3.29a illustrates chromatographically a mixture of CPX, TCC, and SMX at 1mg/L in acetonitrile. Note the fronting of the sulfamethoxazole peak. Normal causes include column channeling, overloading, or ionic interactions. Corrections include replacing the column, changing the stationary phase, increasing the internal diameter, decreasing sample amount, or changing the pH. However, Figure 3.29b shows a chromatogram of these compounds in LGW run under the same conditions, proving the column was not the problem, but instead the sample solvent. Different solvents change the dipole-induced dipole interactions of the analyte, changing the interactions due to structure, polarity, and ionizability with the stationary phase surface adsorption sites. Comparing Figure 3.29a to Figure 3.29b, not only were the retention times shifted and the diode array responses different, but a ghost peak appeared to form in the acetonitrile sample, eluting near the void volume. Sample solvent effects were similar with LC/MS. Consequently, a nitrogen blow down and LGW reconstitution step was added to the extraction procedure. Pure solvent solutions of SMX, TMP, CPX, and TCC were prepared to compare the effects of blowing down to dryness and reconstituting compare to blowing down to approximately 8 - 10% the original volume and then reconstituting. Blowing down to dryness had little effect on the response of sulfamethoxazole or trimethoprim compared to blowing down to approximately 20 μ L of solvent (See Figure 3.30a). The biggest difference was seen in the TCC response (Figure 3.30b).

Figure 3.29a: Ciprofloxacin, Tetracycline and Sulfamethoxazole neat standards (1 mg/L) in acetonitrile analyzed by HPLC with the Waters Series II 996 PDA detector.

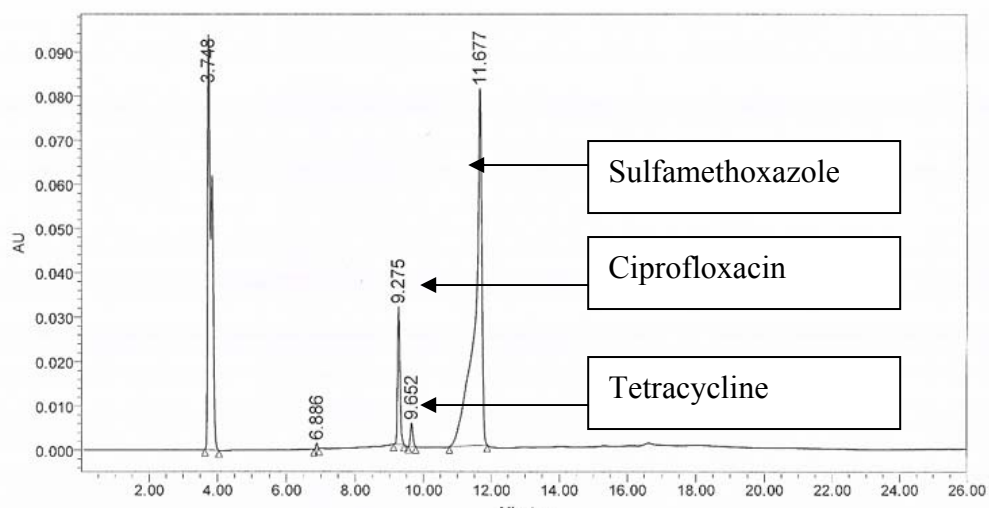


Figure 3.29b: Ciprofloxacin, Tetracycline and Sulfamethoxazole neat standards (1 mg/L) in LGW analyzed by HPLC with the Waters Series II 996 PDA detector.

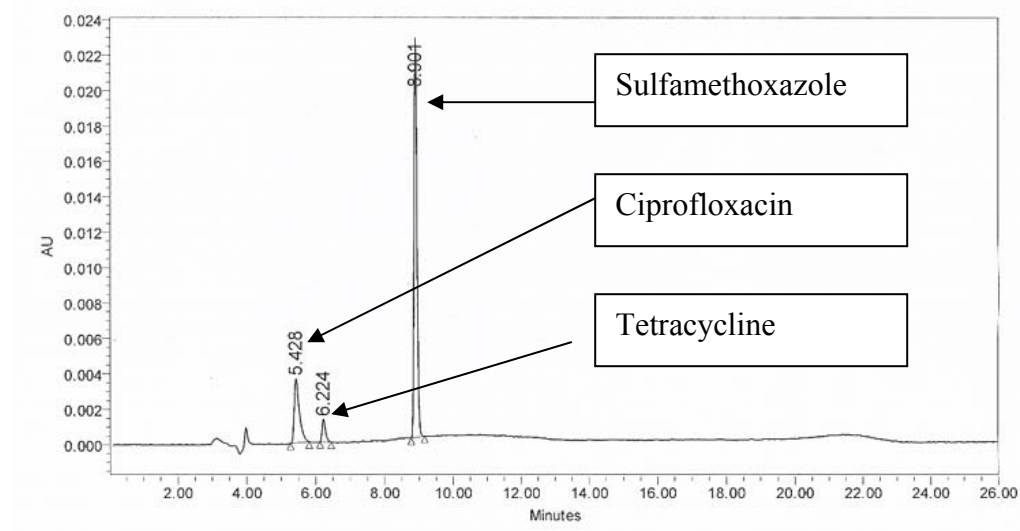


Figure 3.30a: Calibration of SMX in reconstituted solvents.

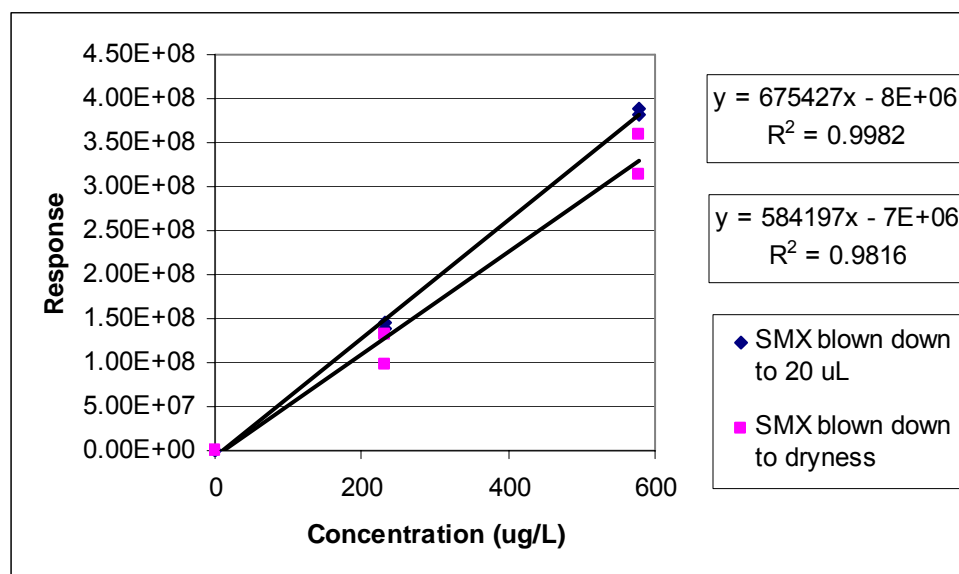
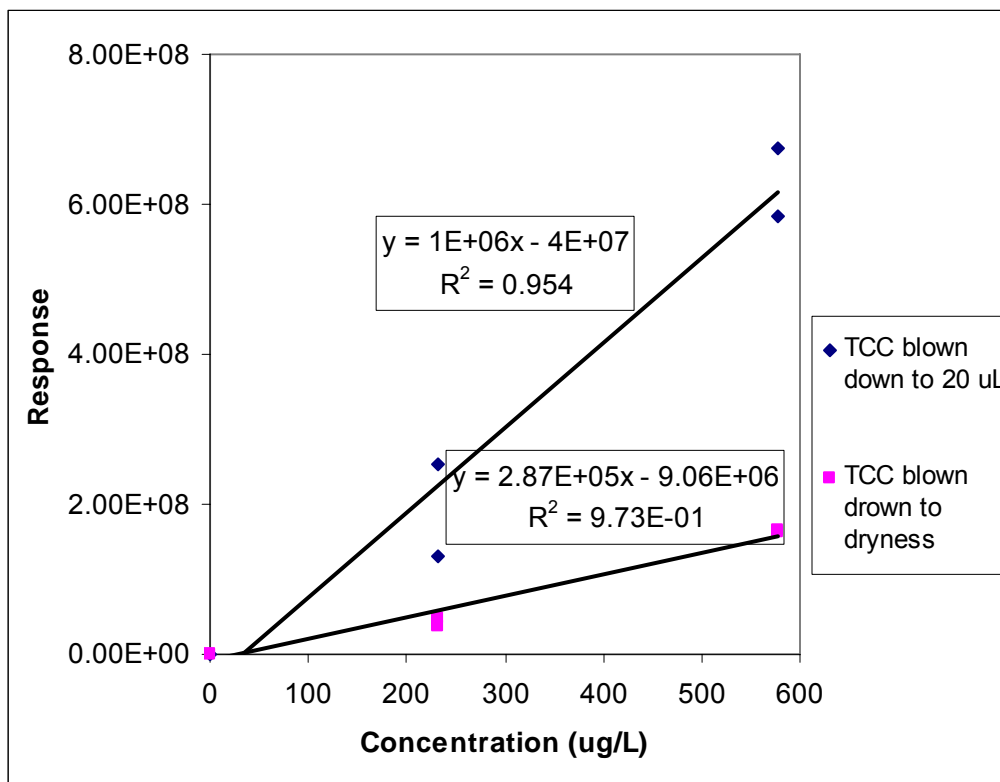


Figure 3.30b: Calibration of TCC in reconstituted solvents.



3.4.4 Instrument Analysis

Matrix calibration curves are essential to calculate the concentration of the target analytes. The following chromatographic figures analyzed on the Waters series II HPLC with model 996 PDA illustrate the elevated background from soil extracts of 0.2M citric acid buffer:methanol and pure methanol from the same unspiked soil (Figures 3.31 and 3.32). The citric acid: methanol extract background response was more elevated than the methanol extract. The baseline maximum of the CAB: methanol extract was 0.015 AU at a retention time around 8 min compared to a baseline maximum of 0.0035 AU around 10 min. Comparing the response of the three analytes (SMX, CPX, and TCC) in the spiked soil extraction, the response in the 0.2M citric acid:methanol (1:1, v:v) extract (Figure 3.33) for sulfamethoxazole was more than twice that in the methanol extract for the same spiked soil (Figure 3.34). Analysis by LCMS/MS offers three degrees of certainty; retention time, the parent mass and daughter ions. Figure 3.35 is an example chromatogram of a Morgan Creek sediment extract comparing the two daughter ions of

trimethoprim (see Table 2.4). Other peaks appear from chemicals that were coextracted; however, only one peak appears to overlap chromatographically in both daughter ion responses. As illustrated before, sample matrix can cause retention time shifts, and the quantifying and confirming breakdown ions add an extra degree of certainty. Therefore, the LC/MS triple quadrupole is preferable for analysis of analytes in complex matrices including all sediment and soil extracts. Figure 3.36 is an example chromatogram of target antibiotic separation and LC/MS/MS identification. Trimethoprim, levofloxacin, ciprofloxacin, tetracycline, and sulfamethoxazole are resolved.

Figure 3.31: Citric acid:methanol extraction of Eastern North Carolina agricultural soil.

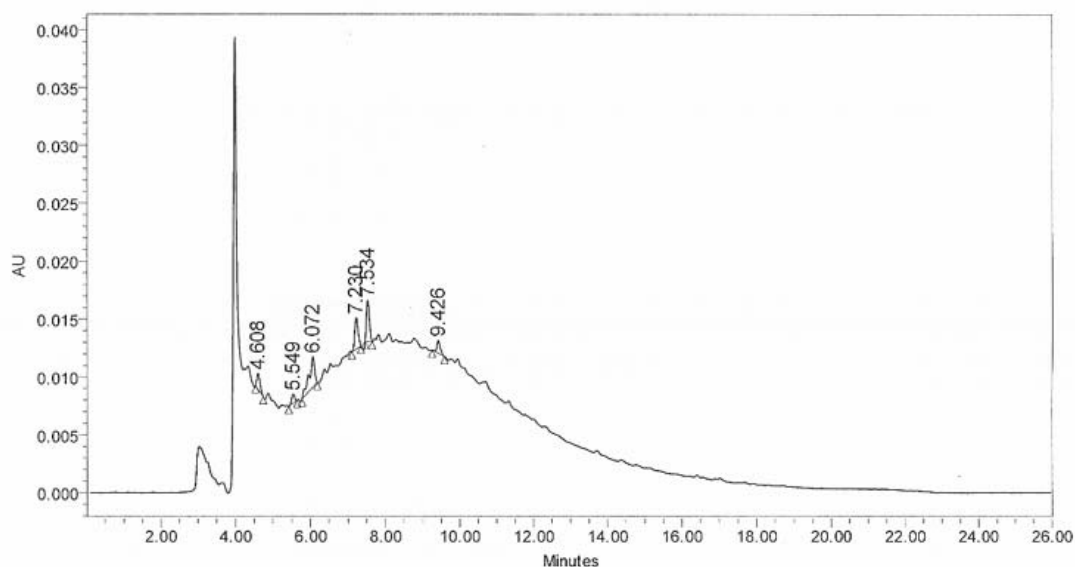


Figure 3.32: Methanol extract of Eastern NC agricultural soil.

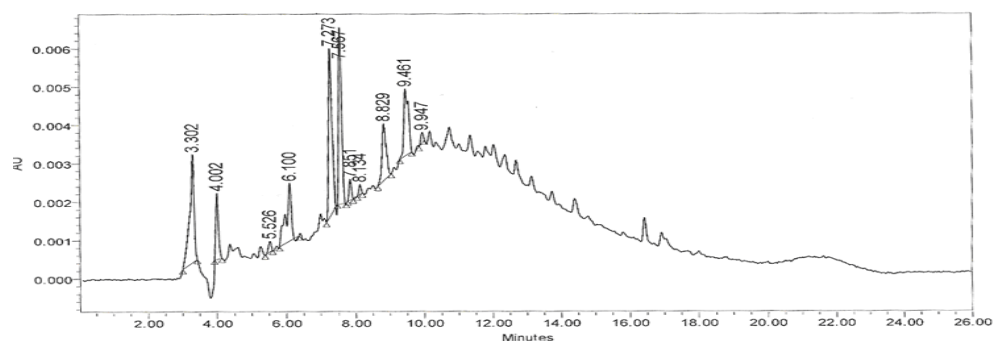


Figure 3.33: 0.2M citric acid:methanol (1:1) extract spiked Eastern NC agricultural soil (15 μg SMX/g soil, 10 μg CPX/g soil; 24 μg TCC/g soil).

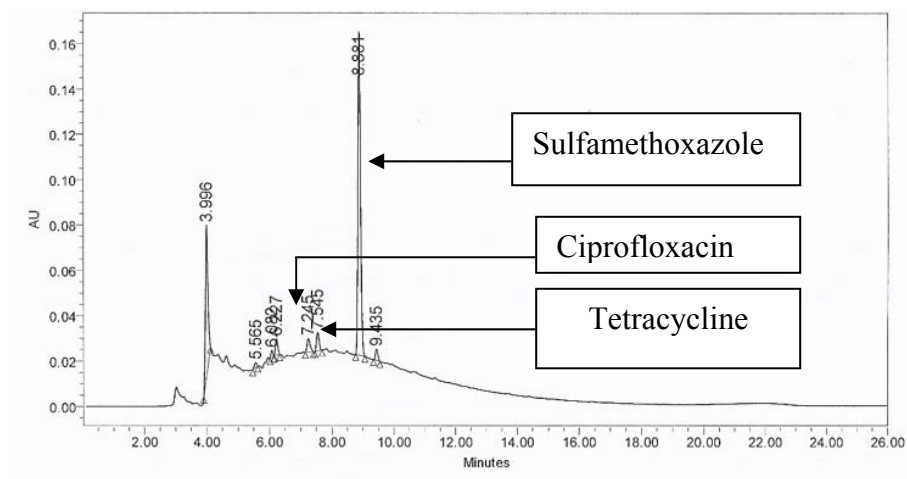


Figure 3.34: Methanol extraction of the spiked Eastern NC agricultural soil (15 μg SMX/g soil; 10 μg CPX/g soil; 24 μg TCC/g soil).

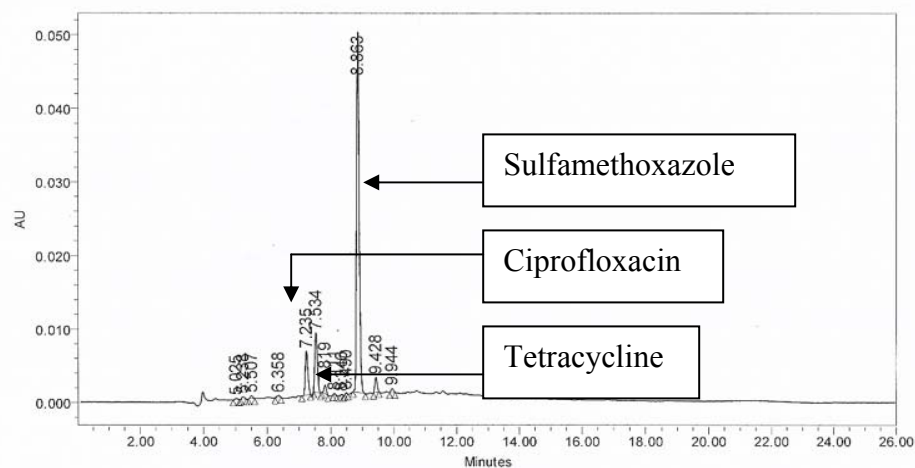


Figure 3.35: LCMS/MS chromatogram of a sediment extract illustrating the importance of the confirmation ion.

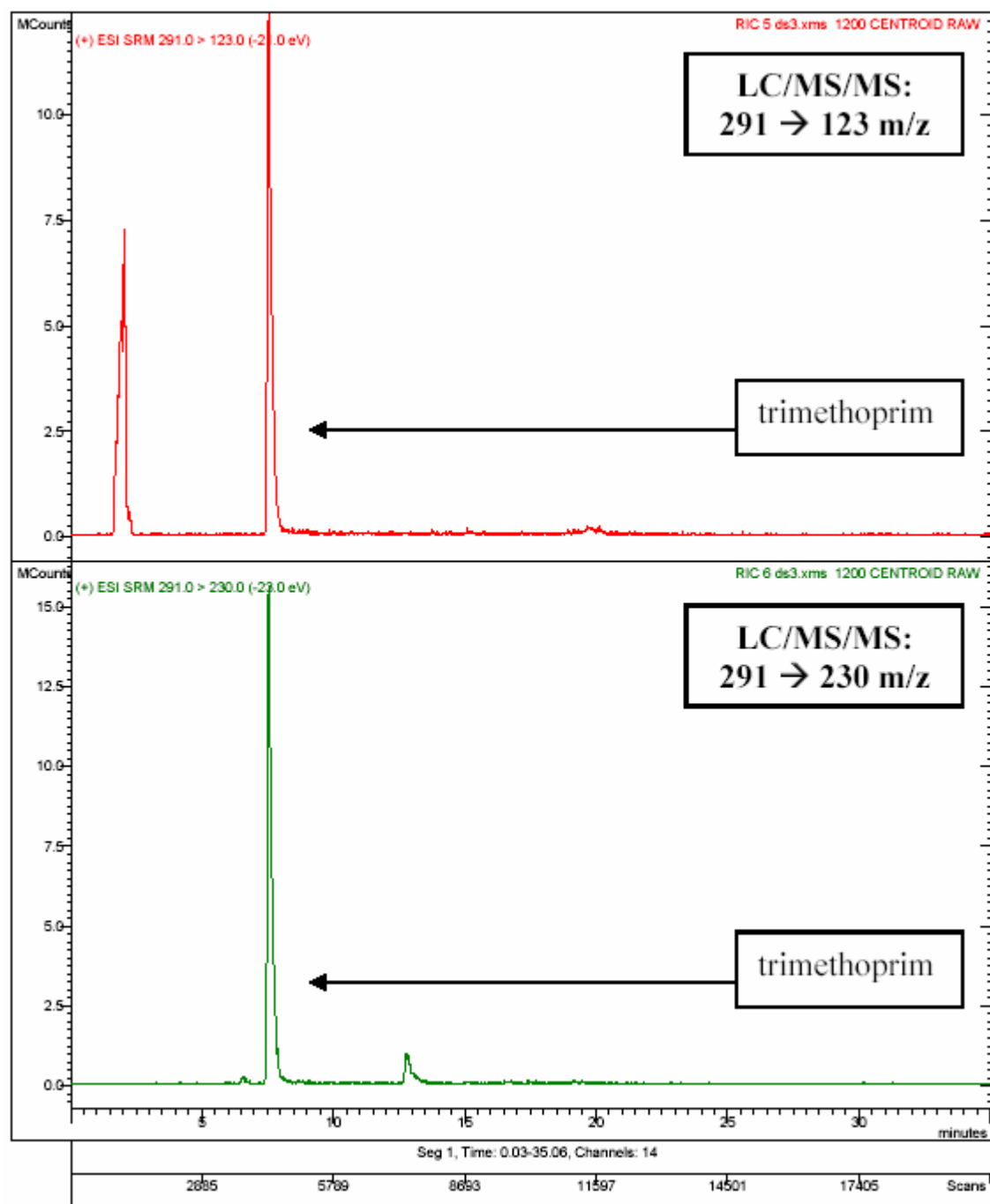


Figure 3.36: An LC-MS/MS example chromatogram of five different antibiotic separations.

Chromatogram Plots

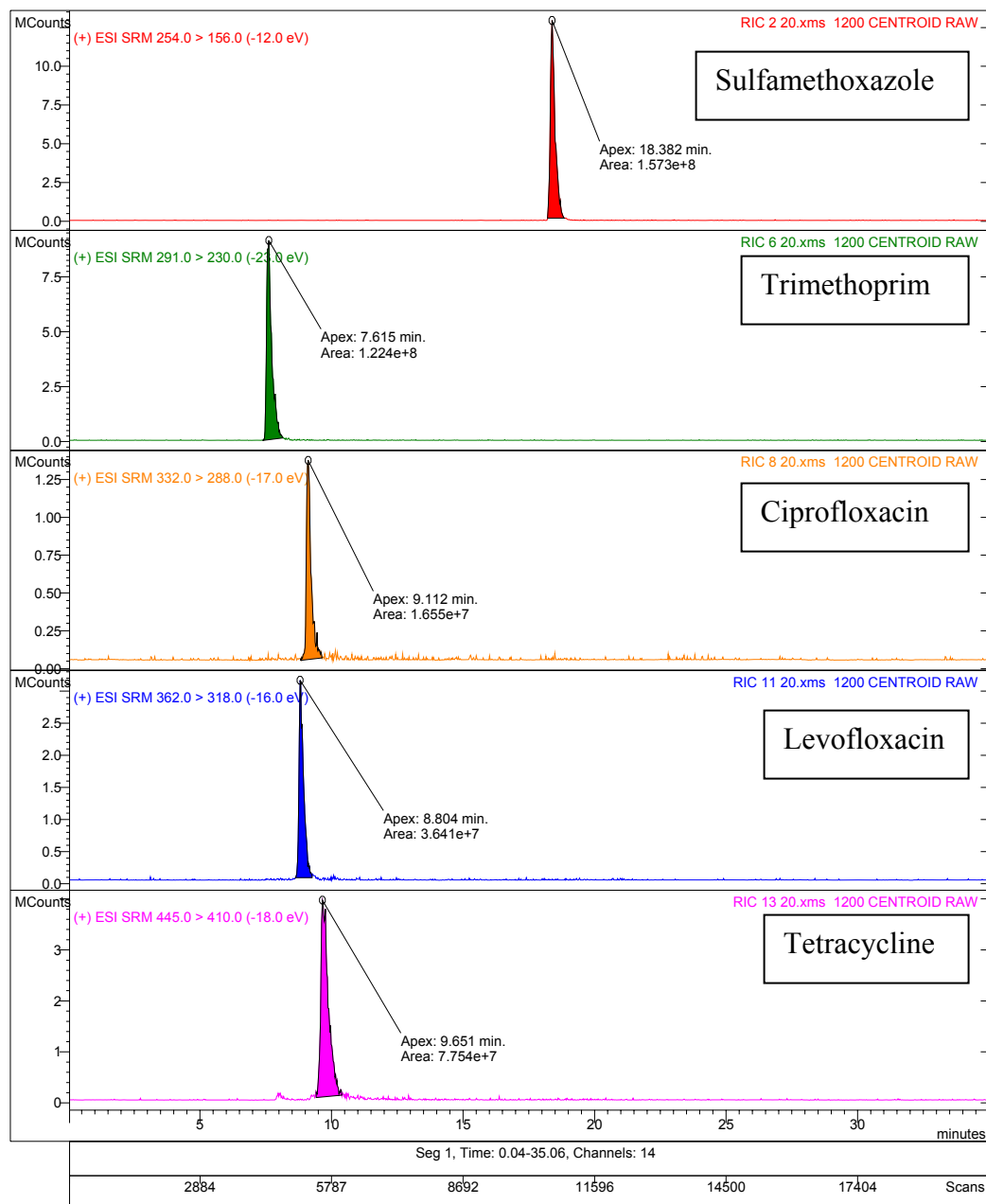
File: ...ocuments and settings\chemicalstastegood\desktop\lcms\032706\20.xms

Sample: 20

Operator:

Scan Range: 1 - 20342 Time Range: 0.04 - 35.06 min.

Date: 3/28/2006 12:10 AM



3.4.5 Standard Addition

Standard Addition was used to quantify antibiotic concentrations in the sediment and the water column. The technique of standard additions is used when the matrix is variable and internal standards are not sufficient to correct for the matrix effects. The technique requires an accurate background correction of the analytical signal intensities but does not account for any instrument drift. When using standard additions on unknown matrices, it is possible to have severe spectral and background correction problems (see Figure 3.37). Compounding the matrix effects, method variability can cause problems with quantitation. The use of a surrogate can help correct for poor method recovery and inconsistency. Figures 3.38a and 3.38b compare the linearity and consistency of a ciprofloxacin standard addition curve to the curve corrected for the relative response of the isotopically labeled ciprofloxacin. The relative response was calculated by dividing the signal intensity of ciprofloxacin by the signal intensity of $^{13}\text{C}_3$ -ciprofloxacin. The concentration based on the standard addition was 5 ng/g in Figure 3.38a, compared to 17 ng/g from the relative response standard addition curve in Figure 3.38b. Standard addition calculations were valid provided that the response of the curve was linear.

Figure 3.37: Example of standard addition for Morgan Creek surface water and OWASA WWTP Effluent for SMX (2/6/2006). (UPS refers to upstream sample ($C_0 = 2$ ng/L); E refers to WWTP effluent ($C_0 = 328$ ng/L); DS refers to downstream sample ($C_0 = 192$ ng/L)).

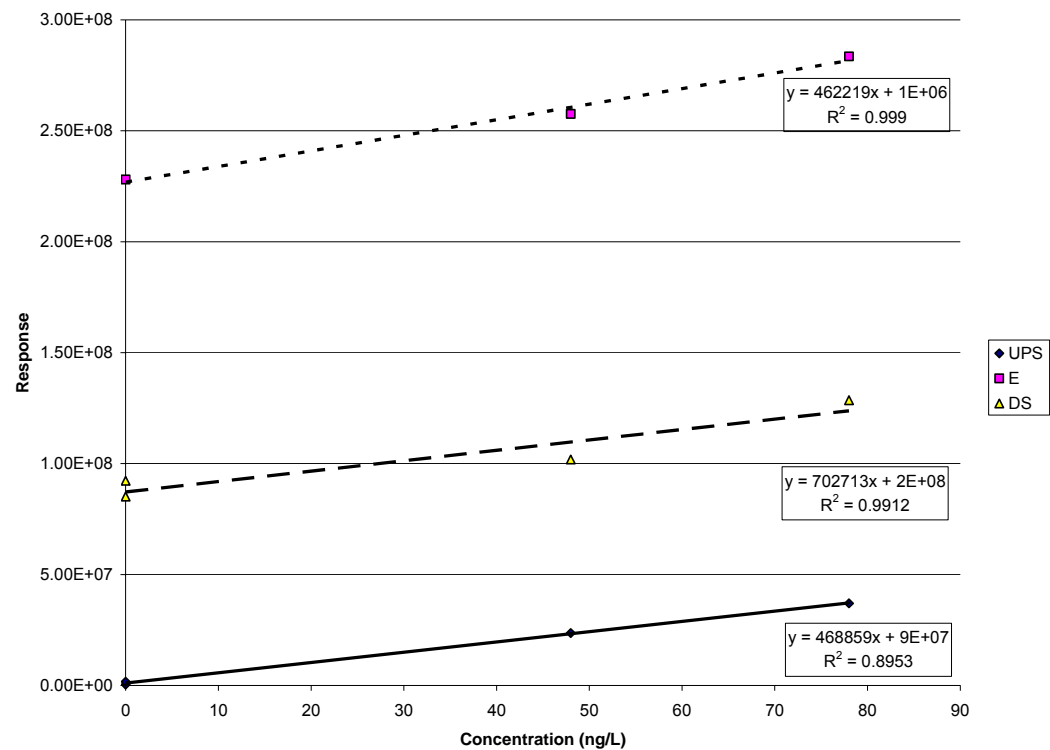


Figure 3.38a: Ciprofloxacin standard addition of a Morgan Creek sediment downstream extraction.

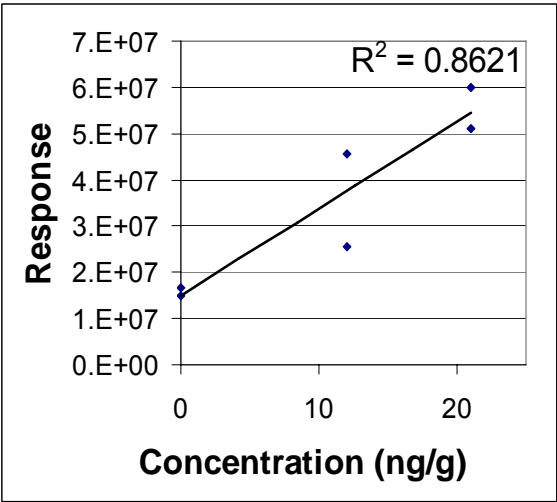
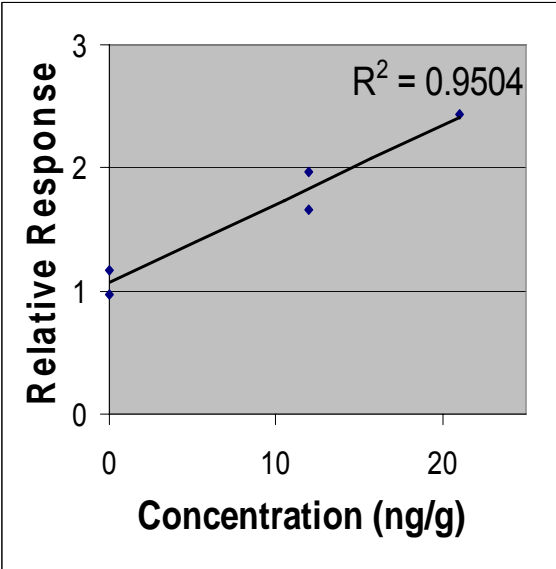


Figure 3.38b: Ciprofloxacin relative standard addition of a Morgan Creek sediment downstream extraction.



3.4.6 Isotopic Dilution

In isotopic dilution, an isotopically labeled version of the target analyte is used as a surrogate for quantitation. It is assumed that the response of the labeled surrogate is proportional in both pure solvent and environmental matrices due to similar chemical behavior. Using this assumption, the labeled surrogate of known concentration should correct for extraction and method errors. The labeled surrogate is spiked into both the environmental sample and a solvent calibration curve at a fixed concentration. The relative response (RR) is calculated using each concentration across the calibration curve as shown in equation 3.1. The RR should be consistent across a linear calibration concentration range. The concentration in the environmental sample is calculated using the RR from the pure matrix as shown in equation 3.2

$$RR = \frac{\text{Area}_{\text{analyte}} \times \text{Concentration}_{\text{labeled}}}{\text{Area}_{\text{labeled}} \times \text{Concentration}_{\text{analyte}}} \quad (3.1)$$

$$\text{Concentration}_{\text{sample}} = \frac{\text{Area}_{\text{analyte}} \times \text{Concentration}_{\text{labeled}}}{\text{Area}_{\text{labeled}} \times RR} \quad (3.2)$$

Two labeled surrogates were used for isotopic dilution; $^{13}\text{C}_6$ -sulfamethoxazole and $^{13}\text{C}_3$ -ciprofloxacin. Example RR calculations are shown in Table 3.9. The RR of sulfamethoxazole is compared to the isotopically labeled version. The isotopically labeled ciprofloxacin was used to compare RR for both levofloxacin (LVX) and ciprofloxacin (CPX). Sulfamethoxazole's calibration linearity is demonstrated in Figure 3.39a. Demonstrations of the linearity of CPX and LVX responses are provided in Figures 3.39b and 3.39c respectively. The detector variations of LVX and CPX appear to mirror each other.

The RR varied slightly from sample set to sample set; therefore, it was imperative to analyze a solvent calibration curve for each run. Comparing standard addition and isotopic dilution calculated concentrations in Table 3.10, there was general agreement for ciprofloxacin (normally less than 20% difference). Results for sulfamethoxazole were surprisingly dissimilar. The concentrations of sulfamethoxazole calculated by the method of isotopic dilution were at least twice those calculated by the method of standard addition.

Carbon-13 is a naturally occurring stable isotope. The surrogate may contain traces of unlabeled SMX; however, the surrogate is spiked into each sample at the same concentration. This spiking would provide an inflated concentration of the SMX calculated by standard addition, but would not explain why every compared concentration was different by a factor of two. The relative ratio of the SMX to surrogate could have changed. It seems unlikely that the carbon-13 would be converted to carbon-12. To examine whether the issue lies with either the instrument response or the method involving complex matrixes, the surrogate could be spiked into soils before solvent extraction, into the soil solvent extract before SPE, and the extracts after SPE.

Table 3.9a: Isotopic dilution relative response of sulfamethoxazole in solvent matrix (LGW) analyzed by LC/MS/MS.

Sulfamethoxazole				
Analyte		Labeled		
Conc (mg/L)	Area	Conc (mg/L)	Area	RR
0	0	0.2	2.47E+08	
0	0	0.2	2.45E+08	
0.104	1.84E+08	0.2	3.00E+08	1.18
0.104	1.97E+08	0.2	3.10E+08	1.22
0.208	3.10E+08	0.2	2.59E+08	1.15
0.208	3.17E+08	0.2	2.85E+08	1.07
0.312	4.52E+08	0.2	2.71E+08	1.07
0.312	4.87E+08	0.2	2.93E+08	1.07
0.416	6.31E+08	0.2	2.85E+08	1.06
0.416	6.53E+08	0.2	2.98E+08	1.05
Average			2.79E+08	1.11
Stdev			2.28E+07	0.07
%RSD			8	6

Table 3.9b: Isotopic dilution relative response of ciprofloxacin in solvent matrix (LGW) analyzed by LC/MS/MS.

Ciprofloxacin				
Analyte		Labeled		
Conc (mg/L)	Area	Conc (mg/L)	Area	RR
0	0	0.4	8.80E+07	
0	0	0.4	9.54E+07	
0.2	1.87E+07	0.4	3.70E+07	1.01E+00
0.2	1.83E+07	0.4	3.24E+07	1.13E+00
0.4	7.64E+07	0.4	8.33E+07	9.17E-01
0.4	5.21E+07	0.4	5.81E+07	8.97E-01
0.6	6.76E+07	0.4	4.61E+07	9.77E-01
0.6	1.05E+08	0.4	8.66E+07	8.09E-01
0.8	1.50E+08	0.4	7.83E+07	9.55E-01
0.8	1.37E+08	0.4	8.32E+07	8.26E-01
Average			6.88E+07	0.94
Stdev			2.32E+07	0.10
%RSD			34	11

Table 3.9c: Isotopic dilution relative response of levofloxacin in solvent matrix (LGW) analyzed by LC/MS/MS.

Levofloxacin				
Analyte		Labeled ¹³ C ₃ -CPX		
Conc (mg/L)	Area	Conc (mg/L)	Area	RR
0	0	0.4	8.80E+07	
0	0	0.4	9.54E+07	
0.2	4.01E+07	0.4	3.70E+07	2.17
0.2	3.98E+07	0.4	3.24E+07	2.45
0.4	1.62E+08	0.4	8.33E+07	1.94
0.4	1.03E+08	0.4	5.81E+07	1.77
0.6	1.47E+08	0.4	4.61E+07	2.12
0.6	2.19E+08	0.4	8.66E+07	1.68
0.8	3.00E+08	0.4	7.83E+07	1.92
0.8	2.84E+08	0.4	8.32E+07	1.71
Average			6.88E+07	1.97
Stdev			2.32E+07	0.27
%RSD			34	13

Figure 3.39a: Calibration curve illustrating the linearity of the sulfamethoxazole response (LC/MS/MS).

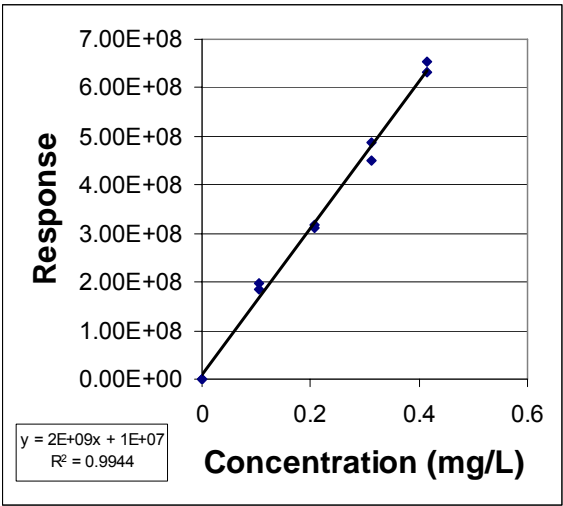


Figure 3.39b: Linearity of ciprofloxacin calibration curve in LGW analyzed by LC/MS/MS.

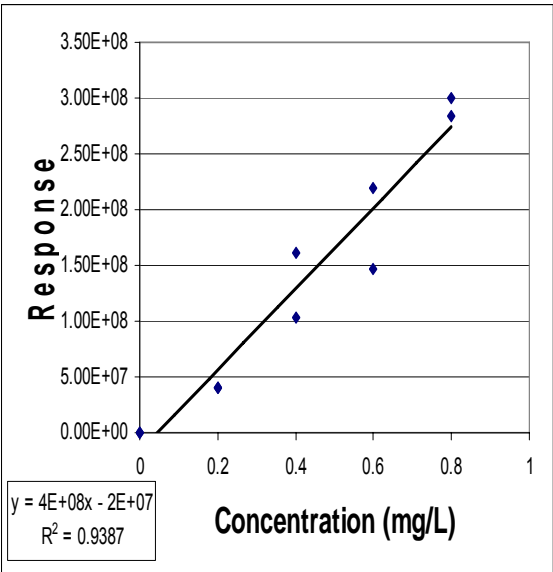


Figure 3.39c: Linearity of levofloxacin calibration curve in LGW analyzed by LC/MS/MS.

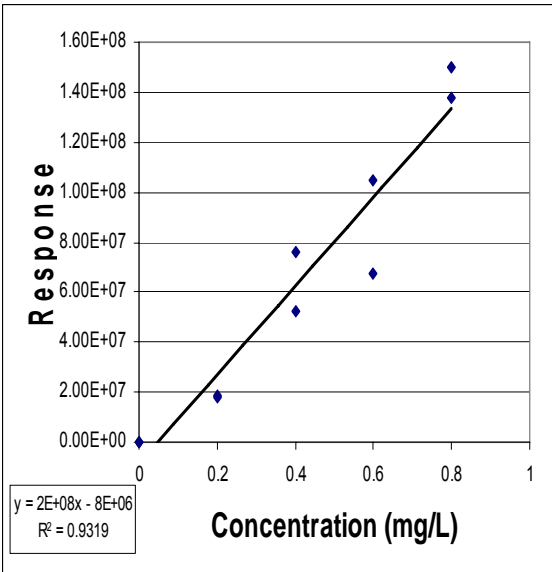


Table 3.10: Comparing standard addition calculated concentrations to isotopic dilution concentrations from Morgan Creek effluent sediment (2/14/06).

	Spike Conc (ng/g)	Standard Addition Conc (ng/g)	Isotopic Dilution Conc (ng/g)	%Difference
CPX	0	13	17	27
	12	25	29	15
	12	25	29	15
	21	34	36	6
SMX	0	0.45	1.2	91
	9	9.45	20	72
	9	9.45	20	72
	15	15.45	31	67

3.5 Environmental Surface Water and Sediment Extractions

On February 6, 2006, the OWASA WWTP released 8.7 MG (13 ft³/s) of UV disinfected effluent into Morgan Creek, contributing to the mean downstream flow of 21 ft³/s. The WWTP effluent therefore accounted for 61% downstream flow. Dilution does not fully account for the decrease in antibiotic concentration 2378 ft downstream for the point of effluent discharge (Table 3.11). The ratio of SMX to TMP in the surface water is slightly less than the pharmaceutical dose of 5:1. The concentrations of antibiotics in the Morgan Creek sandy sediments at the point of wastewater discharge were similar half a mile downstream (Table 3.12). By converting sediment concentrations into parts per trillion (ppt), it appears that sediment levels of antibiotics are much higher than those in the aqueous phase (Table 3.13). Most notable was the concentration of ciprofloxacin, which was over 500 times more concentrated in the sediment. Analysis of the vacuum dried sediment after one month of storage in the dark at 4°C yielded similar concentrations of antibiotics, indicating stability. Included in the analysis was levofloxacin, detected at 30 ng/g sediment (Table 3.14). Results appear to indicate the gradual accumulation of antibiotics in sediments exposed to continuous levels of antibiotics released from the WWTP even though sulfamethoxazole was previously shown not to significantly partition into sandy, low-organic soils in the reactor (*Section 3.3.3*). The sediments in Morgan Creek downstream from the OWASA WWTP have been exposed to a continuous flow of nanogram per liter levels of antibiotics for years, with equilibrium already established, as

compared to the maximum two week exposure of the reactor sediments to a fixed volume of water. None of the aqueous SMX photodegradation byproducts previously identified in *Section 3.3.4* were detected in the sediments.

Table 3.11: Aqueous antibiotic concentrations in surface water (Morgan Creek) around the OWASA WWTP (2/6/2006) (nd = not detected).

	Concentration (ng/L)			Fraction downstream compared to effluent (%)
	Upstream	Effluent	Downstream	
SMX	2.0	328	192	59
TMP	33	110	49	45
CPX	nd	61	15	25
TCC	nd	46	4.0	9.0

Table 3.12: Sediment antibiotic concentrations in surface water (Morgan Creek) around the OWASA WWTP (2/6/2006) (nd = not detected).

	Concentration (ng/g)		
	Upstream	Effluent	Downstream
SMX	nd	0.6	0.7
TMP	nd	4.0	3.0
CPX	nd	25	20
TCC	nd	0.7	2.0

Table 3.13: Comparison of the aqueous and sediment concentrations in surface water (Morgan Creek) around the OWASA WWTP (ppt) (2/6/2006) (nd = not detected).

	Upstream		Effluent		Downstream	
	Water	Sediment	Water	Sediment	Water	Sediment
SMX	2.0	nd	328	600	192	700
TMP	33	nd	110	4000	49	3000
CPX	nd	nd	61	25000	15	20000
TCC	nd	nd	46	700	4.0	2000

Table 3.14: Sediment antibiotic concentrations of sediments extracted from date of collection and one month later (na = not applicable; Note: LVX was not included in the February 16, 2006 analysis).

Date of Analysis	Concentration (ng/g)	
	2/16/2006	3/14/2006
TMP	3	5
CPX	20	17
LVX	na	30

CHAPTER 4

CONCLUSIONS

In the photolysis reactors, sulfamethoxazole was found to be susceptible to photodegradation. However, the presence of natural organic matter and particulates in the water column increased the persistence of sulfamethoxazole in the aqueous phase. Sorption to sediments was negligible in reactors except in the presence of high-organic soil when 15% partitioned over 20 hrs of recirculation. Since most streams and rivers have low organic content in the sediments, the concentration of sulfamethoxazole in those sediments is expected to be low in comparison to other xenobiotics. On the other hand, photolysis byproducts were identified in the aqueous phase, including an isoxazole isomer which was also detected in the effluent discharge of a WWTP and further downstream when low pressure mercury lamps were used to disinfect the effluent.

Sulfamethoxazole, trimethoprim, tetracycline, ciprofloxacin, and levofloxacin were extracted from sediments located at the point of WWTP discharge and 725 m downstream. Concentrations in the sediment were higher than those found in the surface water and effluent, particularly for ciprofloxacin (at least 400 times more concentrated in the sediment). While there have been many studies regarding the occurrence of antibiotics in WWTP effluent and surface water, less is known regarding their fate.

This study found antibiotic accumulation in the sediments, which is also a sink for bacterial accumulation. This finding increases the possibility of microbes developing antibiotic resistance in the sediments.

Further work with the photolysis/water/sediment reactors could include changing the concentrations in the aqueous phase to more environmentally relevant concentrations (mg/L to low $\mu\text{g/L}$ levels). The light source could be changed to a lamp that better simulates natural sunlight, such as a Xenon arc lamp. The residence time of the target antibiotics in the reactor could be increased from hours/days to days/weeks/months. More

work could be done with other antibiotics and in mixtures to compare competition for sorption and photolysis. Microbes from the water and sediments contained in the reactors could be isolated and tested for antibiotic resistance.

Possible avenues of further investigation in terms of the environmental sampling research include collecting water and sediment further downstream and comparing to the antibiotic concentrations at points closer to the treatment plant effluent discharge. More surface water and sediment samples from different locations impacted by municipal discharge should be analyzed and characterized for comparative purposes and will help identify potential areas of antibiotic resistance propagation.

Appendix A: Soil Characterization Procedures

Determination of Soil Ph

1. Calibrate a pH meter/combination electrode with two standard buffers that span the expected pH range of the soil. Generally buffers of pH 4 and 7 will work.
2. Weigh a 50 g sample of freshly sieved soil into a 100 ml beaker.
3. Add 50 ml deionized water and stir the mixture. A stir bar will not work in this situation so a spatula or similar object must be used.
4. Let the solution stand for 30 min and read the pH with the tip of the electrode suspended in the overlying liquid phase. Be sure to gently swirl the slurry while determining the pH.

Gravimetric Soil Moisture Determination (%M)

1. Fill numbered 4 oz jar with field-moist soil
2. Record mass of jar + moist soil
3. Dry in oven @ 105°C for 24 hours. The oven is set for 105°C, so do not adjust.
4. Record mass of jar + dry soil.
5. Consult table of jar masses and subtract mass of jar from determination made in #2 and #4.
6. Calculate soil moisture (%M)

$$\%M = \left(\frac{\text{wetmass}}{\text{drymass}} - 1 \right) 100$$

7. Save the oven-dried sample for determination of soil particle density, total-C, total-N, organic matter content or water holding capacity.

Organic Matter Content of Soils

1. Dry ~ 100 g or more of soils in oven @ 105°C for 24 hours.
2. Fill numbered porcelain crucible with oven-dried soil.
3. Record the mass of crucible + oven-dried soil.
4. Combust at 550°C for 4 h. Remember, it takes the muffle oven >1 h to reach 550°C.
 - a. Do not leave the muffle oven on unattended overnight. These instruments are subject to “core meltdowns”.
5. Allow samples to cool and determine the mass of crucible + ashed soil.

6. Consult the table of crucible masses and subtract the mass of the crucible from the mass of oven-dried soil + crucible (= DW) and the mass of the ashed soil + crucible (= AFDW).
7. Calculate the % organic content (%OM) of the soil:

$$\%OM = \left(\frac{DW - AFDW}{DW} \right) * 100$$

Determination of Soil Texture

1. Soil texture determination requires the following materials: hydrometer, 2 L clear glass graduated cylinder, thermometer, blender, timer and stir rod (optional).
2. Prepare the following reagent:
 - (a) Sodium hexametaphosphate
 40 g sodium hexametaphosphate ($\text{Na}_{15}\text{P}_{13}\text{O}_{40}$ - $\text{Na}_{20}\text{P}_{18}\text{O}_{55}$) → 1 L of DI water.
 Store in 1L polyethylene bottle at room temperature. Infinite shelf life.
3. Weigh 50 g or 100 g of homogenized, oven-dried (24 h @ 105°C) soil and transfer it to the blender cup. Use 50 g if soil is clayey or 100 g if soil is sandy.
4. Fill the blender cup with distilled water to within 10 cm of the rim and add 10 ml of sodium hexametaphosphate. Blend for 15 min.
5. Transfer the soil suspension into the 2L graduated cylinder. Wash remaining soil from the blender cup to the 2 L cylinder with DI water. If 50 g sample is used, make up the volume in the cylinder to 1130 ml. If 100g sample is used, fill to 1205 ml. The volume need not be exact. Mix the suspension thoroughly with the stir rod or by covering and inverting the cylinder so that all sediment is in suspension.
6. **Immediately** after mixing, gently place the hydrometer in the suspension. **Do not drop** the hydrometer in the graduated cylinder as it may break and in the very least will still be bobbing after 40 s. If the solution has a foamy head, add ~1 ml of amyl alcohol with a pasteur pipet to disperse the foam. **Exactly** 40 s from when the stirring stopped, read to the nearest scale division the top of the meniscus on the hydrometer stem.
7. Remove and rinse the hydrometer. Resuspend the soil and take a second 40 s reading exactly as described above. Average these two readings. After the hydrometer has been removed and rinsed for the second time, record the temperature to the nearest 0.1°C using the Omega hand-held LCD unit and the stainless steel thermistor probe.

8. Resuspend the soil particles as described above and take a third hydrometer reading after 120 min of settling time. Record the temperature after the hydrometer has been removed.

To calculate the soil texture:

Correct the hydrometer reading for deviations from 68°F.

- (a) Convert your temperature reading to °F: $^{\circ}\text{F} = (^{\circ}\text{C} \times 9/5) + 32$
- (b) Add 0.2 hydrometer units per °F above 68°F or subtract 0.2 units per °F below 68°F.

Sample correction:

Time	Hydrometer reading	Temp	Corrected reading
40s	25.0	78°F	$25.0 + 0.2(78-68) = 27.0\text{g}$
120 min	10.0	76°F	$10.0 + 0.2(76-68) = 11.6\text{g}$

The principle for these calculations is:

% sand + %silt + %clay = 100%,

where the average 40 s reading gives the silt + clay content

and the 2 h reading gives the clay content

Sample calculation (assuming a 50 g dw sample):

40s reading: % (silt+clay) = $(27.0/50) \times 100 = 54.0\%$

(average) % sand = $100 - 54.0 = 46.0\%$

2h reading: % clay = $(11.6/50) \times 100 = 23.2\%$

% silt = $54.0 - 23.2 = 30.8\%$

Thus, this soil is 46% sand, 31% silt and 23% clay.

Note:

The hydrometer readings are divided by 50 and multiplied by 100 in the case of a 50 g sample to make the percent composition sum to 100. If a 100 g sample is used, no fudge factor is necessary because 100/100 is unity.

Determination of Soil Particle Density (D_p)

1. Dry wet soil sample @ 105 °C for 24 hr.
2. Homogenize soil sample with mortar and pestle.
3. Determine mass of dry pycnometer plus cap (P_a)

4. Fill pycnometer with water (be sure water is approximately at room temp), add cap, dry exterior, and determine mass (P_w)
5. Determine mass of pycnometer/soil/ H_2O (P_{sw})
 - a) Put ~20 ml water in pycnometer
 - b) Put known mass of dry soil (M_s ; use ~40 g) in pycnometer
 - c) Cap, invert, and shake to thoroughly wet soil
 - d) Fill pycnometer, cap, dry exterior and determine mass
6. Calculate particle density (D_p):

$$D_p \text{ (g cm}^{-3}\text{)} = \frac{M_s}{M_s - (P_{sw} - P_w)}$$

Determination of Water Holding Capacity (WHC)

1. Dry at least 20 g soil in 105°C oven for 24 hours.
2. Weigh a small amount of soil homogenized soil (~5 g works well) in a small, tared, weighboat. It is best to use soil that has been pulverized with mortar and pestle. Record the dry soil mass.
3. Saturate a labeled Whatman #19 cm diameter filter paper with H_2O . Use a Kimwipe to remove excess. Weigh and record mean mass of several saturated filters. The largest source of error is in determining the mass of a saturated filter. Filters lose moisture rapidly, so record the mass as soon as possible after saturating and wiping off excess H_2O . Obtain an average mass of a saturated filter paper.
4. Put the wet filter paper in one of the large red funnels and support the funnel in a wire test tube rack. Add the dry, weighed soil to the saturated filter paper. Saturate the dry soil with H_2O and cover the filter cone with foil to keep the filter entirely saturated. Allow the excess water to drip out of the filter cone (~ 2 hr).
5. Pat excess moisture from the bottom of the filter (i.e. beneath the soil) with a kimwipe. Weigh the wet filter + wet soil and record the combined mass.

To calculate Water Holding Capacity:

1. Subtract the average mass of a wet filter from the mass of a wet filter + saturated soil to obtain the mass of water-saturated soil:
 ex. 8.72 g (wet filter+wet soil) - 1.74 g (ave. mass wet filter) = 6.98 g wet soil

2. To obtain mass of H₂O held in saturated soil, subtract:

$$\text{wet soil mass} - \text{dry soil mass} = \text{mass of H}_2\text{O}$$

3. Calculate Water Holding Capacity (WHC):

$$\text{WHC} = \left(\frac{\text{Mass H}_2\text{O}}{\text{Mass dry soil}} \right) * 100$$

Appendix B: Procedure for Total Organic Carbon (TOC) Analysis (Based on Standard Method 5310B)

Sample storage and preparation

1. The holding time between sample collection and analysis is two weeks maximum.
2. Samples should be stored headspace-free in a refrigerator until analysis.
3. Samples that will not be analyzed immediately should be preserved by adding one drop of 0.2 N hydrochloric acid.
4. Take samples out of the refrigerator and allow to warm to room temperature before analysis.
5. Transfer samples from the holding containers into acid-washed TOC vials.
 - a. Pour a small amount of sample into the vial.
 - b. Swish around and throw out.
 - c. Fill the vial with sample up to the rim.

Acid-wash procedure of the TOC vials;

1. Rinse dirty vials three times with tap water.
2. Soak vials overnight in a 10% nitric acid bath.
3. Rinse vials three times with tap water.
4. Rinse vials three times with deionized water.
5. Dry vials overnight in an oven set at 160°C.

Preparation of calibration standards

1. Calibration standards should be prepared each time the analyzer will be run.
2. The calibration standards prepared should bracket the expected range of concentrations of the samples.
3. Four calibration points should be used to develop a calibration curve, including the blank (zero point).
4. The calibration standards are made of potassium hydrogen phthalate (purchased from Nacalai Tesque).
5. Prepare a 1000 mg-C/L stock solution of potassium hydrogen phthalate for subsequent dilutions.
 - a. Stock solution should be kept in a head-space free vial.
 - b. The vial should be amber glass or wrapped aluminum foil to protect the

solution from light (photolabile).

- c. The stock solution lifetime is two months.
- 6. Calibration standards should be made using volumetric flasks and pipets.
 - a. Run calibration standards of 0.0, 0.5, 3.0, and 6.0 mg-C/L.
 - b. Use higher standard concentrations if TOC values are expected to be greater than 6 mg-C/L but less than 10 mg-C/L (maximum concentration).
- 7. Sample calculations for a calibration standard:

Concentration of stock solution: 1000 mg-C/L

Desired final concentration: 10 mg-C/L

Volume: 100 mL

$(10 \text{ mg-C/L}) \times (100 \text{ mL}) \times (1\text{L}/1000 \text{ mL}) = 1 \text{ mg-C/L}$

$(1000 \text{ mg-C/L}) \times V (\text{mL}) \times (1\text{L}/1000 \text{ mL}) = 1 \text{ mg-C/L}$

$V(\text{mL}) = 1 \text{ mL}$

To obtain a 10 mg-C/L calibration solution, 1 mL of stock solution should be diluted to 100 mL with LGW.

- 8. Transfer calibration standards from the 100 mL volumetric flasks to the calibration vials.
 - a. Wash each vial with a small volume of sample
 - b. Fill each vial to 80% full.
- 9. Place the standards into the autosampler tray slots marked S1, S2...S7 in order of increasing concentration.
- 10. Add two drops of 0.2 M hydrochloric acid to the samples and three drops to the calibration standards.
- 11. Run unknown samples in duplicate.
- 12. After every 10 samples, inject an LGW sample and run a check standard of 3.0 or 5.0 mg-C/L.

Preparation of the TOC analyzer

- 1. Turn on the power to the sampling tray and analyzer (one power switch).
- 2. Turn on main valve on the air tank and the valve on the regulator (ultra zero grade air from Sunox).
 - a. Make sure the pressure gauge stays above 500 psi.

- b. Replace air tanks at 500 psi.
- 3. Check the following inside the instrument:
 - a. The carrier gas rotameter in the top left corner of the instrument should be at least 150 cfh.
 - b. The level of the humidifier (glass bottle inside the instrument) should be between the two white lines.
 - i. If not; turn of the instrument.
 - ii. Fill the bottle to the top white line with LGW.
 - iii. Add one potassium hydroxide pellet.
 - c. There should be continuous air bubbles in the IC reaction vessel (plastic).
- 4. Fill the rinsing water vessel (plastic bottle outside the instrument) with LGW.
 - a. Make sure the tubing reaches to the bottom of the vessel with out having tension in the line.
- 5. Turn on the furnace.
 - a. Warm up time to 680°C 20-30 min.
 - i. Press “NEXT” (F1) to get to MAIN MENU.
 - ii. Press “3” and “ENTER” to get to GENERAL CONDITIONS
 - iii. Scroll down to TC FURNACE ON/OFF
- 6. Allow the Baseline to equilibrate
 - a. Press F5 to return.
 - b. Press F2 to get to the MAIN MENU.
 - c. Press 6 and ENTER to go to the MONITOR SCREEN.
 - i. This screen list the status of the five options (furnace, temperature, dehumidifier, baseline position, baseline fluctuation, and baseline noise).
 - ii. All five options must read “OK” before the run can start.
 - iii. Note: If the baseline is out of range:
 - 1. First make sure that the air is turned on to the instrument.
 - 2. Allow the instrument sufficient time to warm up (often during start-up, the baseline will fluctuate).

3. Adjust scale from 1 (the smallest) to 5 or 30 (the largest) to locate the baseline.
 - a. Position is adjusted using a screwdriver to turn the screw at the top of the instrument that reads “Optical Zero.”
7. Perform a mechanical check of the injection arms.
 - a. Note: Never touch anything until the instrument stops moving.
 - b. In MAIN MENU, press 8 and ENTER to get to MAINTENANCE screen.
 - c. Scroll down to MECHANICAL CHECK and press ENTER.
 - d. Hit the ASI button, then test the four arm positions in the following order
 - i. S1
 - ii. V1
 - iii. V43
 - iv. RINS
 - e. Press ARM DOWN so that the needles go into the rinsing tubes.
 - i. Make sure the needles do not hit the sides of the tubes.
 - f. Press RINSE ON and wait for the water to flow through the tubes before hitting RETURN.
 - g. Check the syringe inside the analyzer for air bubbles.
 - i. Use the SYR PUMP DOWN and SYR PUMP UP buttons to loosen air bubbles.
 - ii. Air bubbles can also be dislodged by lightly tapping the syringe.
 - iii. When all air bubbles are removed, leave the syringe in the “up” position.
 - h. Turn of the rinsing mode by pressing the buttons in the following order:
 - i. ASI
 - ii. RINSE OFF
 - iii. RETURN
 - iv. END
 - v. F2 to return to MAIN MENU
8. Enter the sample information by pressing 9 then ENTER in the MAIN MENU to

get to the AUTO SAMPLER screen.

Figure 1: AUTO SAMPLER screen headings

Type	IS	FS	C1	C2	C3	F1	F2	F3	RG	VOL	W	NO	MAX	SD	CV	SP	DIL
NPOC			1	**	**	**	**	**	1	53	4	1	1			0	1
NPOC	1	30	2	**	**	**	**	**	1	53	4	3	5	200	2	5	1
NPOC	31	70	3	**	**	**	**	**	1	53	4	3	5	200	2	5	1

Table 1: Explanation of abbreviations used in the AUTO SAMPLER screen

Abbreviation	Description
NPOC	Non-purgeable organic carbon
IS	Initial sample number
FS	Final sample number
C1, C2, C3	Calibration curve(s) that will be created during the run and used to compare against the samples
F1, F2, F3	Existing calibration curve(s) against which the samples will be compared
RG	Range (options are 1, 5, or 30)
VOL	Injection volume in microliters
W	Number of washes
NO	Number of injections whose standard deviation (SD) and coefficient of variation (CV) should fall within set limits
MAX	The maximum number of injections to obtain the desired SD and CV
SD	Standard deviation
CV	Coefficient of variation
SP	Spurge time
DIL	Dilution Factor

The first line in the AUTO SAMPLER screen sets up the instrument to run a practice calibration curve without sparging or adding acid to the calibration standards. When a number “1” is entered into one of the “C” columns, the instrument creates a new calibration curve and stores it as calibration curve #1. By putting the cursor on this number and entering, the user can vary the parameters of the calibration curve and enter the concentrations used. If making a “dummy” calibration curve, set the spurge time to 0 min. The purpose of the “dummy” calibration curve is to clean out the injection ports and warm up the instrument before making the sample calibration curve.

The second line in the AUTO SAMPLER screen sets up how many samples will be analyzed. In Figure 1, the first sample is located in port 1 and the last sample is located in

port 30. If the user is making a new calibration curve, enter a number (in this case 2) into the first “C” column. This tells the instrument to create this curve from the calibration standards on the sampling tray and use the generated curve to calculate the concentration in the unknown samples.

If the user is going to compare the samples to a calibration curve that already exists and has been stored by a previous user, the user should enter the desired number under one of the “F” columns. The multiple “F” and “C” columns allow the user to create and/or compare their results against multiple curves.

9. Hit NEXT and check that the information on the screen is correct.
10. Hit NEXT again and then START to begin the run.
11. While the samples are running, press SCREEN OFF and then ENTER.
 - a. To turn the screen back on press ENTER.
12. It takes about 2 hrs to run each calibration curve and approximately 20 min to analyze each sample.
13. A set of calibration checkpoints should be inserted every 30 samples.
14. When the run is finished:
 - a. Turn off the air.
 - b. Turn off the instrument.
 - c. Clean the glassware.

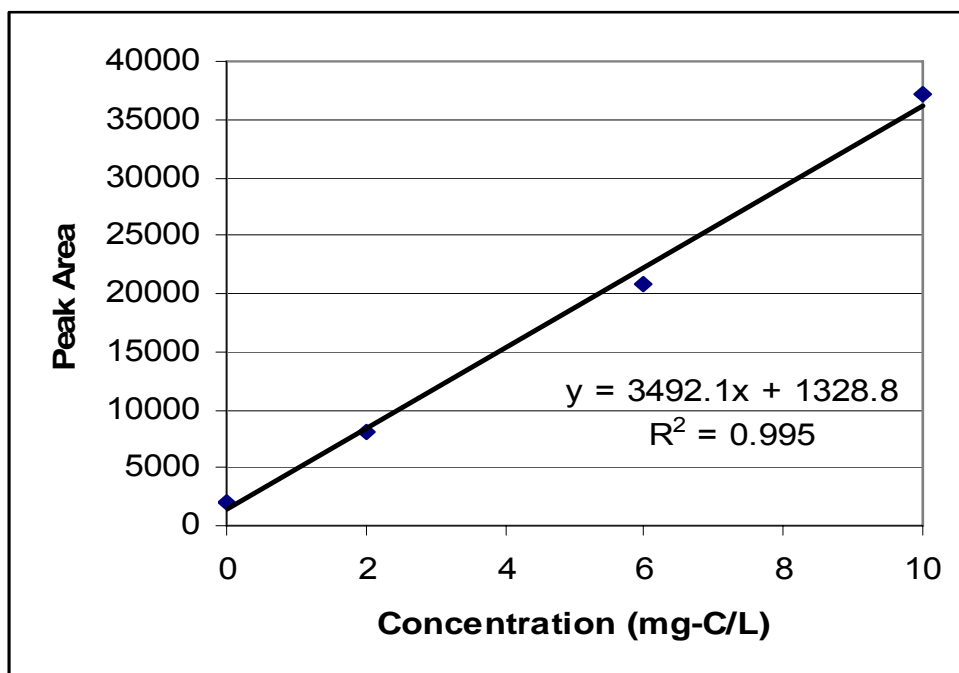
Data Analysis

1. The TOC analyzer outputs the data onto paper. The paper copy consists of the date and time, a summary of the calibration curve used/generated, and the peak areas of each calibration standard. The rest of the output pertains to the unknown samples. Each sample section contains the number of injections, the resulting peak areas, the injections that were discarded, statistical information (mean, standard deviation, and coefficient of variation), and the corresponding concentration (mg-C/L) using the calibration curve.
2. A good calibration curve should have a confidence level greater than 99%. Plot the peak area versus the concentration for the calibration curve. An example is shown in Figure 2 using data from Table 2.

Table 2: Sample data for a calibration curve.

Concentration (mg-C/L)	Peak Area
0	2057
2	8149
6	20789
10	37178

Figure 2: TOC Calibration curve (0-10 mg-C/L).



3. Examine the checkpoints to see if the calibration curve generated reasonable results. If not, make a new calibration curve using the sample run checkpoints and recalculate the concentrations using the peak areas from the printout.

Quality Control and Assurance

1. To insure that the data is sound, it is important to make sure that the procedure is as consistent as possible from run to run.
2. Using the check points every 30 samples as recommended will provide a “double check” of the calibration curve.
3. Check the results to make sure that they are reasonable before reporting them.

4. Duplicates must be within 10% of each other.
5. Check that standards are within 10% of the expected value.
 - a. If not, samples must be reanalyzed.

REFERENCES

- Al-Ahmad, A., F. D. Daschner, *et al.*, (1999). "Biodegradability of cefotiam, ciprofloxacin, meropenem, penicillin G, and sulfamethoxazole and inhibition of waste water bacteria." Archives of Environmental Contamination and Toxicology **37**(2): 158-163.
- Andreozzi, R., M. Raffaele, *et al.*, (2003). "Pharmaceuticals in STP effluents and their solar photodegradation in aquatic environment." Chemosphere **50**(10): 1319-1330.
- Boreen, A. L., X. A. Arnold, *et al.*, (2004). "Photochemical fate of sulfa drugs in the aquatic environment: Sulfa drugs containing five-membered heterocyclic groups." Environmental Science & Technology **38**(14): 3933-3940.
- Brain, R. A., D. J. Johnson, *et al.*, (2004). "Microcosm evaluation of the effects of an eight pharmaceutical mixture to the aquatic macrophytes *Lemna gibba* and *Myriophyllum sibiricum*." Aquatic Toxicology **70**(1): 23-40.
- Brezonik, P. L. and J. Fulkerson-Brekken (1998). "Nitrate-induced photolysis in natural waters: Controls on concentrations of hydroxyl radical photo-intermediates by natural scavenging agents." Environmental Science & Technology **32**(19): 3004-3010.
- Burhenne, J., M. Ludwig, *et al.*, (1999). "Polar photodegradation products of quinolones determined by HPLC/MS/MS." Chemosphere **38**(6): 1279-1286.
- Buxton, G. V., C. L. Greenstock, *et al.*, (1988). "Critical-Review of Rate Constants for Reactions of Hydrated Electrons, Hydrogen-Atoms and Hydroxyl Radicals (.OH/.O-) in Aqueous-Solution." Journal of Physical and Chemical Reference Data **17**(2): 513-886.
- Chee-Sanford, J. C., R. I. Aminov, *et al.*, (2001). "Occurrence and diversity of tetracycline resistance genes in lagoons and groundwater underlying two swine production facilities." Applied and Environmental Microbiology **67**(4): 1494-1502.
- Chelossi, E., L. Vezzulli, *et al.*, (2003). "Antibiotic resistance of benthic bacteria in fish-farm and control sediments of the Western Mediterranean." Aquaculture **219**(1-4): 83-97.
- Clescerl, L. S., A. E. Greenberg, *et al.*, (1999). Standard Methods for Examination of Water and Wastewater. New York, NY, American Public Health Association.
- Doll, T. E. and F. H. Frimmel (2003). "Fate of pharmaceuticals-photodegradation by simulated solar UV-light." Chemosphere **52**(10): 1757-1769.

- Drexel, R. E., G. Olack, *et al.*, (1990). "Organic-Photochemistry .82. Lumitetracycline - a Novel New Tetracycline Photoproduct." Journal of Organic Chemistry **55**(8): 2471-2478.
- Drillia, P., K. Stamatelatou, *et al.*, (2005). "Fate and mobility of pharmaceuticals in solid matrices." Chemosphere **60**(8): 1034-1044.
- Figuerola, R. A., A. Leonard, *et al.*, (2004). "Modeling tetracycline antibiotic sorption to clays." Environmental Science & Technology **38**(2): 476-483.
- Gao, H. Z. and R. G. Zepp (1998). "Factors influencing photoreactions of dissolved organic matter in a coastal river of the southeastern United States." Environmental Science & Technology **32**(19): 2940-2946.
- Gobel, A., A. Thomsen, *et al.*, (2005 b). "Extraction and determination of sulfonamides, macrolides, and trimethoprim in sewage sludge." Journal of Chromatography A **1085**(2): 179-189.
- Gobel, A., A. Thomsen, *et al.*, (2005 a). "Occurrence and sorption behavior of sulfonamides, macrolides, and trimethoprim in activated sludge treatment." Environmental Science & Technology **39**(11): 3981-3989.
- Golet, E. M., A. C. Alder, *et al.*, (2002). "Environmental exposure and risk assessment of fluoroquinolone antibacterial agents in wastewater and river water of the Glatt Valley Watershed, Switzerland." Environmental Science & Technology **36**(17): 3645-3651.
- Golet, E. M., I. Xifra, *et al.*, (2003). "Environmental exposure assessment of fluoroquinolone antibacterial agents from sewage to soil." Environmental Science & Technology **37**(15): 3243-3249.
- Goni-Urriza, M., M. Capdepuy, *et al.*, (2000). "Impact of an urban effluent on antibiotic resistance of riverine Enterobacteriaceae and Aeromonas spp." Applied and Environmental Microbiology **66**(1): 125-132.
- Guardabassi, L., A. Petersen, *et al.*, (1998). "Antibiotic resistance in Acinetobacter spp. isolated from sewers receiving waste effluent from a hospital and a pharmaceutical plant." Applied and Environmental Microbiology **64**(9): 3499-3502.
- Hartmann, A., A. C. Alder, *et al.*, (1998). "Identification of fluoroquinolone antibiotics as the main source of umuC genotoxicity in native hospital wastewater." Environmental Toxicology and Chemistry **17**(3): 377-382.

- Hatchard, C. G. and C. A. Parker (1956). "A New Sensitive Chemical Actinometer .2. Potassium Ferrioxalate as a Standard Chemical Actinometer." Proceedings of the Royal Society of London Series a-Mathematical and Physical Sciences **235**(1203): 518-536.
- Hayashi, N., Y. Nakata, *et al.*, (2004). "New findings on the structure-phototoxicity relationship and photostability of fluoroquinolones with various substituents at position 1." Antimicrobial Agents and Chemotherapy **48**(3): 799-803.
- Himmelsbach, M. and W. Buchberger (2005). "Residue analysis of oxytetracycline in water and sediment samples by high-performance liquid chromatography and immunochemical techniques." Microchimica Acta **151**(1-2): 67-72.
- Hirsch, R., T. Ternes, *et al.*, (1999). "Occurrence of antibiotics in the aquatic environment." Science of the Total Environment **225**(1-2): 109-118.
- Hirsch, R., T. A. Ternes, *et al.*, (1998). "Determination of antibiotics in different water compartments via liquid chromatography electrospray tandem mass spectrometry." Journal of Chromatography A **815**(2): 213-223.
- Holten Lutzhoft, H. C., W. H. Vaes, *et al.*, (2000). "1-Octanol/water distribution coefficient of oxolinic acid; influence of pH and its relation to the interaction with dissolved organic carbon." Chemosphere **40**: 711-714.
- Hooper, D. C. and J. S. Wolfson (1993). Quinolone Antimicrobial Agents. Washington, D.C, American Society for Microbiology.
- Horspool, W. M. and P. Song (1994). CRC Handbook of Organic Photochemistry and Photobiology. Boca Raton, CRC Press.
- Jacobsen, A. M., B. Halling-Sorensen, *et al.*, (2004). "Simultaneous extraction of tetracycline, macrolide and sulfonamide antibiotics from agricultural soils using pressurised liquid extraction, followed by solid-phase extraction and liquid chromatography-tandem mass spectrometry." Journal of Chromatography A **1038**(1-2): 157-170.
- Kalsch, W. (1999). "Biodegradation of the iodinated X-ray contrast media diatrizoate and iopromide." Science of the Total Environment **225**(1-2): 143-153.
- Kim, S., P. Eichhorn, *et al.*, (2005). "Removal of antibiotics in wastewater: Effect of hydraulic and solid retention times on the fate of tetracycline in the activated sludge process." Environmental Science & Technology **39**(15): 5816-5823.
- Klute, A. and A. L. Page (1982). Methods of Soil Analysis. Madison, WI, Society of Agronomy; Soil Science Society of America.

- Kolpin, D. W., E. T. Furlong, *et al.*, (2002). "Pharmaceuticals, hormones, and other organic wastewater contaminants in US streams, 1999-2000: A national reconnaissance." Environmental Science & Technology **36**(6): 1202-1211.
- Kolpin, D. W., M. Skopec, *et al.*, (2004). "Urban contribution of pharmaceuticals and other organic wastewater contaminants to streams during differing flow conditions." Science of the Total Environment **328**(1-3): 119-130.
- Kuhn, H. J., S. E. Braslavsky, *et al.*, (2004). "Chemical actinometry." Pure and Applied Chemistry **76**(12): 2105-2146.
- Kummerer, K. (2001). "Drugs in the environment: emission of drugs, diagnostic aids and disinfectants into wastewater by hospitals in relation to other sources - a review." Chemosphere **45**(6-7): 957-969.
- Kummerer, K. (2002). "Drugs in the environment: emission of drugs, diagnostic aids and disinfectants into wastewater by hospitals in relation to other sources - a review (vol 45, pg 957, 2001)." Chemosphere **48**(3): 383-383.
- Kummerer, K. (2004). "Resistance in the environment." Journal of Antimicrobial Chemotherapy **54**(2): 311-320.
- Lam, M. W. and S. A. Mabury (2005). "Photodegradation of the pharmaceuticals atorvastatin, carbamazepine, levofloxacin, and sulfamethoxazole in natural waters." Aquatic Sciences **67**(2): 177-188.
- Lam, M. W., K. Tantuco, *et al.*, (2003). "PhotoFate: A new approach in accounting for the contribution of indirect photolysis of pesticides and pharmaceuticals in surface waters." Environmental Science & Technology **37**(5): 899-907.
- Larson, R. A. and E. J. Weber (1994). Reaction Mechanisms in Environmental Organic Chemistry. Boca Raton, FL, Lewis.
- Latch, D. E., B. L. Stender, *et al.*, (2003). "Photochemical fate of pharmaceuticals in the environment: Cimetidine and ranitidine." Environmental Science & Technology **37**(15): 3342-3350.
- Le, T. X., Y. Munkage, *et al.*, (2005). "Antibiotic resistance in bacteria from shrimp farming in mangrove areas." Science of the Total Environment **349**(1-3): 95-105.
- Levy, S. B. (1998). "Multidrug resistance - A sign of the times." New England Journal of Medicine **338**(19): 1376-1378.
- Liefer, A. (1988). The Kinetics of Environmental Aquatic Photochemistry. Washington, DC, American Chemical Society.

- Lindberg, R. H., P. Wennberg, *et al.*, (2005). "Screening of human antibiotic substances and determination of weekly mass flows in five sewage treatment plants in Sweden." Environmental Science & Technology **39**(10): 3421-3429.
- Lindsey, M. E., M. Meyer, *et al.*, (2001). "Analysis of trace levels of sulfonamide and tetracycline antimicrobials, in groundwater and surface water using solid-phase extraction and liquid chromatography/mass spectrometry." Analytical Chemistry **73**(19): 4640-4646.
- Loffler, D., J. Rombke, *et al.*, (2005). "Environmental fate of pharmaceuticals in water/sediment systems." Environmental Science & Technology **39**(14): 5209-5218.
- Loffler, D. and T. A. Ternes (2003). "Determination of acidic pharmaceuticals, antibiotics and ivermectin in river sediment using liquid chromatography-tandem mass spectrometry." Journal of Chromatography A **1021**(1-2): 133-144.
- Lorian, V. (1996). Antibiotics in Laboratory Medicine. Baltimore, ML, Williams and Wilkins.
- Lunestad, B. T., O. B. Samuelsen, *et al.*, (1995). "Photostability of 8 Antibacterial Agents in Seawater." Aquaculture **134**(3-4): 217-225.
- Madigan, M. T., J. M. Martinko, *et al.*, (2002). Brock Biology of Microorganisms. Upper Saddle River, NJ, Prentice Hall and Pearson Education.
- Morrison, H., G. Olack, *et al.*, (1991). "Organic-Photochemistry .93. Photochemical and Photophysical Studies of Tetracycline." Journal of the American Chemical Society **113**(21): 8110-8118.
- Murov, S. L. (1973). Handbook of Photochemistry. New York, NY, Dekker.
- Nowara, A., J. Burhenne, *et al.*, (1997). "Binding of fluoroquinolone carboxylic acid derivatives to clay minerals." Journal of Agricultural and Food Chemistry **45**(4): 1459-1463.
- Ohlsen, K., T. Ternes, *et al.*, (2003). "Impact of antibiotics on conjugational resistance gene transfer in *Staphylococcus aureus* in sewage." Environmental Microbiology **5**(8): 711-716.
- Oka, H., Y. Ikai, *et al.*, (1989). "Photodecomposition Products of Tetracycline in Aqueous-Solution." Journal of Agricultural and Food Chemistry **37**(1): 226-231.
- Phillips, R. (1983). Sources and Applications of Ultraviolet Radiations. London, Academic Press.

- Renew, J. E. and C. H. Huang (2004). "Simultaneous determination of fluoroquinolone, sulfonamide, and trimethoprim antibiotics in wastewater using tandem solid phase extraction and liquid chromatography-electrospray mass spectrometry." Journal of Chromatography A **1042**(1-2): 113-121.
- Ronnefahrt, I., U. Traub-Eberhard, *et al.*, (1997). "Comparison of the fate of isoproturon in small- and large-scale water/sediment systems." Chemosphere **35**: 181-189.
- Sassman, S. A. and L. S. Lee (2005). "Sorption of three tetracyclines by several soils: Assessing the role of pH and cation exchange." Environmental Science & Technology **39**(19): 7452-7459.
- Schluter, A., H. Heuer, *et al.*, (2003). "The 64 508 bp IncP-1 beta antibiotic multiresistance plasmid pB10 isolated from a waste-water treatment plant provides evidence for recombination between members of different branches of the IncP-1 beta group." Microbiology-Sgm **149**: 3139-3153.
- Schwarzenbach, R. P., P. M. Geschwend, *et al.*, (1993). Environmental Organic Chemistry. New York, NY, Wiley.
- Simon, N. S. (2005). "Loosely bound oxytetracycline in riverine sediments from two tributaries of the Chesapeake Bay." Environmental Science & Technology **39**(10): 3480-3487.
- Spratt, T. E., S. S. Schultz, *et al.*, (1999). "Different mechanisms for the photoinduced production of oxidative DNA damage by fluoroquinolones differing in photostability." Chemical Research in Toxicology **12**(9): 809-815.
- Stangroom, S. J., C. L. Macleod, *et al.*, (1998). "Photosensitized transformation of the herbicide 4-chloro-2-methylphenoxy acetic acid (MCPA) in water." Water Research **32**(3): 623-632.
- Ternes, T. A., M. Bonerz, *et al.*, (2005). "Determination of pharmaceuticals, iodinated contrast media and musk fragrances in sludge by LC/tandem MS and GC/MS." Journal of Chromatography A **1067**(1-2): 213-223.
- Thiele-Bruhn, S. (2003). "Pharmaceutical antibiotic compounds, in soils - A review (vol 166, pg 145, 2003)." Journal of Plant Nutrition and Soil Science-Zeitschrift Fur Pflanzenernahrung Und Bodenkunde **166**(4): 546-546.
- Thiele-Bruhn, S. and I. C. Beck (2005). "Effects of sulfonamide and tetracycline antibiotics on soil microbial activity and microbial biomass." Chemosphere **59**(4): 457-465.

- Thiele-Bruhn, S., T. Seibicke, *et al.*, (2004). "Sorption of sulfonamide pharmaceutical antibiotics on whole soils and particle-size fractions." Journal of Environmental Quality **33**(4): 1331-1342.
- Turiel, E., G. Bordin, *et al.*, (2005). "Study of the evolution and degradation products of ciprofloxacin and oxolinic acid in river water samples by HPLC-UV/MS/MS-MS." Journal of Environmental Monitoring **7**(3): 189-195.
- Turiel, E., A. Martin-Esteban, *et al.*, (2006). "Multiresidue analysis of quinolones and fluoroquinolones in soil by ultrasonic-assisted extraction in small columns and HPLC-UV." Analytica Chimica Acta **562**(1): 30-35.
- Wessels, J. M., W. E. Ford, *et al.*, (1998). "The complexation of tetracycline and anhydrotetracycline with Mg^{2+} and Ca^{2+} ; a spectroscopic study." Journal of Physical Chemistry B **102**: 9323-9331.
- Witte, W. (1998). "Medical consequences of antibiotic use in agriculture." Science **279**(5353): 996-997.
- Xia, K., A. Bhandari, *et al.*, (2005). "Occurrence and fate of pharmaceuticals and personal care products (PPCPs) in biosolids." Journal of Environmental Quality **34**(1): 91-104.
- Yang, S. W. and K. Carlson (2003). "Evolution of antibiotic occurrence in a river through pristine, urban and agricultural landscapes." Water Research **37**(19): 4645-4656.
- Ye, Z. (2005). Occurrence, Fate, and Transformation of Antibiotics during Drinking Water Treatment. Chapel Hill, NC, University of North Carolina-Chapel Hill.
- Zhou, W. and D. E. Moore (1994). "Photochemical Decomposition of Sulfamethoxazole." International Journal of Pharmaceutics **110**(1): 55-63.